

**EVALUATING THE EFFECTS OF PROCESS PARAMETERS IN COLD
CHAMBER HIGH PRESSURE DIE CASTING**

A Thesis

*Submitted In partial fulfillment of the requirement of the
requirement for award of degree of*

**MASTER OF ENGINEERING
IN
PRODUCTION AND INDUSTRIAL ENGINEERING**

Submitted by

VIRENDER UPNEJA
ROLL NO: 820982005

Under the guidance of:

Dr. Vinod Kumar

Associate Professor, MED
THAPAR UNIVERSITY

Mr. Lalit Kumar

Lecturer, MED
THAPAR UNIVERSITY



**DEPARTMENT OF MECHANICAL ENGINEERING,
THAPAR UNIVERSITY
PATIALA-147004, INDIA
DECEMBER -2012**

CERTIFICATE

I hereby declare that the thesis entitled "EVALUATING THE EFFECTS OF PROCESS PARAMETERS IN COLD CHAMBER HIGH PRESSURE DIE CASTING" is an authentic record of my study carried out as requirement for the award of degree of Master of Engineering in Production and Industrial Engineering at Thapar University, Patiala, under the guidance of Dr. Vinod Kumar, Associate Professor and Mr. Lalit Kumar, Lecturer of Department of Mechanical Engineering, Thapar University, Patiala during January 2012 to December 2012. The matter embodied in this thesis has not been submitted in part or full to any other University or institute for the award of any degree.

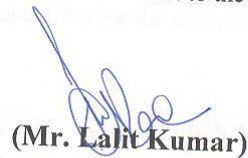


Virender Upneja

This is to certify that above declaration made by the student concerned is correct to the best of my knowledge & belief.

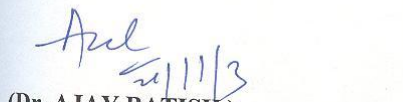


(Dr. Vinod Kumar)
Associate Professor, MED
Thapar University,
Patiala, 147004




(Mr. Lalit Kumar)
Lecturer, MED
Thapar University,
Patiala, 147004

Countersigned by:



(Dr. AJAY BATISH)
Professor and Head
Department of Mechanical Engineering
Thapar University, Patiala, 147004



(Dr S.K. MOHAPATRA)
(Dean of Academic Affairs)
Thapar University, Patiala

ACKNOWLEDGEMENT

With deep sense of gratitude I express my sincere thanks to my guides, **Dr. Vinod Kumar , and Mr. Lalit Kumar** for their valuable guidance, proper advice and constant encouragement of my work in this Thesis from the initial level .I also feel very much obliged to **Dr. AJAY BATISH**, Professor & Head, of Mechanical Engineering Department.

I would like to thanks all the members and employees of Mechanical Engineering Department, Thapar University, Patiala for their everlasting support.

I am also very thankful to my friends for their cooperation.

I offer my regards to all of those who supported me in any respect during the completion of the work.

Lastly, and most importantly, I wish to thank my parents, my wife and my little baby girl. They supported me and loved me. To them I dedicate my thesis.



VIRENDER UPNEJA

Registration No. 82098205

ME(Production and Industrial Engineering)

ABSTRACT

High Pressure Die Casting (HPDC) is an efficient, economical process offering a broader range of shapes and components than many other manufacturing techniques. High Pressure Die Casting is a process by which a molten non-ferrous material is forced under high pressure into reusable tool steel molds. These molds, called dies, can be designed to produce complex shapes with a high degree of accuracy and repeatability, with smooth or textured surfaces. High Pressure Die Casting is best suited for high volume production runs and can produce the least expensive parts. A variety of materials are available for the High Pressure Die Casting process. The included materials and process charts can be used to help determine which are best suited for a specific application.

Experiments in industrial environment were conducted producing wire clamp using commercially treated A356 (Al-Si) and ADC 12 (Al-Si) alloy. The different process parameter were varied such as injection pressure, pouring temperature, coating type, cooling type to understand their affect on the final product.

The objective of this study is to evaluate the main effects i.e. thermal characteristics (temperature of the molten metal), injection pressure of the molten metal, type of coating (oil coating, oil + graphite coating, Dycot coating), and the type of cooling (air cooling, water cooling and oil cooling) on density of the material, hardness of the material and the surface roughness of the material. The methodology used to calculate the effect of various parameters will also be studied using parameterization approach in design of experiment is Taguchi approach. Taguchi's approach provides a powerful and efficient method for designing products that operate consistently and optimally over a variety of conditions This approach allows quality considerations to be included at an early stage of any new venture; in the design phase for a product, during routine maintenance or during installation of a manufacturing process An experimental model for Multi Response Signal To Noise (MRSN) ratio encompassing three responses namely surface roughness, density and hardness has been employed to carry out the experimental study and subsequent analysis. Analysis of Variance (ANOVA) was performed for all the responses and the effect of the factors was explained with the help of main effect plots. Micro structural analysis for all the trials was done.

The major finding and conclusion of this research is that control of various parameter such as pouring temperature, injection pressure, coating type cooling type enhances the quality of product and suggest the different combination of process parameter which helps the product to sustain in the market.

Some limitation of numerical modelling and metallurgical analysis were also identified during this research and recommendations were made to improve the surface roughness, hardness & density of aluminium alloy wire clamps.

<u>TITLE</u>	<u>PAGE NO.</u>
LIST OF FIGURES	v-viii
LIST OF TABLES	ix-xi
Chapter 1 INTRODUCTION TO COLD CHAMBER DIE CASTING	1-14
1.1 Introduction	1
1.2 History of Die Casting	1
1.3 Advantages of Die Casting	2
1.4 Die Casting Process	3
1.5 Process Cycle	3
1.6 Equipments	5
1.7 Die Construction	9
1.8 Die Casting Alloys	13
1.9 Organization of Study	13
Chapter 2 LITERATURE REVIEW	15-30
2.1 Introduction	15
2.2 Summary of Literature	29
2.3 Problem formulation	29
2.4 Objectives	30
2.5 Work Plan	30

Chapter 3	DESIGN OF EXPERIMENT	31-49
3.1	Introduction	31
3.2	Establishment of Objective Function	32
3.3	Selection of Factors	32
3.4	Degree of Freedom (dof)	32
3.5	Orthogonal Array	33
3.6	Description of Die Casting Machine	36
3.7	Description of Pit Furnace	38
3.8	Experimental Set up	40
3.9	Measuring and Test Equipment Used	40
3.10	Composition of Work Material	41
3.11	Analysis of Results	46
Chapter 4	RESULTS AND ANALYSIS (A356)	50-73
4.1	Introduction	50
4.2	Results of Surface Roughness	51
4.3	Analysis of Variance- Surface Roughness	51
4.4	Results for S/N ratio – Surface Roughness	53
4.5	Optimal Design For Roughness	56

4.6	Results for Density	58
4.7	Analysis of Variance- Density	59
4.8	Results for S/N ratio – Density	69
4.9	Optimal Design for Density	64
4.10	Results of Hardness	66
4.11	Analysis of Variance- Hardness	66
4.12	Results for S/N Ratio – Hardness	69
4.13	Optimal Design for Hardness	71
Chapter 5 RESULTS AND ANALYSIS (ADC12)		74-93
5.1	Introduction	74
5.2	Results of Surface Roughness	75
5.3	Analysis of Variance- Surface Roughness	75
5.4	Results for S/N ratio – Surface Roughness	77
5.5	Optimal Design For Roughness	80
5.6	Results for Density	81
5.7	Analysis of Variance- Density	83
5.8	Results for S/N ratio – Density	84
5.9	Optimal Design for Density	86
5.10	Results of Hardness	88
5.11	Analysis of Variance- Hardness	88

5.12	Results for S/N Ratio – Hardness	91
5.13	Optimal Design for Hardness	93
Chapter 6 MULTI RESPONSE OPTIMIZATION		94-99
6.1	Introduction	94
6.2	Comparison for Roughness	96
6.3	Comparison for Density	98
6.4	Comparison for Hardness	99
Chapter 7 MICRO STRUCTURE		100-105
7.1	Introduction	100
7.2	Microstructure Analysis	105
Chapter 8 RESULTT AND CONCLUSION		106-107
8.1	Results	106
REFERENCES		108-114

LIST OF FIGURES

<u>Figure No.</u>	<u>Title</u>	<u>Page No.</u>
Figure 1.1	High Pressure Die Casting Process	4
Figure 1.2	Hot chamber machine	6
Figure 1.3	Hot chamber die casting	6
Figure 1.4	Cold chamber die casting machine	7
Figure 1.5	Description of cold chamber die casting	8
Figure 1.6	Schematic view of cold chamber die casting	8
Figure 1.7.1	Single cavity die	9
Figure 1.7.2	Multiple-cavity die	10
Figure 1.7.3	Unit die	10
Figure 1.7.4	Combination dies	10
Figure 3.1	High Pressure Cold Chamber Die Casting Machine	37
Figure 3.2	High Pressure Cold Chamber Die Casting Machine	38
Figure 3.3	Pit Furnace	39
Figure 3.4	Rockwell Hardness Testing Machine	41
Figure 3.5	Raw material of A356 and ADC12 before casting	42
Figure 3.6	Final Sample of Material of A356 and ADC12 After Casting	44
Figure 4.1	Fish bone diagram	50

Figure 4.2	Bar chart for percentage contribution in roughness	52
Figure 4.3	Main effect plots for mean Roughness	53
Figure 4.4	Pie chart for surface roughness for s/n ratio	54
Figure 4.5	Bar chart for surface roughness for s/n ratio	55
Figure 4.6	Main Effect Plot for S/N Ratio of Roughness	56
Figure 4.7	Bar chart for percentage contribution in density	60
Figure 4.8	Pie chart for percentage contribution in density	60
Figure 4.9	Main effect plots for mean Density	61
Figure 4.10	Pie chart for Density for s/n ratio	63
Figure 4.11	Main Effect Plot for S/N Ratio for Density	64
Figure 4.12	Bar chart for percentage contribution in Hardness	67
Figure 4.13	Pie chart for percentage contribution in Hardness	67
Figure 4.14	Main effect plots for mean Hardness	69
Figure 4.15	Bar chart for Hardness for s/n ratio	70
Figure 4.16	Main Effect Plot for S/N Ratio for Hardness	71
Figure 5.1	Fish bone diagram	74
Figure 5.2	Bar chart for percentage contribution in roughness	76
Figure 5.3	Pie chart for surface roughness for means	76
Figure 5.4	Main effect plots for mean Roughness	77

Figure 5.5	Bar chart for surface roughness for s/n ratio	78
Figure 5.6	Pie chart for S/N Ratio of Roughness	79
Figure 5.7	Main Effect Plot for S/N Ratio of Roughness	79
Figure 5.8	Bar chart for percentage contribution in density	83
Figure 5.9	Pie chart for percentage contribution in density	83
Figure 5.10	Main effect plots for mean Density	84
Figure 5.11	Pie chart for Density for s/n ratio	85
Figure 5.12	Main Effect Plot for S/N Ratio for Density	86
Figure 5.13	Bar chart for Means in Hardness	89
Figure 5.14	Pie chart for Means in Hardness	90
Figure 5.15	Main effect plots for mean Hardness	90
Figure 5.16	Pie chart for Hardness for s/n ratio	92
Figure 5.17	Main Effect Plot for S/N Ratio for Hardness	92
Figure 6.1	Bar chart for comparisons of Means in Roughness	96
Figure 6.2	Bar chart for comparisons of Means in Density	97
Figure 6.3	Bar chart for comparisons of Means in Hardness	98
Figure 7.1	Microstructure of A356 and ADC 12 Pouring Temperature 770 ⁰ , and Injection pressure 100 Kg/cm ² , Oil Coating, Air Cooling.	100

- Figure 7.2 Microstructure of A356 and ADC 12 Pouring Temperature 770⁰, and Injection pressure 90 Kg/cm², Oil Graphite Coating, Water Cooling. 101
- Figure 7.3 Microstructure of A356 and ADC 12 Pouring Temperature 770⁰c, and Injection pressure 120 Kg/cm², Dycot Coating, Oil Cooling. 102
- Figure 7.4 Microstructure of A356 and ADC 12, Pouring Temperature 790⁰, and Injection pressure 100 Kg/cm², Oil Graphite Coating, Oil Cooling.103
- Figure 7.5 Microstructure of A356 and ADC 12, Pouring Temperature 790⁰, and Injection pressure 90 Kg/cm², Dycot Coating, Air Cooling. 104
- Figure 7.6 Microstructure of A356 and ADC 12, Pouring Temperature 790⁰, and Injection pressure 120 Kg/cm², Oil Coating, and Water Cooling.105
- Figure 7.7 Microstructure of A356 and ADC 12, Pouring Temperature 730⁰, and Injection pressure 100 Kg/cm², Dycot Coating, Water Cooling.106
- Figure 7.8 Microstructure of A356 and ADC 12, Pouring Temperature 730⁰, and Injection pressure 90 Kg/cm², Oil Coating, Oil Cooling.107
- Figure 7.9 Microstructure of A356 and ADC 12, Pouring Temperature 730⁰, Injection pressure 120 Kg/cm², Oil Graphite Coating, Air Cooling.108

LIST OF TABLES

<u>Table No.</u>	<u>Title</u>	<u>Page No.</u>
Table 3.1	Factors of interest and their respective levels	32
Table 3.2	Degree of freedom	33
Table 3.3	Orthogonal Array	35
Table 3.4	Specification of Die Casting Machine	36
Table 3.5	Chemical composition of work piece materials	43
Table 3.6	Analysis of the Result	45
Table 3.7	Response Characteristics	49
Table 4.1	Results for Surface Roughness	51
Table 4.2	Analysis of Variance for means of surface roughness	52
Table 4.3	Response Table for Means surface roughness	53
Table 4.4	Analysis of Variance for SN ratios of surface roughness	54
Table 4.5	Response Table for S/N Ratio of Surface Roughness	55
Table 4.6	Significant factor and Their Levels	57
Table 4.7	Results of Density	58
Table 4.8	Analysis of Variance for Means density	59

Table 4.9	Response Table for Means for Density	61
Table 4.10	Analysis of Variance for S/N ratio for Density	62
Table 4.11	Response Table for Means for Density	63
Table 4.12	Significant Factor and their Levels	64
Table 4.13	Results of Hardness	66
Table 4.14	Analysis of Variance for Mean Hardness	67
Table 4.15	Response Table for Means for hardness	68
Table 4.16	Analysis of Variance for S/N Ratio of Hardness	70
Table 4.17	Response Table for S/N Ratio of Hardness	71
Table 4.18	Significant Factors and Their Levels	72
Table 5.1	Results for Surface Roughness	75
Table 5.2	Analysis of Variance for means of surface roughness	76
Table 5.3	Response Table for Means surface roughness	77
Table 5.4	Analysis of Variance for SN ratios of surface roughness	78
Table 5.5	Response Table for S/N Ratio of Surface Roughness	79
Table 5.6	Significant factor and Their Levels	80
Table 5.7	Results of Density	82
Table 5.8	Analysis of Variance for Means density	82
Table 5.9	Response Table for Means for Density	83
Table 5.10	Analysis of Variance for S/N ratio for Density	85
Table 5.11	Response Table for S/N Ratio for Density	85
Table 5.12	Significant Factor and their Levels	86
Table 5.13	Results of Hardness	88

Table 5.14	Analysis of Variance for Mean Hardness	89
Table 5.15	Response Table for Means for hardness	90
Table 5.16	Analysis of Variance for S/N Ratio of Hardness	91
Table 5.17	Response Table for S/N Ratio of Hardness	92
Table 5.18	Significant Factors and Their Levels	93
Table 6.1	Analysis of results for A356 casting	94
Table 6.2	Analysis of results for ADC12 casting	95
Table 6.3	Percentage Contribution for roughness for means.	96
Table 6.4	Percentage Contribution for Density for means.	97
Table 6.5	Hardness for means in A356 and ADC 12 alloy	98

1.1 INTRODUCTION

High Pressure Die Casting (HPDC) is an efficient, economical process offering a broader range of shapes and components than many other manufacturing techniques. High Pressure Die Casting is a process by which a molten non-ferrous material is forced under high pressure into reusable tool steel molds. These molds, called dies, can be designed to produce complex shapes with a high degree of accuracy and repeatability, with smooth or textured surfaces. High Pressure Die Casting is best suited for high volume production runs and can produce the least expensive parts. A variety of materials are available for the High Pressure Die Casting process. The included materials and process charts can be used to help determine which are best suited for a specific application. [64]

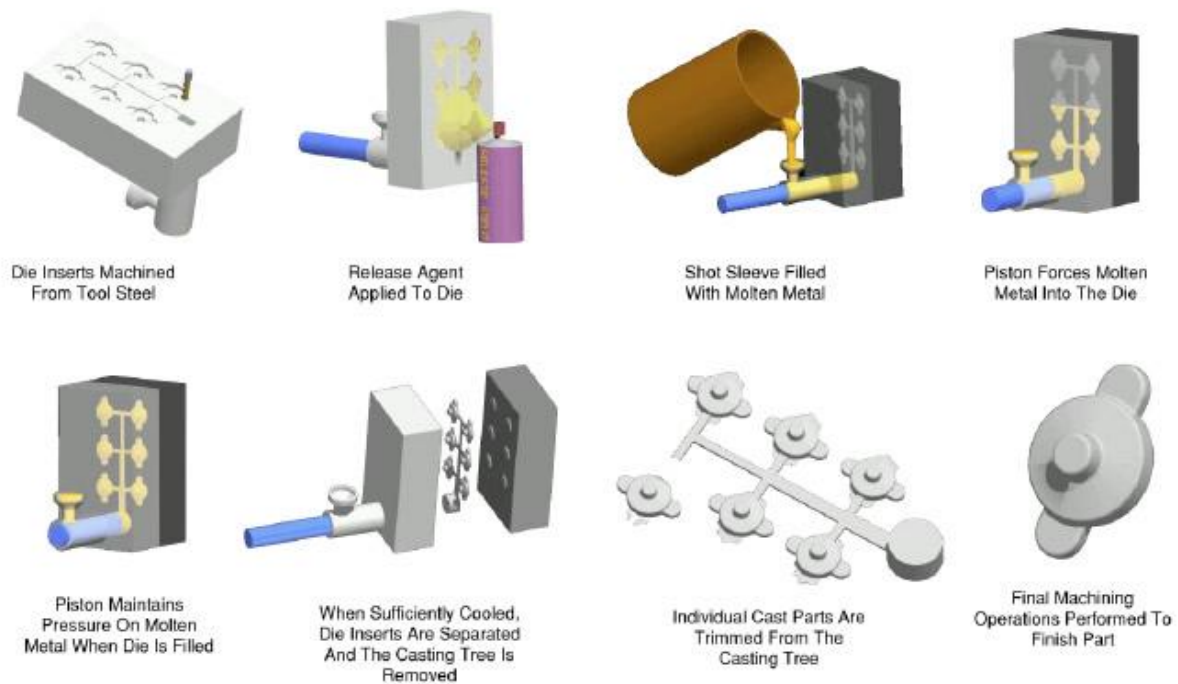


Fig1.1 High pressure die casting process [64]

1.2 HISTORY

The earliest examples of die casting by pressure injection - as opposed to casting by gravity pressure - occurred in the mid-1800s. A patent was awarded to Sturges in 1849 for the first manually operated machine for casting printing type. The process was limited to printer's type for the next 20 years, but development of other shapes began to increase toward the end of the century. By 1892, commercial applications included parts for phonographs and cash registers, and mass production of many types of parts began in the early 1900s.

The first die casting alloys were various compositions of tin and lead, but their use declined with the introduction of zinc and aluminium alloys in 1914. Magnesium and copper alloys quickly followed, and by the 1930s, many of the modern alloys still in use today became available.

The die casting process has evolved from the original low-pressure injection method to techniques including high-pressure casting at forces exceeding 4500 pounds per square inch squeeze casting and semi-solid die casting. These modern processes are capable of producing high integrity, near net-shape castings with excellent surface finishes. [1]

1.2.1 The Future of Die Casting

Continuous refinement in both the alloy used in die casting and the process itself, has expanded the die casting applications into almost every known market. Once limited to only lead, today's die caster can produce casting in variety of sizes shapes and wall thickness that are strong durable and dimensionally precise [1]

1.3 THE ADVANTAGES OF DIE CASTING

Die casting is an efficient, economical process offering a broader range of shapes and components than any other manufacturing technique. Parts have long service life and may be designed to complement the visual appeal of the surrounding part. Designers can gain a number of advantages and benefits by specifying die cast parts. [1]

1.3.1 High-speed production

Die casting provides complex shapes within closer tolerances than many other mass production processes. Little or no machining is required and thousands of identical castings can be produced before additional tooling is required. [3]

1.3.2 Dimensional accuracy and stability

Die casting produces parts that are durable and dimensionally stable, while maintaining close tolerances. They are also heat resistant. [3]

1.3.3 Strength and weight

Die cast parts are stronger than plastic injection moldings having the same dimensions. Thin wall castings are stronger and lighter than those possible with other casting methods. Plus, because die castings do not consist of separate parts welded or fastened together, the strength is that of the alloy rather than the joining process.[3]

1.3.4 Multiple finishing techniques

Die cast parts can be produced with smooth or textured surfaces, and they are easily plated or finished with a minimum of surface preparation.

1.3.5 Simplified Assembly

Die castings provide integral fastening elements, such as bosses and studs. Holes can be cored and made to tap drill sizes, or external threads can be cast.

1.4 DIE CASTING PROCESS

Die casting is a manufacturing process that can produce geometrically complex metal parts through the use of reusable molds, called dies. The die casting process involves the use of a furnace, metal, die casting machine, and die. The metal, typically a non-ferrous alloy such as aluminum or zinc, is melted in the furnace and then injected into the dies in the die casting machine. There are two main types of die casting machines - Hot chamber machines (used for alloys with low melting temperatures, such as zinc) and cold chamber machines (used for alloys with high melting temperatures, such as aluminium). However, in both machines, after the molten metal is injected into the dies, it rapidly cools and solidifies into the final part, called the casting

The castings that are created in this process can vary greatly in size and weight, ranging from a couple ounces to 40 kg. One common application of die cast parts are housings - thin-walled enclosures, often requiring many ribs and bosses on the interior. Metal housings for a variety of appliances and equipment are often die cast. Several automobile components are also manufactured using die casting, including pistons, cylinder heads, and engine blocks. Other common die cast parts include propellers, gears, bushings, pumps, valves and electrical components such as wire clamps. [4]

1.5 Process Cycle

The process cycle for die casting consists of five main stages, which are explained below. The total cycle time is very short, typically between 2 seconds and 1 minute. [3]

1.5.1 Clamping

The first step is the preparation and clamping of the two halves of the die. Each die half is first cleaned from the previous injection and then lubricated to facilitate the ejection of the next part. The lubrication time increases with part size, as well as the number of cavities and side-cores. Also, lubrication may not be required after each cycle, but after 2 or 3 cycles, depending upon the material. After lubrication, the two die halves, which are attached inside the die casting machine, are closed and securely clamped together. Sufficient force must be applied to the die to keep it securely closed while the metal is injected. The time required to close and clamp the die is

dependent upon the machine - larger machines (those with greater clamping forces) will require more time. This time can be estimated from the dry cycle time of the machine. [5]

1.5.2 Injection

The molten metal, which is maintained at a set temperature in the furnace, is next transferred into a chamber where it can be injected into the die. The method of transferring the molten metal is dependent upon the type of die casting machine, whether a hot chamber or cold chamber machine is being used. The difference in this equipment will be detailed in the next section. Once transferred, the molten metal is injected at high pressures into the die. Typical injection pressure ranges from 6894757 to 137895140 Pascal. This pressure holds the molten metal in the dies during solidification. The amount of metal that is injected into the die is referred to as the shot. The injection time is the time required for the molten metal to fill all of the channels and cavities in the die. This time is very short, typically less than 0.1 seconds, in order to prevent early solidification of any one part of the metal. The proper injection time can be determined by the thermodynamic properties of the material, as well as the wall thickness of the casting. A greater wall thickness will require a longer injection time. In the case where a cold chamber die casting machine is being used, the injection time must also include the time to manually ladle the molten metal into the shot chamber. [5.]

1.5.3 Cooling

The molten metal that is injected into the die will begin to cool and solidify once it enters the die cavity. When the entire cavity is filled and the molten metal solidifies, the final shape of the casting is formed. The die cannot be opened until the cooling time has elapsed and the casting is solidified. The cooling time can be estimated from several thermodynamic properties of the metal, the maximum wall thickness of the casting, and the complexity of the die. A greater wall thickness will require a longer cooling time. The geometric complexity of the die also requires a longer cooling time because the additional resistance to the flow of heat. [1]

1.5.4 Ejection

After the predetermined cooling time has passed, the die halves can be opened and an ejection mechanism can push the casting out of the die cavity. The time to open the die can be estimated from the dry cycle time of the machine and the ejection time is determined by the size of the casting's envelope and should include time for the casting to fall free of the die. The ejection mechanism must apply some force to eject the part because during cooling the part shrinks and adheres to the die. Once the casting is ejected, the die can be clamped shut for the next injection. [1]

1.5.5 Trimming

During cooling, the material in the channels of the die will solidify attached to the casting. This excess material, along with any flash that has occurred, must be trimmed from the casting either manually via cutting or sawing, or using a trimming press. The time required to trim the excess material can be estimated from the size of the casting's envelope. The scrap material that results from this trimming is either discarded or can be reused in the die casting process. Recycled material may need to be reconditioned to the proper chemical composition before it can be combined with non-recycled metal and reused in the die casting process. [1]

1.6 Equipment

The two types of die casting machines are Hot chamber machine and Cold chamber machine.

1.6.1 Hot Chamber Die Casting Machines

Hot chamber machines are used for alloys with low melting temperatures, such as zinc, tin, and lead. The temperatures required to melt other alloys would damage the pump, which is in direct contact with the molten metal. The metal is contained in an open holding pot which is placed into a furnace, where it is melted to the necessary temperature. The molten metal then flows into a shot chamber through an inlet and a plunger, powered by hydraulic pressure, forces the molten metal through a gooseneck channel and into the die. Typical injection pressures for a hot chamber die casting machine are between 6894757 to 137895140 Pascal. After the molten metal has been injected into the die cavity, the plunger remains down, holding the pressure while the casting solidifies. After solidification, the hydraulic system retracts the plunger and the part can be ejected by the clamping unit. Prior to the injection of the molten metal, this unit closes and clamps the two halves of the die. When the die is attached to the die casting machine, each half is fixed to a large plate, called a platen. The front half of the die, called the cover die, is mounted to a stationary platen and aligns with the gooseneck channel. The rear half of the die, called the ejector die, is mounted to a movable platen, which slides along the tie bars. The hydraulically powered clamping unit actuates clamping bars that push this platen towards the cover die and exert enough pressure to keep it closed while the molten metal is injected. Following the solidification of the metal inside the die cavity, the clamping unit releases the die halves and simultaneously causes the ejection system to push the casting out of the open cavity. The die can then be closed for the next injection. [5]

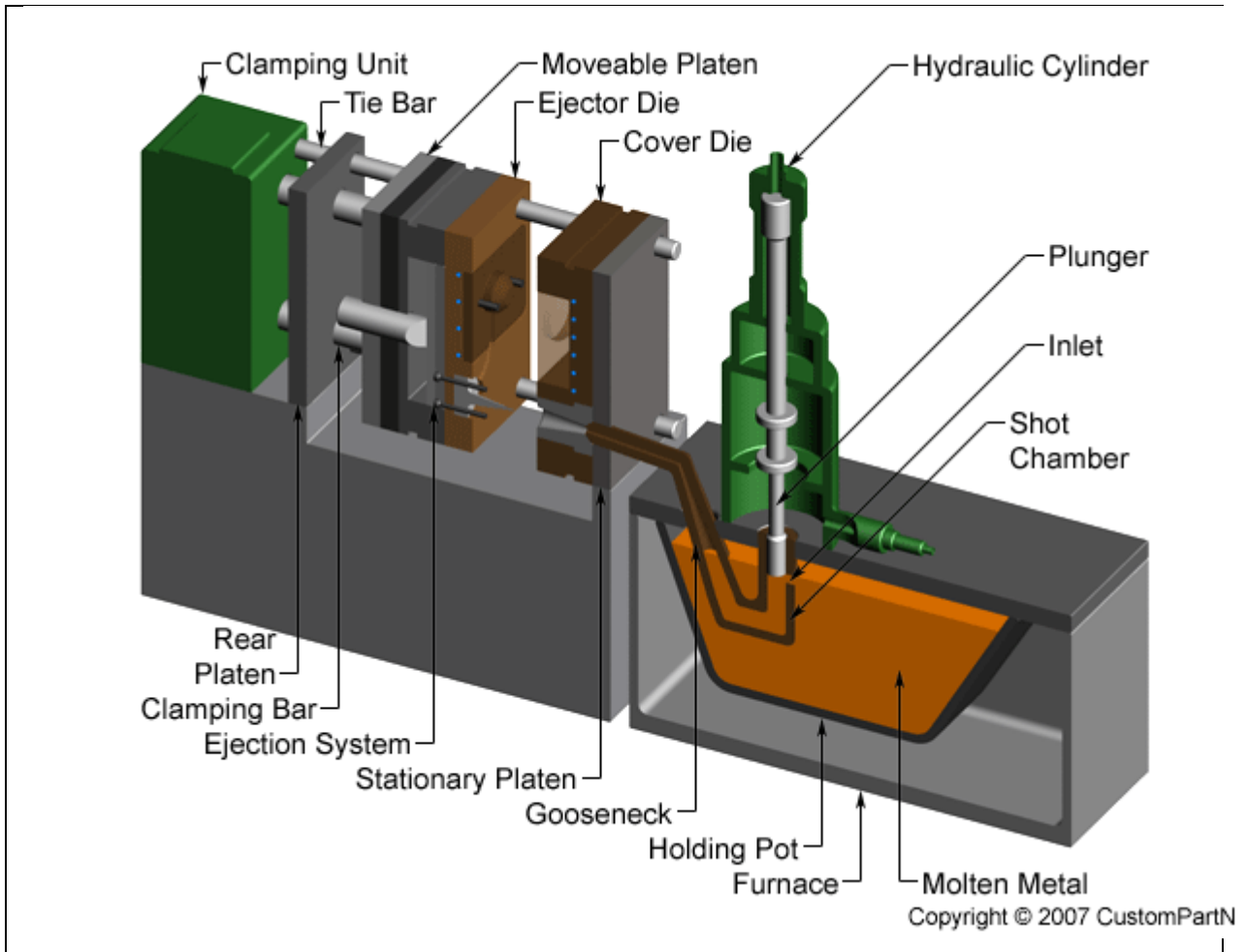


fig 1.2 Hot chamber machine [4]

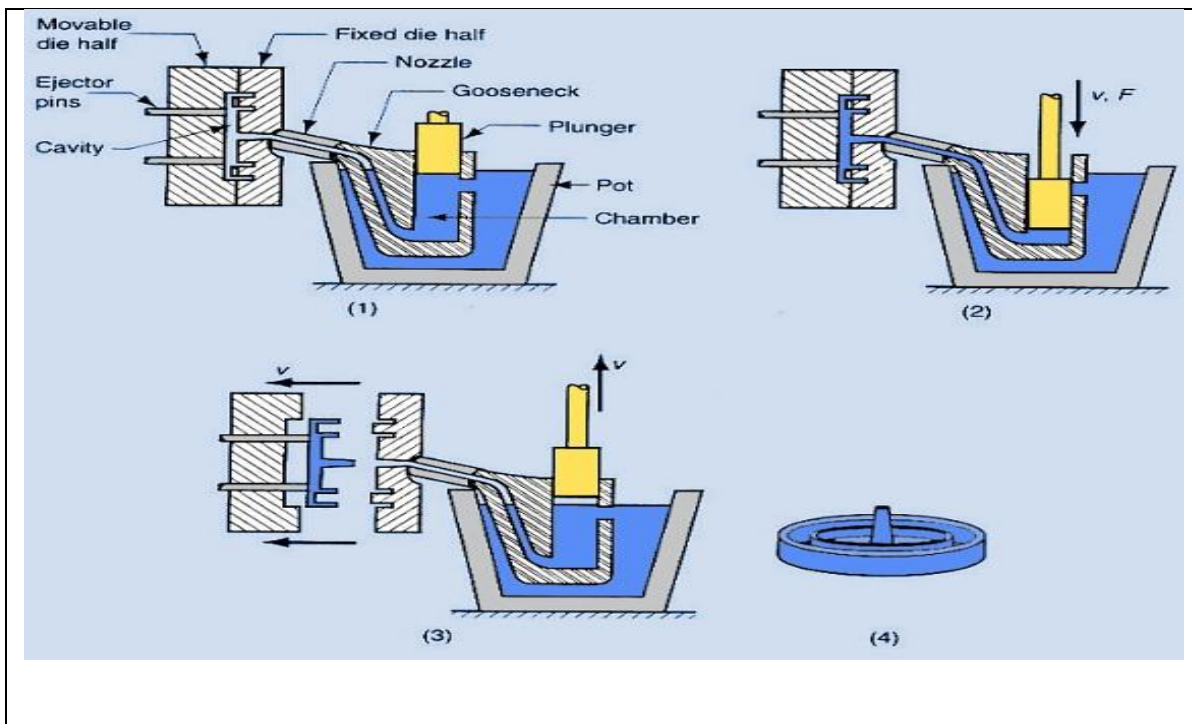


fig 1.3 Hot chamber die casting [4]

1.6.2 Cold Chamber Die Casting Machine

Cold chamber machines are used for alloys with high melting temperatures that cannot be cast in hot chamber machines because they would damage the pumping system. Such alloys include aluminium, brass, and magnesium. The molten metal is still contained in an open holding pot which is placed into a furnace, where it is melted to the necessary temperature. However, this holding pot is kept separate from the die casting machine and the molten metal is ladled from the pot for each casting, rather than being pumped. The metal is poured from the ladle into the shot chamber through a pouring hole. The injection system in a cold chamber machine functions similarly to that of a hot chamber machine, however it is usually oriented horizontally and does not include a gooseneck channel. A plunger, powered by hydraulic pressure, forces the molten metal through the shot chamber and into the injection sleeve in the die. The typical injection pressures for a cold chamber die casting machine are between 13789514 and 137895140 Pascal. After the molten metal has been injected into the die cavity, the plunger remains forward, holding the pressure while the casting solidifies. After solidification, the hydraulic system retracts the plunger and the part can be ejected by the clamping unit. The clamping unit and mounting of the dies is identical to the hot chamber machine

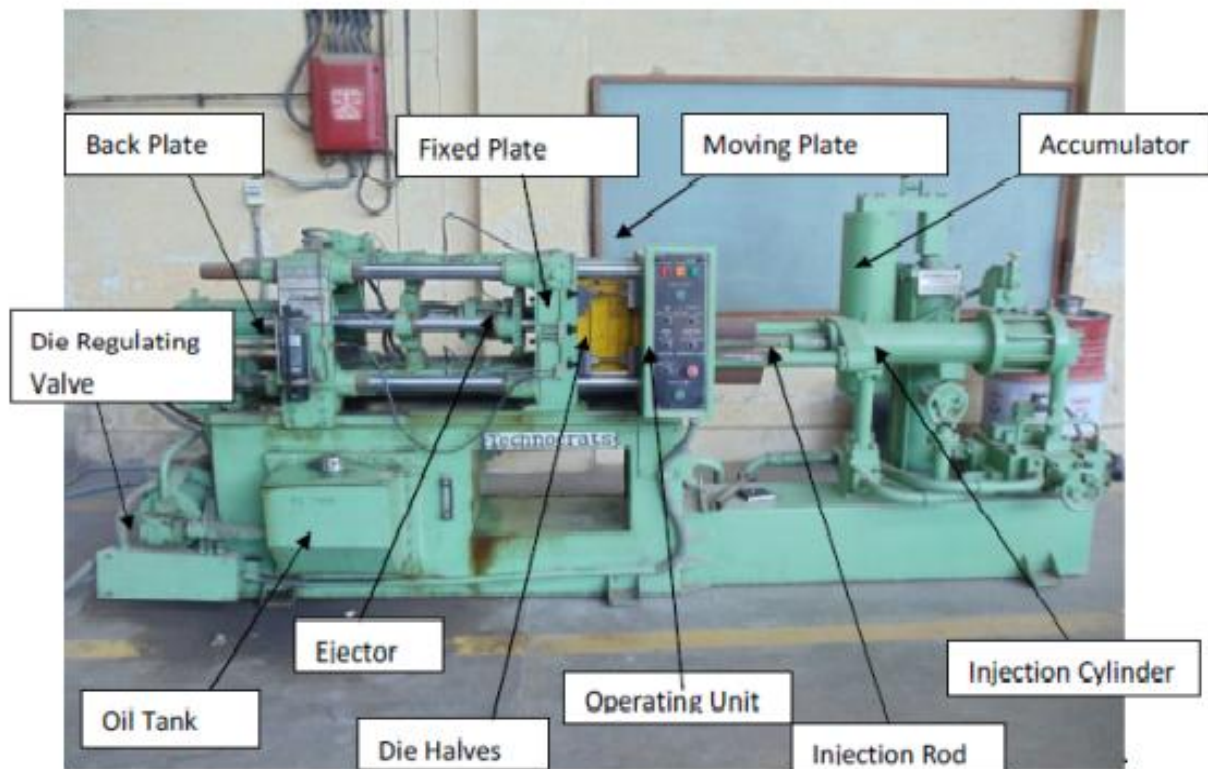


Fig 1.4 Cold chamber die casting machine in workshop at Thapar University, Patiala

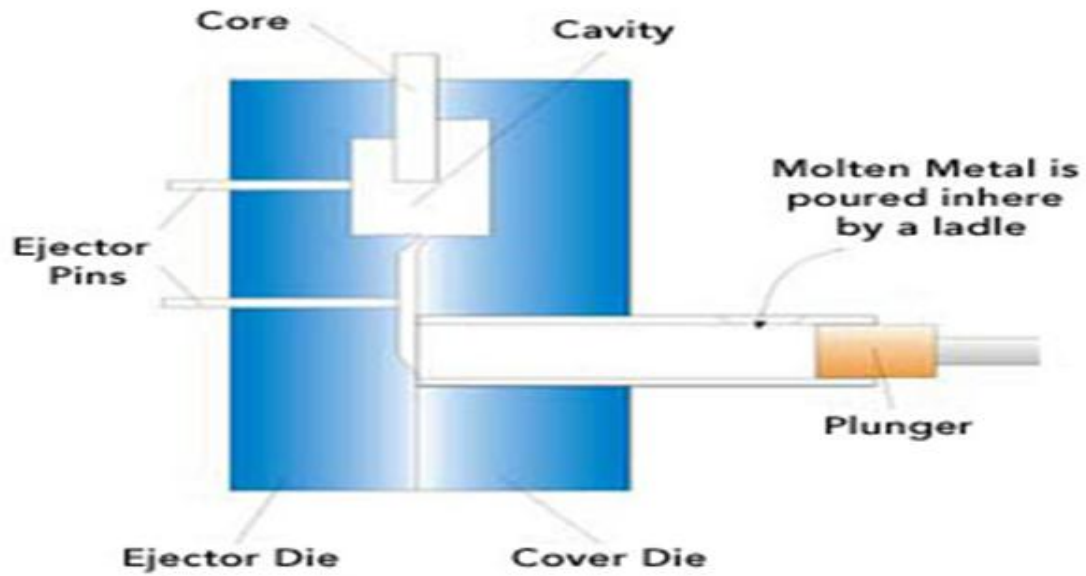


Fig 1.5 Description of cold chamber die casting [4]

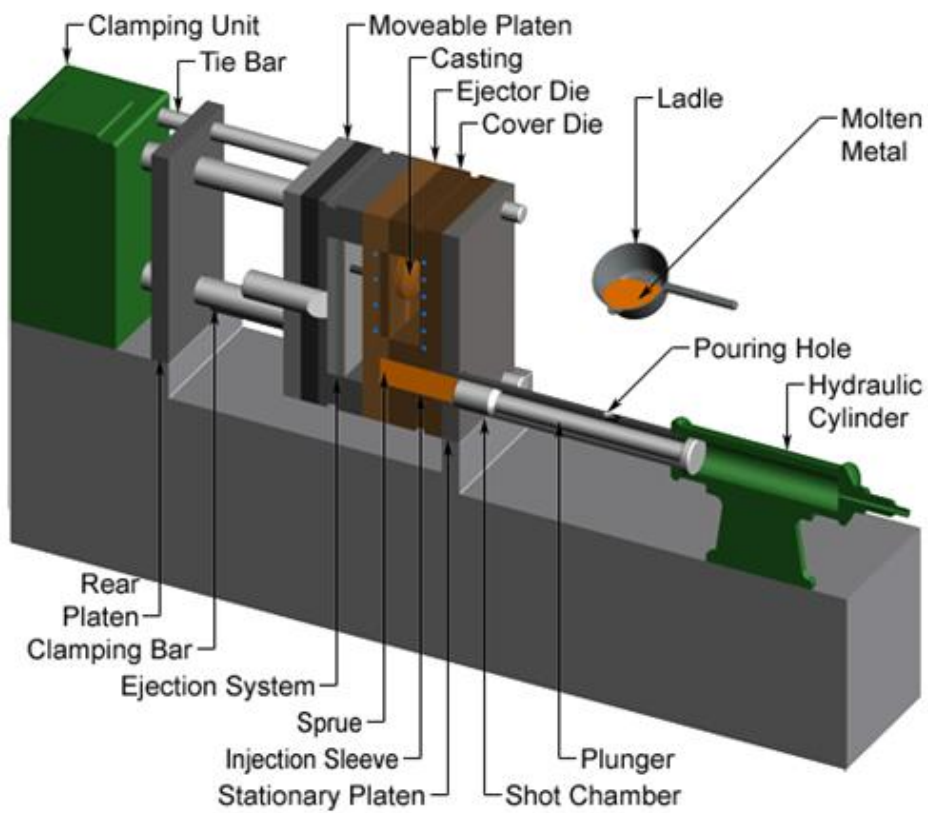


Fig 1.6 Schematic view of cold chamber die casting [4]

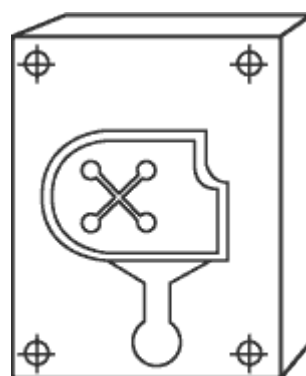
1.7 DIE CONSTRUCTION

Dies or die casting tooling are made of alloy tool steel in at least two sections, one is fixed die half or cover half and the ejector die half, to permit the removal of casting. Modern dies also may have moveable slides, cores or other section to produce holes, threads and other desired shapes in casting. Sprue hole is in the fixed die that allows the molten metal to enter the die and fill the cavity. The fixed die usually contain the runner (passage way) and gates (inlet) that route the molten metal to the die cavity. Dies also includes locking pins to secure the two halves, ejector pins to help remove the cast part and opening for coolant and lubricants. When the die casting machine closes, the two die halves are locked and held together by the machines hydraulic pressure. The surface where the ejector and fixed die halves of the die meet and locked is referred as die parting line. The total projected surface area of the part being cast, measured at the die parting line and the pressure required of the machine to inject metal into the die cavity governs the clamping force of the machine. [1]

Die casting dies have four basic functions.

- Holding molten metal in the shape of the desired casting.
- Provides a mean for molten metal to get to a space where it will be held to the desired shape.
- Remove heat from the molten metal to allow the metal to solidify.
- To provide means for removal of casting.

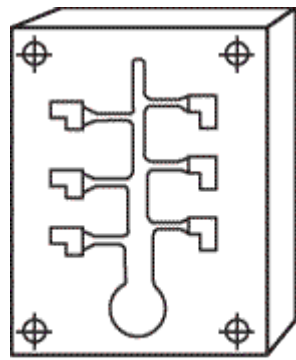
Single cavity to produce one component



Single-Cavity Die

Fig 1.7.1

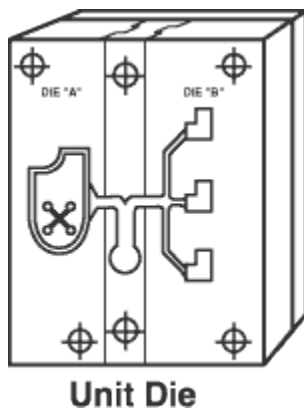
Multiple cavity to produce a number of identical parts[1]



Multiple-Cavity Die

Fig 1.7.2

Unit die to produce different parts at one time[1]



Unit Die

Fig 1.7.3

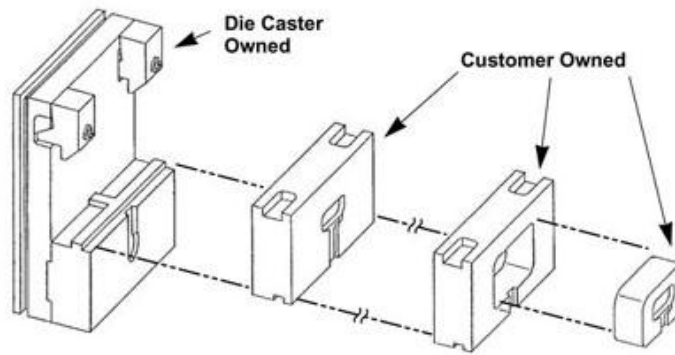


Fig 1.7.4

Combination die to produce several different parts for an assembly.[1]

Die are generally of moveable and stationary type.

In a simple two part die cavities may be created in the fixed member (the whole of impression in fixed platen) or whole of the impression in moving platen. The form of the component sometime makes only one of these positions practically. But in general the die designer must choose that which offers the best product, well finished and at fastest rate.

It is essential that casting shall be retained by ejector half of the die during the opening stroke, and this is the best achieved by making the impression in such a way that the solidified metal tend to deposit on the ejector die and away from the opposite fixed die member.

1.7.1 Die Coating

The function of the die coating is to provide a layer deposited on the walls to control the different condition of metal alloy and for its solidification and to facilitate release of the casting & prolong die life, etc.

The principal functions required of a coating for die casting are:

- Control of the metal flow to ensure that it reaches all parts of the die at a sufficient temperature to prevent the formation of seams, cold laps, etc.
- Control of heat transfer to obtain better solidification and ensure that the castings are properly fed.
- Easy release: since castings are extracted at just below the solidification temperature, Easy release ensures that castings do not come out deformed.
- Good surfaces, and therefore a reduction in finishing costs. Longer die life, therefore Increased productivity and reduced maintenance. These results are directly in line with the characteristics of DYCOTE. (FOSECO, the Logo and DYCOTE are Trade Marks of the Foseco Group of Companies, used under licence).

1.7.2 Coating Application Method

The coating can be applied using several methods:

- Brush
- Spray
- Immersion

For dies the quickest and most suitable method is spray application. Brush application is reserved for plain areas, or for small details that must be coated in a different way from the rest of the die. Immersion application is mainly used for copper alloys, where the coating also has to cool the die.
[6]

1.7.3 Die Paint

Die paint is applied to the pouring basin which provide insulation to the pouring basin. Usually die paint is a combination of calcium silicate (5% to 10%), bentonite (5% to 7%), rest of the material is tracoat.[6]

1.7.4 Spoon Paint

Spoon paint is also applied in the ladle to avoid sticking of metal and it also helps to retain the temperature.[6]

1.7.5 Die Temperature

Dies generally are preheated to a temperature of around 300 to 400 °C, this can be achieved by repeating the trial shorts or can be achieved by heating up the dies by some external source.

1.7.6 Cooling of die

Cooling of the die is necessary (in case of high production) so that temperature of the die may not increase beyond its limit. Moreover cooling with water and/or air decreases its solidification time by taken heat from the molten metal. Cooling may be done on various parts on the die for a particular delay on other parts and cooling time may provide directional solidification. Cooling with water or air is accomplished by air or water solenoid valves. Cooling and delay time is set by providing a timer accordingly to the type of casting. [2]

1.8 Die Casting Alloys

Die casting alloys are normally non-ferrous and there is a large number available with a wide range of physical and mechanical properties covering almost every conceivable application a designer might require. Aluminium and zinc alloys are the most widely used, Followed by magnesium, zinc-aluminium (ZA) alloys, copper, tin and lead. Zinc, lead and tin based alloys are classified as low melting point metals because they turn melt at less than 725°F (385°C). Zinc-aluminium (ZA) alloys have a slightly higher melting range of 800°F to 900°F (426°C to 482°C). Aluminium and magnesium alloys are considered to be moderate melting point alloys, being cast in the 1150°F to 1300°F (621°C to 704°C) range. Copper alloys are considered to be high melting point alloys, over 1650°F (899°C). Low melting point alloys are cast in hot chamber machines. Intermediate and high melting point alloys are cast in cold chamber machines.[1]

1.8.1 CHOOSING THE PROPER ALLOY

Each of the metal alloys available for die casting offers particular advantages for the completed part.[1]

Zinc

The earlier alloy to cast, it offers high ductility, high impact strength, and easily plated. Zinc is economical for small parts, has low melting point and promotes long die life.

Aluminium

Aluminium alloy is light in weight, while processing high dimensional stability for complex shapes and thin walls. Aluminium has good corrosion resistance and mechanical properties, high thermal and electrical conductivity, as well as strength at high temperatures.

Magnesium

The earliest alloy to machine, magnesium has an excellent strength to weight ratio and is lightest alloy commonly die cast.

Copper

This alloy possesses high hardness, high corrosion resistance, and high mechanical properties of alloy cast. It offers excellent wear resistance and dimensional stability, with strength approaching that of steel parts.

Lead and Tin

These alloys offer high density and are capable of producing parts with extremely close dimensions. They are also used for special form of corrosion resistance. Alloys of aluminium are used in die casting more extensively than alloys of any other base metal. The die casting process consumes almost twice as much tonnage of aluminium alloys as all other casting processes combined.[1]

Die casting is especially suited to production of large quantities of relatively small parts. Aluminium die castings weighing up to about 5 kg are common, but castings weighing as much as 50 kg are produced when the high tooling and casting-machine costs are justified.

1.8.2 ALUMINUM ALLOYS

Aluminium die casting alloys are lightweight, offer good corrosion resistance, ease of casting, good mechanical properties and dimensional stability. Although a variety of aluminium alloys can be die cast from primary or recycled metal, most designers select a standard alloy. Special alloys for special applications are available but their use usually involves significant cost premiums.

1.9 Organization of Study

Whole study has been divided into six chapters.

Chapter 1: This chapter gives the introduction of cold chamber die casting process. This chapter also includes the brief description of various types of dies, types of metals/alloys that can be used in die casting process. It also includes the advantages of die casting.

Chapter 2: This chapter includes the literature review of die casting process. The total literature has been categorized into six categories. It also includes the summary of literature and problem formulation.

Chapter 3: This chapter gives the description of design of experiment and experimental design of study, the experimental set up, process parameters levels and orthogonal array for experiment.

Chapter 4: This chapter includes the observation table of the responses in A356 aluminium alloy and also include the analysis of the observed data using ANOVA. It gives us the idea about the significant and non significant input factors. The optimal design is also included in this chapter.

Chapter 5: This chapter includes the observation table of the responses in ADC12 aluminium alloy and also include the analysis of the observed data using ANOVA. It gives us the idea about the significant and non significant input factors. The optimal design is also included in this chapter.

Chapter 6: This chapter includes the comparison of results obtained in A356 and ADC 12 alloy.

Chapter 7: This chapter includes the different microstructure obtained during the phase transformation in A356 and ADC 12 alloy.

Chapter 8: This chapter includes all the observation and results obtained in the study.

2.1 INTRODUCTION

The aim of literature review in this section is as follows.

1. To understand the effect of various process parameters such as pouring temperature, injection pressure, cooling medium to minimize the defect produced in the High Pressure Die Casting.
2. To understand the heat transfer of casting system.
3. To understand the effect of thermal control factor such as interfacial heat transfer, duration and sequence of cooling, cooling media flow rate.
4. To understand the effect of various die coating and lubrication on the quality of casting.
5. To understand the relationship between thermal condition of casting and its microstructure

The literature has been categorized into the following sections:

- a) **Effect Of Process Parameters**
- b) **Thermal Control Factors**
- c) **Effect Of Pressure**
- d) **Effect Of Die Lubricants & Coating**
- e) **Microstructure**
- f) **Micro Porosity**

Effect of Process Parameter

Ching Chih Tai et al.[7] In this paper the main concentration on the the design of runner and gating system is very important factor in deciding the quality of die casting, poor design leads to various defects such as gas porosity, also in this paper integration of numerical simulation in to optimization of runner and gating system for a typical telecommunication part

Lalit Kumar et al.[2] In this thesis report the main effects i.e. thermal characteristics (temperature of the molten metal), injection pressure of the molten metal, type of coating (oil coating, oil + graphite coating, dycot coating), and the type of cooling (air cooling, water

cooling and oil cooling) on density of the material, hardness of the material and the surface roughness of the material in High Pressure Die casting on work material LM6 was studied.

Stephanie Dalquist et al.[8] In this paper the environmental impact of die casting by examining the life cycle of the process was studied . It is possible to consider the environmental impact of the metal forming process as well as the impact of associated processes such as metal preparation and die preparation.

Jiang Zheng et al. [9] This paper demonstrated that it is very essential to optimize the process parameter for good surface quality of the cast, as the optimization of the combination of processes is time-consuming. In this work, an evaluation system for the surface defect of casting has been established to quantify surface defects, and artificial neural network was introduced to generalize the correlation between surface defects and die-casting parameters, such as mold temperature, pouring temperature, and injection velocity.

B. Baradarani et al. [10] Investigated the effect of small addition of zirconium on the hardness, grain size, precipitate type and size of cast A356 aluminium alloy was investigated. The cast alloys were solution treated and then artificially aged for different periods of time. Hardness tests and scanning electron microscope (SEM), energy dispersive X-ray (EDX) and X-ray diffraction (XRD) studies were carried out on the as-cast, as-solutionised and age-hardened specimens. Incoherent, coarse Al₃Zr particles formed in the microstructure during the solidification of the alloy and caused grain refinement in the as-cast structure, the hardness of the alloy to remain constant at high temperatures for long periods of time due to the slow diffusion of Zr in the α -Al

C.G. Kang et al.[11] studied that Semi-solid die casting of Al alloy is suitable for complicated large parts of near net shape without defect and excellent mechanical properties in comparison with conventional casting process. Die design for the product with high quality in semi-solid die casting is required to prevent micro porosity, inflow of oxidized substances, and liquid segregation. Therefore, shape and size of runner, position and size of overflow and air vent, and arrangement of heating line are very important. Micro porosity, unfilled phenomena, turbulent flow, and liquid segregation occurs during semi-solid die casting

P.W. Cleary et al.[12] In this paper the geometric complexity and high fluid speeds involved in HPDC combine to give strongly three-dimensional fluid flow with significant free surface fragmentation and splashing. A Lagrangian simulation technique that is particularly well suited to modelling HPDC is smoothed particle hydrodynamics (SPH). Materials are

approximated by particles that are free to move around rather than by fixed grids, enabling the accurate prediction of fluid flows involving complex free surface motion. Validation of isothermal SPH flow predictions for the casting of a servo piston head using water analogue experiments is presented. Comparison with MAGMA soft predictions provides information of the relative strengths of these two approaches.

Guilherme et al.[13] This paper describes the results obtained in a study performed in partnership between Lab Fund/DEM/PGCEM/UEDESC and the WEG Motors Department of Industrial Engineering for the Quality Control and Aluminium Die Casting. It involves the combination of an experimental DOE (design of experiments) methodology and of a commercial numeric applicative. The influence of the speed injection parameters in the first and second phases and of the upset pressure over the die casting parts quality, in 305 aluminium alloys is investigated. Initially, an experiment planning was performed, where several combinations of the three injection parameters were used, in order to enable the evaluation of their influence on the occurrence of foundry defects, such as porosities and cold shuts.

Peng et al[14] The current paper focuses on the influence of the process parameters on the peak values of the interfacial heat transfer coefficient (IHTC) at metal/die interface during high pressure die casting (HPDC) process. A “step shape” casting and AM50 alloy were used during the experiment. The IHTC was determined by solving the inverse thermal problem based on the measured temperature inside the die.

Chen Zheng et al[15] In this study The effects of processing parameters on the microstructures of the semi-solid A356 Al-alloy slurries were investigated, and the formation mechanism and morphology controlling of the spherical primary α (Al) grains were discussed.

Peng et al. [16] investigated the effects of process parameters, casting thickness, and alloys on the metal-die interfacial heat-transfer coefficient (IHTC) in the HPDC process. Experiment was carried out on a cold-chamber die-casting machine with two casting alloys AM50 and ADC12. A special casting, namely, “step-shape” casting, was used and cast against a H13 steel die. The IHTC was determined using an inverse approach based on the temperature measurements inside the die. Results showed that the IHTC was different at different steps and changes as the solidification of the casting proceeds. Process parameters only influenced the IHTC in its peak value, and for both AM50 and ADC12 alloys. Results also showed that a closer contact between the casting and die could be achieved when the casting alloy is ADC12 instead of AM50, which consequently leads to a higher IHTC.

Horacio Ahuett et al. [17] determined the quality of a die cast product to a great extent by the mechanism of cavity fill. The evolution of this process has received attention both in industry and literature. Because of its effect on the cost of a numerical simulation, the question of whether or not the filling stage takes place under isothermal conditions needs to be addressed. They analyze the process of fill in die casting and presents relations that can be used to predict those conditions under which heat release may be significant. They also introduced and discussed the effects of heat released during fill on the prediction of die casting die deflections

J.D. Zhu et al. [18] In this paper the effect of hydrogen on the casting, transport of hydrogen in liquid by diffusion, and Darcy flow in the mushy zone. For simulating the nucleation of hydrogen pores, the initial pore radius is assumed to be a function of the secondary dendrite arm spacing, whereas pore growth is based on the assumption that hydrogen activity within the pore and the liquid are in equilibrium

S. M. H. Mirbagheri et al.[19] studied a computational model that has been developed for determination of metallostatic pressure on the heat transfer coefficient, resistance of metal–mold interface and solidification time for solving of heat transfer equations. The simulation of interface resistance is based on the zero thickness element (ZTE), using the finite element method (FEM). The pressure gradient has been imposed by an experimental function, which obtained based on experimental data.

Vinod Kumar et al.[20] Investigated that parting line plays an important role which affects not only parting surface generation but also mold structure and cost. Parting line is easy to be determined for some regular product and hard for some irregular products. For irregular and complicated shaped castings FEM based and CAD based methods are evolved. New types of methods called MESHFREE METHODS are getting popularity nowadays for the parting line and parting direction in die casting.

Thermal Control Factors

R.W. Lewis et al.[21] In this paper it is observed that the major objectives of the solidification analysis is to predict the presence of hot spots, i.e., a location in a casting that solidifies last. The primary and most obvious phenomenon during solidification is the transfer of heat from the cooling metal to the mold. The benefit of this correlation is in its ability to

approximate the combined effects of geometry variation, insulation, chills, die coatings, air gap formation, etc. during the numerical simulation and its use in the optimal design of heat transfer at the metal-mold interface.

G. Doura et al.[22] In this paper A heat transfer coefficient gauge has been built, obeying particular rules in order to ensure the relevance and accuracy of the collected information. The gauge body is made out of the same materials as the die casting die (H13). It is equipped with six thermocouples located at different depths in the body and with a sapphire light pipe. The light pipe is linked to an optic fibre, which is connected to a monochromatic pyrometer. Thermocouples and pyrometer measurements are recorded with a data logger. A high pressure die casting die was instrumented with one such gauge.

Guo Zhipeng et al.[23] The present work focused on the determination of the interfacial heat transfer coefficient (IHTC) between metal and die during the high pressure die casting (HPDC) process. Experiments were carried out on an aluminium alloy, ADC12, using “step shape” casting—so-called because of its shape. The IHTC was successfully determined by solving one of the inverse heat problems using the nonlinear estimation method first used by Beck. The calculation results indicated that the IHTC immediately increased after liquid metal was brought into the cavity by the plunger and decreased as the solidification process of the liquid metal proceeded

A. Hamasaiid et al. [24] Found that the main measurements during the trial included velocity and the position of the piston that delivers the metal into the die, the pressure in the die cavity and at the tip of the piston, the alloy surface temperature, and the die temperature at different depths from the surface of the die. The temperature data were analyzed using an inverse method to determine the HTC at the casting die interface during solidification. This article examines in detail the influence of the piston velocity and in-cavity pressure on heat transfer at the casting-die interface during casting and solidification of the magnesium AZ91D alloy

K. Gnanamurthy et al.[25] This paper reviews a range of metals including metal foams and recommends a structured concurrent engineering process between foundry man and 3 designer to realise lightweight cast components

V. Jaiganesh et al[26] In this paper, the variability assessment part of the capability studies of a measuring instrument used in a statistical process control studies in a jobbing foundry has been assessed. The inferences regarding the suitability of the measurement system has

been drawn on the basis of the guidelines proposed by the Automotive Industry Action Group (AIAG).

Guo Zhipeng et al.[27] The present work focused on the determination of the interfacial heat transfer coefficient (IHTC) between metal and die during the high pressure die casting (HPDC) process. Experiments were carried out on an aluminium alloy, ADC12Z, using “step shape” casting—so-called because of its shape. The IHTC was successfully determined by solving one of the inverse heat problems using the nonlinear estimation method first used by Beck. The calculation results indicated that the IHTC immediately increased after liquid metal was brought into the cavity by the plunger and decreased as the solidification process of the liquid metal proceeded

Yongyou Cao et al.[28] In this paper High-pressure die cast B390 alloy was prepared on a 350 ton cold chamber die casting machine. The metal/die interfacial heat transfer coefficient of the alloy was investigated. Considering the filling process, a “finger”-shaped casting was designed for the experiments. This casting consisted of five plates with different thicknesses (0.05 inch or 1.27 mm to 0.25 inch or 6.35 mm) as well as individual ingates and overflows. Experiments under various operation conditions were conducted, and temperatures were measured at various specific locations inside the die.

Persson et al. [29] experimentally evaluated the temperature variations in the surface layer of hot work tool steel during actual brass die casting. A special method was developed to measure the temperature in the surface layer of the mould at different depths. Untreated, borided, and physical vapour deposition (PVD) coated (CrN) tools were included. Temperature profiles in the surface layer of the mould were recorded and details of the thermal cycling were obtained. Starting with a tool of room temperature, the tool temperature range averages during the initial 20 casting events. Simultaneously, within a surface layer of about 2mm thickness, the maximum stress is reduced to a constant level. Based on the temperature profiles, the maximum surface temperature of the mould and the thickness of the tool surface layer within which fatigue damage can occur were estimated to about 826 °C and 1.5 mm, respectively. This limited thickness results from the decrease in temperature range and, consequently, stress from the tool surface and inwards. Finally, no notable influence of the investigated surface engineering on the thermal conditions was found.

Patrzalek et al.[30] investigated feedback and modelling on high pressure die casting processes to investigate them as a whole. The research is specifically aimed at high pressure

die casting processes but analogous processes (such as injection molding and thixomoulding) that used cooling channels to stabilize or balance die temperature profiles could also benefit from this research. A key element of this research program was the development and construction of a small, prototype casting system that could be used to explore the validity of any developed, thermal models.

H. Yamagataa et al. [31] investigated the effect of average cooling rates on the microstructure of the hypereutectic Al–20% Si alloy, using the novel Universal Metallurgical Simulator and Analyzer Platform. The quantitative measurements of the primary Si size and the Secondary Dendrite Arm Spacing of the non-equilibrium α -aluminum as a function of the cooling rates was performed for the laboratory test samples. This research was carried out in order to analyze the microstructure of the high pressure die cast cylinder block and to understand its complex solidification process.. Research revealed that some primary Si particles nucleated from the beginning of the melt pouring into the shot sleeve prior to the injection process while the α -aluminum dendrites and eutectic Si nucleated in the die cavity. Therefore, it was proven that the injected hypereutectic Al–20% Si liquid melt had solid primary Si particles.

Matthew Patrzalek et al.[32] The research is specifically aimed at high pressure die casting processes but analogous processes (such as injection moulding and thixomoulding) that used cooling channels to stabilise or balance die temperature profiles could also benefit from this research. A key element of this research program was the development and construction of a small, prototype casting system that could be used to explore the validity of any developed, thermal models.

Horacio Ahuett-Garza et al.[33] In this paper the process of fill in die casting and presents relations that can be used to predict those conditions under which heat release may be significant. In order to put the relevance of fill conditions in context, the effects of heat released during fill on the prediction of die casting die deflections are introduced and discussed

Henry hu et al.[34] In high pressure die casting processes, proper temperature control of a die yields high casting production rates and superior quality components. In order to better understand the effect of water flow rates on die temperature, a computer-based data acquisition and control system (DACs) has been developed and employed to monitor and

record data of internal water flow rates and local temperatures of an industrialized die insert installed in a die casting process simulator

Giulio Timelli et al.[35] In this paper The influence of solution heat treatment time and temperature on the microstructure and mechanical properties and the mode of fracture of a high-pressure die-cast AlSi7MgMn alloy is reported. Metallographic and image analysis techniques have been used to quantitatively examine the microstructural changes occurring during solution heat treatment. A solution heat treatment of 15 minutes at 475 °C, or even more at 525 °C, is sufficient to spheroidize the eutectic Si, as well as coarsen and increase the interparticle distance of the eutectic Si. Increasing the solution temperature from 475 °C to 525 °C improves the mechanical properties.

Emma Sjolander et al.[36] In this paper It is shown that the changes occurring during solution treatment are relatively well understood, and that the equilibrium phase diagram can be used to predict the stability of phases at the solution treatment temperature. The influence of quench rate and natural ageing on subsequent artificial ageing needs to be studied further, but some conclusions can be drawn. These include: (1) An increase in quench rate above 4 °C/s gives a small increase in yield strength after ageing, while the concomitant influence on elongation is more complicated and depends on the alloy. (2) Natural ageing is shown to have a large influence on subsequent artificial ageing response of Al–Si–Mg alloys, while there is a significant lack of knowledge for Cu-containing alloys.

H.Moller et al.[37] Investigated that the automotive industry has many possible applications for semi-solid metal (SSM)–high-pressure die casting (HPDC) parts, the newly developed heat treatment cycles, as well as the traditional heat treatment cycles, were applied to A356 brake callipers cast using a LK DCC630 HPDC machine. Vickers hardness measurements at a cross section of the brake callipers were performed, indicating that similar values can be obtained when using the significantly shorter heat treatment cycles. Finally, the typical tensile properties that can be obtained for SSM-HPDC A356 brake callipers are compared with those manufactured by gravity die casting. Results indicate that the differences in microstructures (globular or dendritic) do not have a noteworthy effect on the heat treatment response.

Hiroshi horikawa et al.[38] Observed that thermal conductivity of aluminium alloy is improved by the addition of silicon where said invention is characterised by an aluminium alloy casting material with excellent thermal conductivity comprising 5-10% mass of silicon, 0.1-0.5% by mass of magnesium and the remainder comprising aluminium and inevitable impurities and where on aging treatment is performed

Effect of pressure

C.G. Kang et al.[39] Studied that die design for the product with high quality in semi-solid die casting is required to prevent micro porosity, inflow of oxidized substances, and liquid segregation. Therefore, shape and size of runner, position and size of overflow and air vent, and arrangement of heating line are very important. Micro porosity, unfilled phenomena, turbulent flow, and liquid segregation occur during semi-solid die casting. To prevent these phenomena, defect analysis of product according to the change of injection velocity is carried out and optimal injection velocity for high quality product is proposed and simulated

Rosendo Zamora et al.[40] In this paper an experimental study of the optimum maximum plunger speed in the slow phase of a high-pressure die casting machine with horizontal cold chamber is presented. A special apparatus that uses a photoelectric sensor to determine the instant at which the working fluid reaches the runner was developed and installed in the injection chamber. The measured volumes of air remaining in the chamber at this instant for various maximum plunger speeds were compared with those predicted by a three dimensional numerical model based on a finite element formulation and the volume of fluid method for treating the free surface

Effect of Die Lubricants & Coating

R. Kimura et al.[41] Investigated that the insulating ability of powder lubricant is higher than that of conventional oil-soluble or water-soluble lubricants. This will be effective to prevent the formation of scattered chill structure. Influence of the components and composition of powder lubricants on insulating ability and lubricating ability were investigated. Thus, it was found that the lubricant contains 40 mass% or more of wax that will be appropriate for die lubricant. On the other hand, the high insulating lubricant contains 25 mass% of wax that will be suitable for sleeve lubricant

James L. Graff .[42] This paper describes our results on how different spraying parameters (dilution length, spray angle, air pressure, liquid pressure, etc.) and die lubricant compositions affect the thermal balance of die casting dies based upon the heat fluxes and heat transfer coefficients measured.

C. Mitterer et al.[43] investigated in die casting, tools are exposed to erosion, corrosion and soldering due to the frequent contact of the tool surface to the casting alloy, due to heat checking and gross cracking ,due to thermal fatigue and oxidation due to high pouring

temperatures. The gradual destruction of die surfaces during service decreases casting piece quality and limits die lifetime. Hard coatings based on nitrides or carbides of transition metals may protect the steel surface from erosion and soldering of aluminium and improve the resistance against thermal cracking. Thus, they may replace the thick oxide-based die coatings nowadays used in foundries hard coating based on TiN have been proven to increase the life time of aluminium die-casting dies by several hundreds of percent due to a reduction of erosion, corrosion and soldering processes and due to an increase of the thermal fatigue limit .In addition for these coatings the pouring temperatures may not be sufficient to form a protective oxide layer during service Finally, we have been able to show that the PACVD technology is very well suited to coating large and heavy dies of complex shape with a uniform coating thickness and homogeneity

Yucong Wang et al.[44] demonstrated the applications of PVD coatings to extend die-casting die life, mainly by reducing molten metal corrosion and erosion to the die. However, die steci heat checking (or thermal cycling induced cracking) resistance is affected significantly by the PVD coatings. This paper presents the results of a systematic study involving three H series and two managing hot work tool steels with and without TiN, TiAlN and CrN PVD coatings, in terms of heat checking resistance, hardness and impact toughness changes, as well as molten aluminium corrosion resistance. TiN, TiAlN, and CrN PVD coatings can provide significant corrosion and erosion resistance to molten aluminium.

D. Heim et al.[45] studied that advantage of providing hard coating and The coatings are also expected to prevent the aluminium from soldering onto the tool surface. Lifetime increases in cores and moulds are reported with coatings deposited by CVD, PVD and PACVD. PACVD offers the possibility to coat the tools at temperatures below their tempering temperature (in contrast to CVD), and there is no need to move the tools during the process or to adjust the target arrangement of the tools to coat uniformly as in PVD.

A. Lousa et al.[46] In this paper Chromium nitride coatings are known to give reasonable solutions to the requirements of semisolid forming tools and of pressure die-casting of low-melting-point metals and alloys. These hard coatings have good mechanical behaviour when working at high temperatures. They show enhanced hardness and good wear and corrosion resistance, as well as reduced adhesion to the molten or semisolid metal. We have developed a related hard coating based on multilayered stacking of CrN and Cr metal layers with bilayer thickness down to 22 nm

Microstructure

M.S. Dargusch et al.[47] In this paper we have studied that effect of silicon content on the Al-Si alloy. Increasing the silicon content above the eutectic level results in an increase in the number of coarse faceted Mg₂Si particles in the microstructure. Creep rates at 100 hours were found to decrease with increasing silicon content in AS-type alloys

H. Yamagataa et al.[48] Investigated the effect of average cooling rate on the microstructure of AL-SI alloy, and the result was investigated by using the novel Universal Metallurgical Simulator and Analyzer Platform. This research was carried out in order to analyze the microstructure of the high pressure die cast cylinder block and to understand its complex Solidification process. The Equivalent Diameter of the primary Si decreased from 89.7±17.3 to 16.5±3.8_μm and the Secondary Dendrite Arm Spacing from 22.1±5.9 to 5.1±0.8_μm with an increase in the cooling rate from 4.9 to 82.9 °C/s.

Anthony E. Hughes et al.[49] In this paper The broad range of microstructural characteristics associated with the high strength Al alloys have been examined in detail. Perhaps the most attention has been paid to the AA2024-T4 legacy alloy where the microstructure is complicated by the broad compositional variation of second phases, particularly the constituent particles. The role of these features on corrosion has been described and areas where the role of the microstructure is still not clearly understood have been identified and discussed

S. Otarawanna et al.[50] In this paper it was found that the intensification pressure(IP)play a major role in defect prevention, At high IP, defect bands form in the gate region and appear to be assisting the feeding during the intensification stage.

H. Moller et al.[51] As the automotive industry has many possible applications for semi-solid metal (SSM)–high-pressure die casting (HPDC) parts, the newly developed heat treatment cycles, as well as the traditional heat treatment cycles, were applied to A356 brake Callipers cast using a LK DCC630 HPDC machine; Results indicate that the differences in microstructures (globular or dendritic) do not have a noteworthy effect on the heat treatment response. This implies that the short heat treatment cycles originally developed for globular SSM-HPDC A356 castings can be successfully applied to dendritic liquid A356 castings too.

Nonjabuliso et al.[52] The objective of this work was to determine the time for sufficient dissolution of the eutectic phase in this Al-Zn-Mg-Cu alloy. Solution heat treatment was carried out at 473°C for various time periods and the samples were quenched in water. The

samples were then artificially aged at 120°C for 24 hrs. A component of the eutectic was observed to have dissolved and another component transformed to new intermetallic phases for all solution heat treatment times at 473°C.

Micro porosity

J.A. Taylor et al.[53] In this paper, This work identifies the role that iron plays in porosity formation and reports a threefold effect in an Al-5 pct Si-1 pct Cu-0.5 pct Mg alloy. In addition to a detailed analysis of casting porosity profiles, metallographic and thermal studies also point to inadequacies in the existing theories regarding the role of iron and suggest that a new theory is required to understand the observed behaviour.

A.S. Sabau et al.[54] The results show that the effect of micro porosity on the interdendritic fluid flow cannot be neglected. The predictions of porosity profiles are validated by comparison with independent experimental measurements by other researchers on aluminum A356 alloy test castings designed to capture a variety of solidification conditions.

J.D. Zhu et al.[55] Developed a numerical model for predicting micro porosity formation in aluminum castings , which describes the redistribution of hydrogen between solid and liquid phases, the transport of hydrogen in liquid by diffusion, and Darcy flow in the mushy zone. For simulating the nucleation of hydrogen pores, the initial pore radius is assumed to be a function of the secondary dendrite arm spacing, whereas pore growth is based on the assumption that hydrogen activity within the pore and the liquid are in equilibrium. One of the key features of the model is that it uses a two-stage approach for porosity prediction.

V.D. Tsoukalas et al. [56] In this investigation, an effective approach based on multivariable linear regression (MVLRL) and genetic algorithm (GA) methods has been developed to determine the optimum conditions leading to minimum in AlSi9Cu3 aluminium alloy die castings. Experiments were conducted by varying holding furnace temperature, die temperature, plunger velocities in the first and second stage, and multiplied pressure in the third stage using L27 orthogonal array of Taguchi method. The experimental results from the orthogonal array were used as the training data for the MVLRL model to map the relationship between process parameters and porosity formation of the die cast parts

Yoshihiko hangai et al.[57] In this paper The non-destructive and three-dimensional quantitative evaluation of porosity in aluminium alloy die castings is proposed to identify

whether the predominant cause of pore formation is shrinkage or entrapped gas. The validity of this method of evaluation was shown by comparing two different regions with different ratios of pores formed by shrinkage and gas. It was shown that the proposed evaluation can be used as a quantitative indication of porosity.

Thoguluva et al.[58] In this paper, different types of casting dies are discussed. Parts produced by die-casting can be sharply defined with smooth or textured surfaces and are suitable for a wide variety of attractive and serviceable finishes. Die-casters can produce castings in a variety of shapes, sizes and wall thicknesses that are light-weight, strong, durable and dimensionally precise. Die-casting process has been well-researched and systematically quantified in terms of thermodynamics, heat transfer and fluid flow. Design factors causing thermal fatigue should be identified to extend the die life.

Kevin morasch[59] In this paper a restoration process for restoring surface porosity defect on a component surface is examined. The restoration surface is subsequently sprayed with a restoration spray to restore the surface porosity defects. The component surface then finishes to create a final component substantially free of surface porosity.

Guo Zhi-peng et al. [60] focuses on the determination of the interfacial heat transfer coefficient (IHTC) at the metal–die interface in the high pressure die casting (HPDC) process. Experiment was conducted and a “step shape” casting was used to cast a magnesium alloy AM50 against a H13 steel die. Based on the temperature measurements inside the die, IHTC was determined by applying an inverse approach. The influences of the step thickness and process parameters on the IHTC were investigated. Results show that the shape of IHTC profiles is different at different steps and the duration for IHTC to maintain a higher value grows as the step thickness increases. The influence of process parameters is mainly on the IHTC peak value. For thinner steps, a higher fast shot velocity leads to a higher IHTC peak value. But for thicker steps such as Step 5, the casting pressure shows a more prominent influence on the IHTC peak value. Also, at these thicker steps a lower initial die surface temperature always leads to a higher IHTC peak value.

Zhipeng et al. [61] focused on the determination of the interfacial heat transfer coefficient (IHTC) between metal and die during the high pressure die casting (HPDC) process. Experiments were carried out on an aluminum alloy, AM50 AGAINST A H13 STEEL, using “step shape” casting—so-called because of its shape. The IHTC was successfully determined by solving one of the inverse heat problems using the nonlinear estimation method first used by Beck. The calculation results indicated that the IHTC immediately increased after liquid

metal was brought into the cavity by the plunger and decreased as the solidification process of the liquid metal proceeded. The liquid metal eventually solidified completely, a condition when the IHTC tended to be stable. Casting thickness played an important role in affecting the IHTC between the metal and die not only in terms of its value but also in terms of its change tendency. Also, under the test conditions, different change tendencies of the metal solid fraction were found between castings with different thicknesses and the die.

W. D. Griffiths et al. [62] investigated the effect of contraction and distortion of a casting during cooling within a mould; it can force their respective surfaces together, with the associated increased interfacial pressure resulting in increased interfacial heat transfer. The heat transfer mechanisms between the casting and the die surfaces were evaluated to produce a simple model of interfacial heat transfer which included conduction through the points of actual contact, in parallel with conduction through the interfacial gas between the points of actual contact, both mechanisms being in series with the heat transfer by conduction through the die coating. The magnitude of the thermal resistances for the different heat transfer paths evaluated in the model showed that the heat transfer through the points of actual contact, and through the interfacial gas, had similar thermal resistances, and were approximately four times greater than the thermal resistance associated with the die coating itself

R. K. Nayak et al. [63] described the main difficulties associated with numerical simulation of solidification processes is the lack of thermo-physical properties and/or boundary conditions. Temperature distributions in investment castings and shells are of great influence on the quality of investment castings. To improve the simulation prediction of casting defects, interface heat transfer coefficient (IHTC) between casting and fused silica shell need to be optimised. Simulation and experimental analysis have been carried out using the optimised IHTC for an austenitic stainless steel investment casting component. With the correct choice of the initial IHTC value, a thermal simulation is sufficient to accurately predict the cooling curves without resorting to the use of a fully coupled thermo mechanical simulation. In addition, it is observed that use of optimised IHTC is quite helpful to predict the defects in the casting accurately and it helps to design the gating system for investment casting process.

2.2 Summary of Literature

A lot of work has been done in the field of high pressure cold chamber die casting process in different type of process parameters, different type of thermal control factors such as Interfacial heat transfer coefficient, type of cooling, heat treatment, cooling circuit duration and flow rate. Alloy composition and its condition influence the wear rate .With increase in temperature hardness and wear rate resistance also increases.Heat treatment of all aluminium alloy improved abrasive wear resistance. Increase in pressure in HPDC reduces the density of aluminium alloy. Effect of process parameters helps in predicting the micro porosity at various stage of casting. Die coating and lubrication maintain a thermal balance with in the part and helps in improving the mechanical properties of aluminium alloy. The effect of average cooling rate on the microstructure of AL-SI alloy, and the result Creep rates at 100 hours were found to be decreased. With increasing silicon content in AS-type alloys and the equivalent diameter of the primary Si decreased from the Secondary Dendrite Arm Spacing with an increase in the cooling rate.

2.3 PROBLEM FORMULATION

Based on the literature survey and the subsequent analysis of gaps the present work aims to investigate the effect of various parameters in a High Pressure Die Casting Process on the properties of aluminium alloy and optimize the parameters using multi-response optimization methodology. The experiments have been conducted using aluminium alloys A356 and ADC12. The process parameters varied were the thermal characteristics (temperature of the molten metal), the injection pressure of molten metal, Coating thickness and solidification rate. The properties and quality of die cast components are directly related to the microstructure of die cast component. This research study has been carried out on the High Pressure Die Casting Machine available at S.L Casting &Allied Industries, Focal point, Patiala

2.4 OBJECTIVES

- To evaluate the effect of process parameter (pouring temperature, injection pressure, coating thickness and solidification rate) on the properties of the cast metal.
- To evaluate the significant interactions between the above factors.
- To analyze the machined surface for microstructure and hardness to study the change in material properties as a result of the experimentation.

This has been done by factorial analysis of variance. The factor analysis parameterization approach has been used to study the effect of various factors at appropriate levels. Multiple

regression models have been used to determine the best-fit relationship between the response and the model parameter. After studying the effect of parameters using a parametric approach a study on material properties and effect of process parameters has been completed.

2.5 WORK PLAN

Following activity have been carried out to complete the project

1. Preparatory work
 - (a) Selection of die casting alloy.
 - (b) Procurement of material to make the required alloy and preparation of samples.
 - (c) The samples will be cut by hand hack saw and machined on the grinding machine at GRIMT, Radaur(Haryana).
2. After finalization of the significant process parameters detailed experiments were carried out with all possible variations, included in the study.
3. Measurements were taken for each process variable and results were analyzed using ANOVA to arrive at a method which satisfies the requirement of the cast product.
4. Study of material properties.
5. Multi response optimisation was done using MRSN technique

3.1 INTRODUCTION

The effect of various process parameters was studied after the machining of die cast parts. Different Parameters (viz. temperature of the molten metal, injection pressure of the molten metal, type of coating, and the type of cooling) was studied using parameterization approach developed by Taguchi.[66]

The full factorial design is referred as the technique of defining and investigating all possible conditions in an experiment involving multiple factors while the fractional factorial design investigates only a fraction of all the combinations. Although these approaches are widely used, they have certain limitations: they are inefficient in time and cost when the number of the variables is large; they require strict mathematical treatment in the design of the experiment and in the analysis of results; the same experiment may have different designs thus produce different results; further, determination of contribution of each factors is normally not permitted in this kind of design. The Taguchi method has been proposed to overcome these limitations by simplifying and standardizing the fractional factorial design. The methodology involves identification of controllable and uncontrollable parameters and the establishment of a series of experiments to find out the optimum combination of the parameters which has greatest influence on the performance and the least variation from the target of the design [66].

3.2 ESTABLISHMENT OF OBJECTIVE FUNCTION

The objective of the study is to evaluate the main effects i.e. thermal characteristics (temperature of the molten metal), injection pressure of the molten metal, type of coating (oil coating, oil + graphite coating, dycot coating), and the type of cooling (air cooling, water cooling and oil cooling) on work piece material (A356 & ADC12) aluminium alloy, density of the material, hardness of the material and the surface roughness of the material.

3.3 SELECTION OF FACTORS

The determination of which factors to investigate depends on the responses of interest. The factors that are believed to affect the responses were identified using cause and effect

analysis, and brainstorming. The lists of factors studied with their levels are given in the Table 3.1

Table 3.1(a): Factors of interest and their respective levels for work material A356

FACTOR	Level-1	Level-2	Level-3
Pouring temperature of the molten metal (A)	770	790	730
Injection pressure of the molten metal kg/cm ² (B)	100	90	120
Type of coating (C)	Oil coating	Oil + Graphite Coating	Dycot coating
Type of cooling (D)	Air cooling	Water cooling	Oil cooling

Table 3.1(b): Factors of interest and their respective levels for work material ADC12

FACTOR	Level-1	Level-2	Level-3
Pouring temperature of the molten metal (A)	770	790	730
Injection pressure of the molten metal kg/cm ² (B)	100	90	120
Type of coating (C)	Oil coating	Oil + Graphite Coating	Dycot coating
Type of cooling (D)	Air cooling	Water cooling	Oil cooling

3.4 DEGREE OF FREEDOM (dof)

The number of factors and their interactions and level for factors determine the total degree of freedom required for the entire experimentation. Table 3.2 gives the degrees of freedom of each factor along with total degrees for the freedom of experiment. The degree of freedom for each factor is given by the number of levels minus one.

dof for each factor : k-1

Where k is the number of level for each factor

Table 3.2: Degree of freedom

Factor	A	B	C	D	Total
Degree of Freedom	2	2	2	2	8

3.5 ORTHOGONAL ARRAY

Orthogonal array (OA) plays a critical part in achieving the high efficiency of the Taguchi method. OA is derived from factorial design of experiment by a series of very sophisticated mathematical algorithms including combinatorial, finite fields, geometry and error-correcting codes. The algorithms ensure that the OA to be constructed in a statistically independent manner that each level has an equal number of occurrences within each column; and for each level within one column, each level within any other column will occur an equal number of times as well. Then, the columns are called orthogonal to each other. OA is available with a variety of factors and levels in the Taguchi method. Since each column is orthogonal to the others, if the results associated with one level of a specific factor are much different at another level, it is because changing that factor from one level to the next has strong impact on the quality characteristic being measured.

The selection of orthogonal array depends on:

- The number of factors and interactions of interest
- The number of levels for the factors of interest

Taguchi's orthogonal arrays are experimental designs that usually require only a fraction of the full factorial combinations. The arrays are designed to handle as many factors as possible in a certain number of runs compared to those dictated by full factorial design. The columns of the arrays are balanced and orthogonal. This means that in each pair of columns, all factor combinations occur same number of times. Orthogonal designs allow estimating the effect of each factor on the response independently of all other factors.

Once the degrees of freedom are known, the next step, selecting the orthogonal array (OA) is easy. The number of treatment conditions is equal to the number of rows in the orthogonal array and it must be equal to or greater than the degrees of freedom. Once the appropriate orthogonal array has been selected, the factors can be assigned to the various columns. [66]

To select an appropriate orthogonal array for experiments, the total degrees of freedom must be computed. The degrees of freedom are defined as the number of comparisons between process parameters that must be made to determine which level is better and, specifically, how much better it is. For example, a two-level process parameter counts for one degree of freedom. The degrees of freedom associated with interaction between two process parameters are given by the product of the degrees of freedom for the two process parameters. In the present study, the interaction between the die casting parameters is neglected. Therefore, there are eight degrees of freedom owing to the four sets of input parameters in the cold chamber die casting process. Once the degrees of freedom are known, the next step is to select an appropriate orthogonal array to fit the specific task. The degrees of freedom for the orthogonal array should be greater than, or at least equal to, those for the process parameters. In this study, an L9 orthogonal array with five columns and nine rows was used. This array has eight degrees of freedom and it can handle four process parameters. Each die casting parameter was assigned to a column and nine die casting parameter combinations were tested. Therefore, only nine experiments are required to study the entire casting parameter space using the L9 orthogonal array. The experimental layout for the casting parameters using the L9 orthogonal array is shown in Table 3.3.

Table 3.3(a): Orthogonal Array L9 For material A356

Trial No.	Pouring temp. °C	Injection pressure kg/cm ²	Coating type	Cooling Medium
1	770	100	Oil Coating	Air Cooling
2	770	90	Oil+ graphite	Water Coolig
3	770	120	Dycot	Oil Cooling
4	790	100	Oil+ graphite	Oil Cooling
5	790	90	Dycot	Air Cooling
6	790	120	Oil Coating	Water Coolig
7	730	100	Dycot	Water Coolig
8	730	90	Oil Coating	Oil Cooling
9	730	120	Oil+ graphite	Air Cooling

Table 3.3(b): Orthogonal Array L9 For material ADC12

Trial No.	Pouring temp. °C	Injection pressure kg/cm ²	Coating type	Cooling Medium
1	770	100	Oil Coating	Air Cooling
2	770	90	Oil+ graphite	Water Coolig
3	770	120	Dycot	Oil Cooling
4	790	100	Oil+ graphite	Oil Cooling
5	790	90	Dycot	Air Cooling
6	790	120	Oil Coating	Water Coolig
7	730	100	Dycot	Water Coolig
8	730	90	Oil Coating	Oil Cooling
9	730	120	Oil+ graphite	Air Cooling

3.6 DESCRIPTION OF DIE CASTING MACHINE

The experiments have been conducted on Horizontal Cold Chamber Pressure Die Casting Machine of Technocrats made model TDC- 120 available at S.L Casting and Allied Industry,D-217,Focal point , Patiala. Die casting machine used for the experiments is same by look but differ by capacity as available in Thapar University, Patiala shown in the figure 3.1 and figure 3.2 The main parts of the machine are control box panel, fixed plate, moving plate, back plate, accumulator, injection cylinder, injection plunger, ejector system, oil tank, die regulating valve, pressure regulating valve. The injection pressure can be varied through the pressure regulating valve. Control is provided on the machine for die opening time, closing time and the ejector time for the ejection of cast product. The machine can be operated in manual as well as in automatic mode. The main specifications of the machine are given in table 3.4.

Table 3.4: Specification of Die Casting Machine

Locking force	120 tones
Injection force	20 tons
Hydraulic ejection force	9 tons
Die mounting plates	650 x 650 (mm)
Space between tie bars	428 x 428 (mm)
Max. die height	450 mm
Min. die height	200 mm
Tie bar diameter	72 mm
Die opening stroke	300 mm
Injection stroke	275 mm
Ejection stroke	75 mm
Distance between centre and bottom	120 mm

injection	
Electric motor capacity	11 kw
Working pressure	100/35 kg/cm ²
Hydraulic pump (vane type)	30/60 ltr./min
Oil tank capacity	350 ltr.
Machine weight	4.6 tons
Shot capacity (Max. Injection Weight)	1500 gm

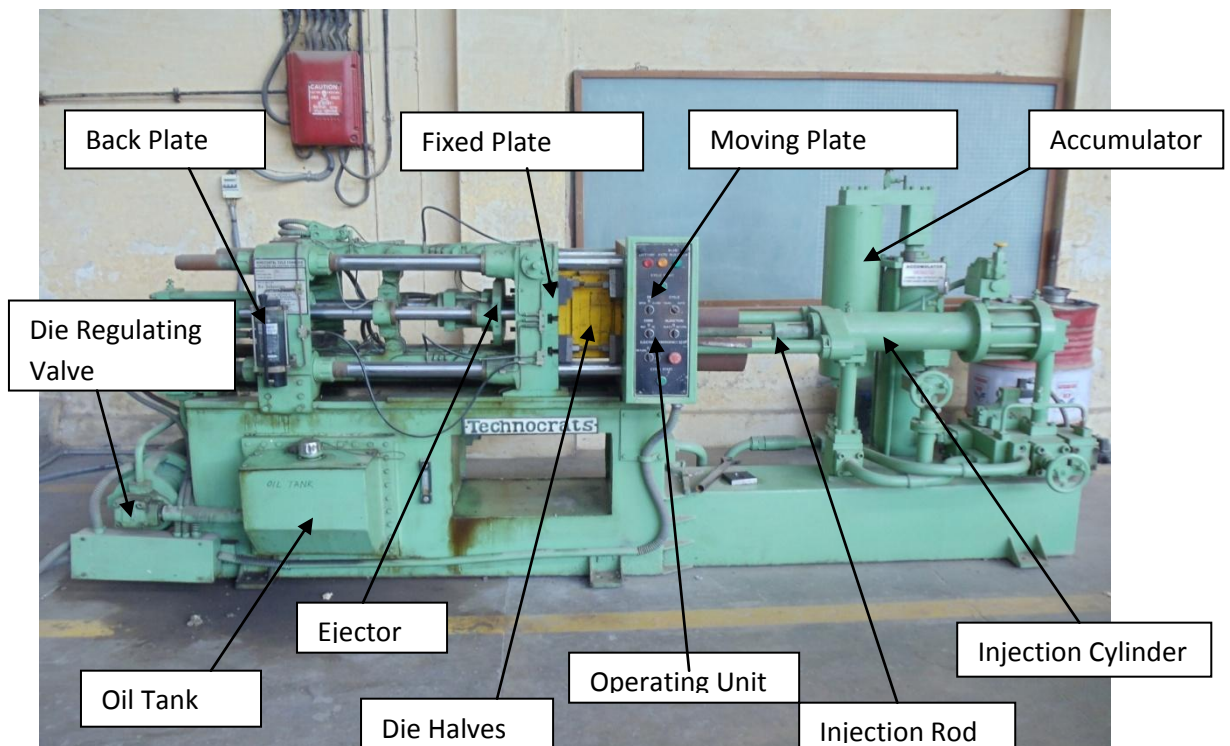


Figure 3.1 High Pressure Cold Chamber Die Casting Machine (80 Tons) at Thapar University

3.6.1 Operating mode

- Manual Mode: In this mode the machine is not under the casting programme. Direction of operations depends upon the decision of operator.
- Automatic Mode: Machines operations can be programmed e.g. die opening time, die closing time; casting ejection time can be controlled.

- Stop Button: The machine stops when stop button is pushed.

3.6.2 Display indication

- Pressure gauge: the pressure gauges are used to display the pressure of injection of molten metal and to display the pressure of the accumulator.



Figure 3.2 High Pressure Cold Chamber Die Casting Machine (120 Tons) at S.L Casting & Allied Industry, D-217, Focal Point, Patiala

3.7 DESCRIPTION OF PIT FURNACE

The metal was melted in a Pit type furnace the maximum temperature that can be achieved is up to 1100°C . The Pit furnace used for the experiments available at S.L Casting & Allied Industry, Patiala is (shown in the Figure 3.3) .The melting temperature can be varied and measured by pyrometer indicator.



Pit Furnace

Figure 3.3: Pit Furnace

3.8 EXPERIMENTAL SET UP

The machine was operated at standard operating conditions except the injection pressure which was varied at 100,90,120 kg/cm² for A356 and ADC12 work material, as per experimental design. The other factors which were varied as per experimental design are the coating (oil coating, oil + graphite coating and dycot), the cooling medium of the cast product (air cooled, water cooled, oil cooled), the pouring temperature of the molten metal for A356 and ADC 12 work material are (770⁰ C, 790⁰ C, 730⁰ C,) . The metal was poured in the injection chamber in the injection sleeve with the aid of pouring spoon. L9 orthogonal was used for conducting the experiments. All the trial conditions using L9 orthogonal array are listed in Table 3.1. All the experiments were conducted on HPDC at S.L Casting and Allied Industry, Focal Point, Patiala.

The Pit furnace was used for melting both the material, ie A356 and ADC12 alloy separately at different temperature conditions as per experimental design. The temperature was measured by manual pyrometer indicator.

3.8.1 Dies for Experiment

Dies used for the casting of the final product i.e. wire clamp were made of alloy tool steel in two sections, one was fixed die half and the other was ejector die half, to permit the removal of casting. Dies included locking pins to secure the two halves, ejector pins to help remove the cast part.

3.9 MEASURING AND TEST EQUIPMENT USED

Rockwell hardness and surface roughness tests were conducted on all the samples, produced after each of the 9 trials. Also, density was measured using a weighing machine, and micrometer. The details of important test equipment used in experimental study are given below.

3.9.1 Surface Roughness Tester

Surface roughness was measured using the Mitutoyo Surf test model SJ-400 available in Metrology laboratory at Thapar Univesity,Patiala,Punjab, India. The equipment uses the stylus method of measurement, has profile resolution 0.000125µm (on 8µm range)and measure roughness up to 800µm. A tracing length of 4.8 mm was used for analysis.

3.9.2 Rockwell Hardness Tester

Hardness was measured on a Rockwell Hardness Tester, (model AVERY 6402) England, available at Strength of Material Laboratory, Thapar University, Patiala. The hardness measurement is dependent on the diameter of indentation on the samples. The indents formed in the pyramid shaped steel ball indenter were measured on B scale with a minor load of 10 kg for 20 Seconds.

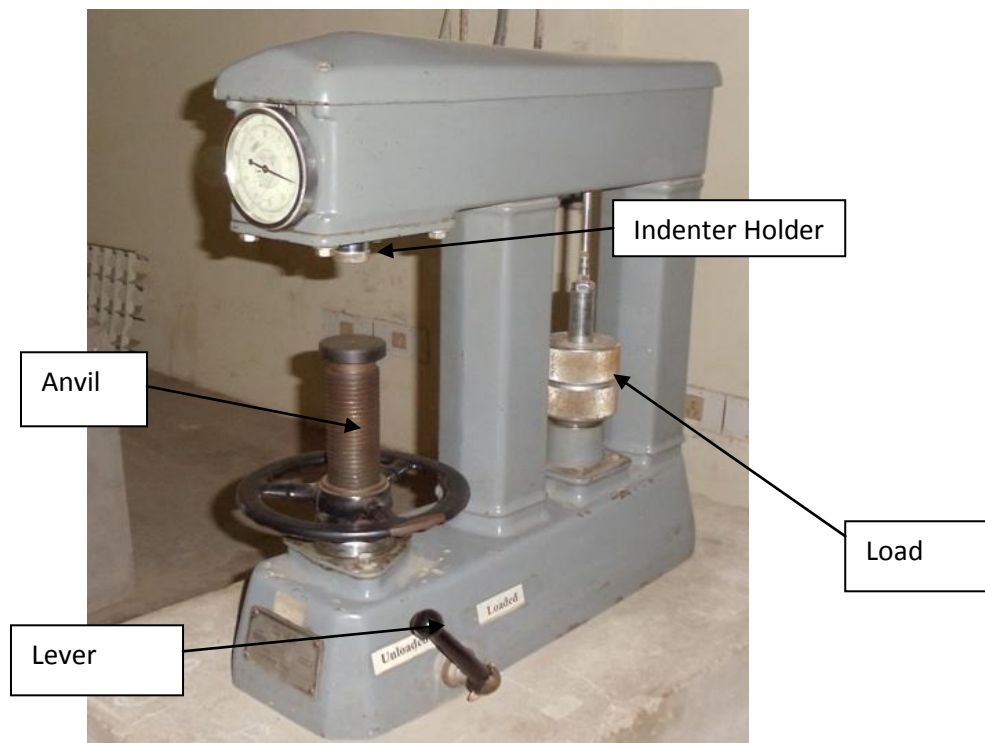


Figure 3.4: Rockwell Hardness Testing Machine

3.10. COMPOSITION OF WORK MATERIAL

The Aluminium alloy A356 and ADC12 was used for the experiments. The percentage composition of the work piece material is provided in Table 3.5. The work pieces are shown in the Figure 3.5(a), 3.5(b) and work pieces after casting as a final sample are shown in Figure 3.6(a), 3.6(b).



Figure 3.5(a): Raw material of A356 before casting



Figure 3.5(b): Raw material of ADC12 before casting

Table 3.5: Chemical composition of work piece materials

	% composition of aluminium alloy A356													
	Si	Fe	Cu	Mn	Mg	Zn	Cr	Be	Ni	Ti	Pb	Sn	Sr	Sb
Value	6.9	0.2	0.1	0.0	0.3	0.0	0.0	0.0	0.0	0.15	0.0	0.0	<0.	0.0
	001	10	02	82	20	520	184	005	240	2	034	040	00	68
		3										8	01	9
												0		
	Na	B	Zr	Ga	Co	V	Ca	Ag	Cd	In	Bi	Hg	La	Ba
Value	0.0	0.0	0.0	0.0	<0.	0.0	<0.	0.0	<0.	<0.0	<0.	0.0	<0.	<0.
	022	01	04	054	000	064	000	004	000	0030	001	033	00	00
	4	60	52	0	50	3	10	0	10		00	2	03	01
	Ba	P	Ce	Li	Al									
Value	<0.	0.0	<0.	<0.	92.									
	000	03	00	000	030									
	10	61	15	10	6									

	% composition of aluminium alloy ADC12													
	Si	Fe	Cu	Mn	Mg	Zn	Cr	Be	Ni	Ti	Pb	Sn	Sr	Sb
Value	10.	0.9	2.0	0.2	0.2	0.9	0.0	0.0	0.2	0.15	0.1	0.0	<0.	0.0
	200	10	00	82	70	820	084	005	001	2	034	800	00	08
	Na	B	Zr	Ga	Co	V	Ca	Ag	Cd	In	Bi	Hg	La	Ba
Value	0.0	0.0	0.0	0.0	<0.	0.0	<0.	0.0	<0.	<0.0	<0.	0.0	<0.	<0.
	032	01	03	054	000	064	000	004	000	0030	001	023	00	00
	4	60	52	0	50	3	10	0	10		00	2	03	01
	Ba	P	Ce	Li	Al									
Value	<0.	0.0	<0.	<0.	84.									
	000	03	00	000	771									
	10	61	15	10	6									



Figure 3.6(a): Final Sample of Material of A-356 after casting



Figure 3.6(b): Final Sample of Material of ADC-12 after casting

3.11 ANALYSIS OF RESULTS

The results for surface hardness, density and hardness after each of the 9 trials conducted with repetition are given in table: 3.6.

Table 3.6(a) Analysis of results for A356 casting

Trial No.	Pouring temp. °C	Injection pressure kg/cm ²	Coating type	Cooling type	Mean surface roughness R _a	Mean Density	Mean Hardness
1	770	100	Oil Coating	Air Cooling	1.105	2.6733	75.3333
2	770	90	Oil+ graphite	Water Coolig	2.93	2.6617	85.6667
3	770	120	Dycot	Oil Cooling	1.53	2.6838	87.3333
4	790	100	Oil+ graphite	Oil Cooling	1.67	2.6772	80
5	790	90	Dycot	Air Cooling	1.82	2.6624	82.3333
6	790	120	Oil Coating	Water Coolig	1.545	2.6761	81
7	730	100	Dycot	Water Coolig	2.13	2.6711	76
8	730	90	Oil Coating	Oil Cooling	2.075	2.6645	75.6667
9	730	120	Oil+ graphite	Air Cooling	2.84	2.6853	79.3333

Table 3.6(b) Analysis of results for ADC12 casting

Trial No.	Pouring temp. °C	Injection pressure kg/cm ²	Coating type	Cooling type	Mean surface roughness R _a	Mean Density	Mean Hardness
1	770	100	Oil Coating	Air Cooling	2.78	2.760004	90.5
2	770	90	Oil+ graphite	Water Coolig	1.68	2.7051	84
3	770	120	Dycot	Oil Cooling	1.78	2.7649	104
4	790	100	Oil+ graphite	Oil Cooling	1.39	2.725	104.5
5	790	90	Dycot	Air Cooling	2.12	2.725	107
6	790	120	Oil Coating	Water Coolig	3.66	2.784	95
7	730	100	Dycot	Water Coolig	1.86	2.75	112
8	730	90	Oil Coating	Oil Cooling	1.75	2.725	91.5
9	730	120	Oil+ graphite	Air Cooling	1.81	2.784	89

3.10.1 Analysis of Variance

The knowledge of the contribution of individual factors is critically important for the control of the each response. The analysis of variance (ANOVA) is a common statistical technique to determine the percent contribution of each factor for results of the experiment. It calculates parameters known as sum of squares (SS), pure SS, degree of freedom (dof), variance, F-ratio and percentage contribution of each factor. Since the procedure of ANOVA is a very complicated and employs a considerable of statistical formula, only a brief description of is given as following.

The Sum of Squares (SS) is a measure of the deviation of the experimental data from the mean value of the data.

Let 'A' be a factor under investigation

$$SS_T = \sum_{i=1}^N (y_i - \bar{T})^2$$

Where N = Number of response observations, \bar{T} is the mean of all observations

y_i is the i , th response

Factor Sum of Squares (SS_A) - Squared deviations of factor (A) averages from overall average

$$SS_A = \left[\sum_{i=1}^{k_A} \left(\frac{A_i^2}{n_{Ai}} \right) \right] - \frac{T^2}{N} \quad \text{(Equation 3.1)}$$

Where

A_i = Average of all observations under A_i level = A_i / n_{Ai}

T = sum of all observations

\bar{T} = Average of all observations = T / N

n_{Ai} = Number of observations under A_i level

Error Sum of Squares (SS_e) - Squared deviations of observations from factor (A) averages

$$SS_e = \sum_{j=1}^{k_A} \sum_{i=1}^{n_{Ai}} (y_i - \bar{A}_j)^2 \quad \text{(Equation 3.2)}$$

$$SS'_A = SS_A - (V_e)(v_A) \quad \text{(Equation 3.3)}$$

SS'_A is expected sum of squares due to factor A, and the percent contribution to the total variation can be calculated as:

$$P = \frac{SS'_A}{SS_T} \times 100 \quad \text{(Equation 3.4)}$$

3.10.2 Signal-to-Noise Ratio

The parameters that influence the output can be categorized into two classes, namely controllable (or design) factors and uncontrollable (or noise) factors. Controllable factors are those factors whose values can be set and easily adjusted by the designer. Uncontrollable factors are the sources of variation often associated with operational environment. The best settings of control factors as they influence the output

parameters are determined through experiments. From the analysis point of view, there are three possible categories of the response characteristics explained below.

r is the number of tests in a trial (noise of repetitions regardless of noise levels)

$\sum_{i=1}^r y_i^2$ = summation of all response values under each trial

MSD = Mean square deviation

y_j = Observed value of the response characteristic

y_o = nominal or target value of the results

The three different response characteristics are given by the following.

1) Higher is Better. The S/N for higher the better is given by:

$$(S/N)_{HB} = -10 \log (MSD_{HB})$$

$$\text{Where } MSD_{HB} = \frac{1}{r} \sum_{j=1}^r \left(\frac{1}{y_j^2} \right) \quad (\text{Equation 3.5.})$$

MSD_{HB} = Mean Square Deviation for higher-the-better response.

2) Nominal is Better. The S/N for nominal is better is:

$$(S/N)_{NB} = -10 \log (MSD_{NB})$$

$$\text{Where } MSD_{NB} = \frac{1}{r} \sum_{j=1}^r (y_j - y_o)^2 \quad (\text{Equation 3.6.})$$

Lower is Better. In this design situation, the surface roughness and hardness is the type of “lower is better”, which is a logarithmic function based on the mean square deviation (MSD), given by

$$S / N_{LB} = -10 \log(MSD) = -10 \log \left[\left(\frac{1}{r} \sum_{i=1}^r y_i^2 \right) \right] \quad (\text{Equation 3.7.})$$

$$\text{Where } MSD_{LB} = \frac{1}{r} \sum_{j=1}^r (y_j^2)$$

3.10.3 Signal to noise ratio for response characteristics

The parameters that influence the output can be categorized in two categories, controllable factors and uncontrollable factors. The control factors that may contribute to reduced variation can be quickly identified by looking at the amount of variation present in response. The uncontrollable factors are the sources of variation often associated with operational environment. For this experimental work, response characteristics have given in the Table 3.7.

Table 3.7: Response Characteristics

Response name	Response type	Units
Density	Higher the better	gm/cm ³
Hardness	Higher the better	HRB
Surface Roughness	Lower the better	Microns

3.10.4 Measurement of F-value of Fisher's F ratio

The principle of the F test is that the larger the F value for a particular parameter, the greater the effect on the performance characteristic due to the change in that process parameter. F value is defined as:

$$F = \frac{MS \text{ for the term}}{MS \text{ for the error term}} \quad (\text{Equation 3.8})$$

Depending on F-value, percentage contribution is calculated of each factor and interaction.

Computation of average performance:

Average performance of a factor at certain level is the influence of the factor at this level on the mean response of the experiments.

4.1 INTRODUCTION

The effect of various input parameters i.e. thermal characteristics (temperature of the molten metal), injection pressure of the molten metal, type of coating (oil coating, oil + graphite coating, dycot coating), and the type of cooling (air cooling, water cooling and oil cooling). The three responses were selected for experimentation namely, surface roughness, density, hardness. The experiment was conducted using A356 and ADC12 aluminium alloy. The assignment of factor was carried out using statistical software MINITAB 16. All the factors were varied at three levels. The degree of freedom required for the experiment was calculated to be 8, thus orthogonal array that can be used should have degree of freedom (DOF) less than or equal to 8. L9, which can accommodate factors with 3-levels, was thus used for conduct of experiments to measure three responses namely the surface roughness, density and hardness. After conducting the 9 trials the mean value for all the above factors are tabulated. For the analysis of result Analysis of Variance (ANOVA) was performed.

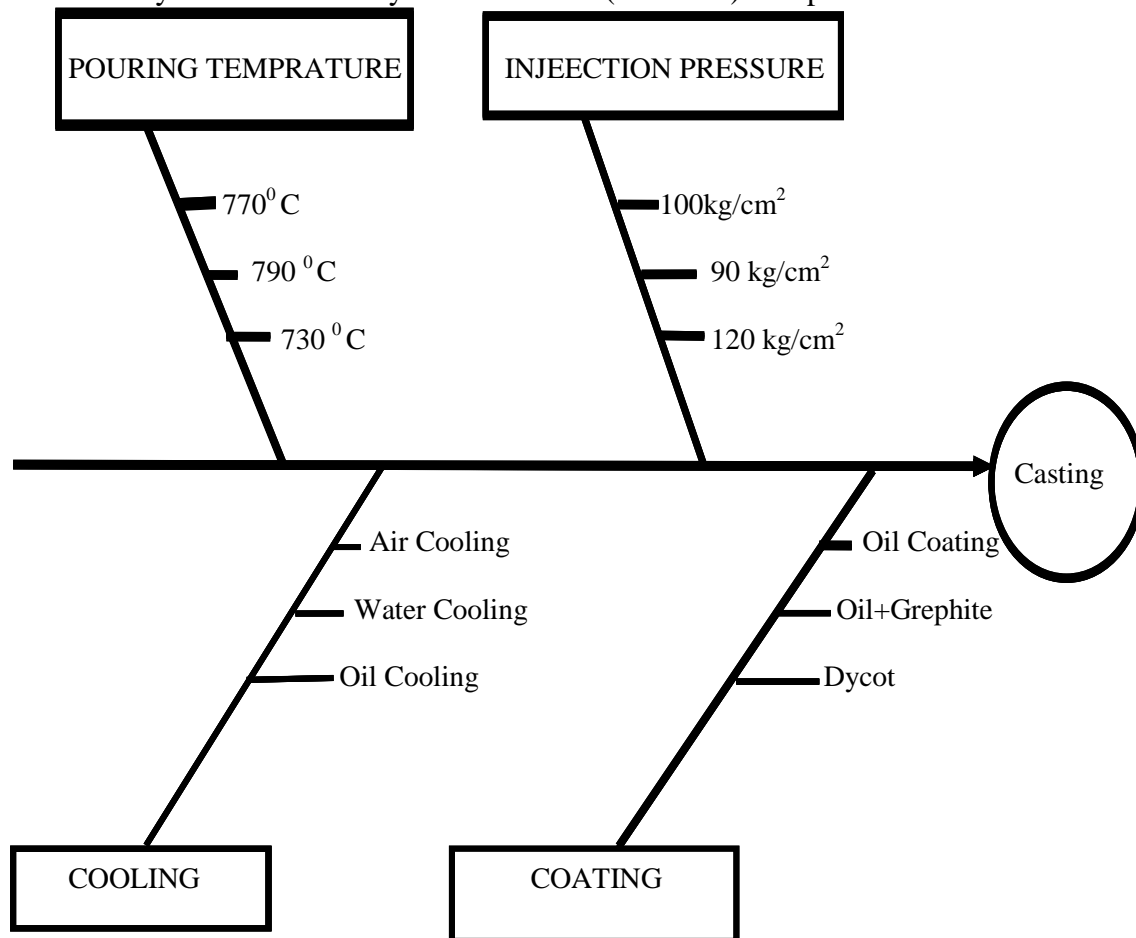


Figure 4.1: Fish bone diagram for process parameter and factors affecting them.

4.2 RESULTS OF SURFACE ROUGHNESS (R_a)

Surface roughness was measured using the Mitutoyo Surf test model SJ-400 available in the Metrology laboratory at Thapar University, Patiala. The result of surface roughness for each of the 9 experiments is given in Table 4.1.

Table 4.1: Results for Surface Roughness of A356 Alloy (R_a)

Trial No.	Pouring temp.	Injection pressure	Coating type	Cooling type	Mean surface roughness	S/N ratio
1	770 ⁰	100	Oil Coating	Air Cooling	1.105	-0.86725
2	770 ⁰	90	Oil+ graphite	Water Coolig	2.93	-9.33735
3	770 ⁰	120	Dycot	Oil Cooling	1.53	-3.69383
4	790 ⁰	100	Oil+ graphite	Oil Cooling	1.67	-4.45433
5	790 ⁰	90	Dycot	Air Cooling	1.82	-5.20143
6	790 ⁰	120	Oil Coating	Water Coolig	1.545	-3.77857
7	730 ⁰	100	Dycot	Water Coolig	2.13	-6.56759
8	730 ⁰	90	Oil Coating	Oil Cooling	2.075	-6.34036
9	730 ⁰	120	Oil+ graphite	Air Cooling	2.84	-9.06637

4.3 ANALYSIS OF VARIANCE- SURFACE ROUGHNESS

The results were analyzed using ANOVA for identifying the significant factors affecting the surface roughness. ANOVA results for the mean surface roughness at 95% confidence interval are given in Table 4.2. The variation data for each factor was tested for F value to find significance of each factor. The principle of F-test is that the larger the F values for a particular parameter, the greater the effect of performance characteristics due to the change in that process parameter. ANOVA analysis showed that Coating (F value 4.34055) was the

only factor that significantly affects the surface roughness. All other factors, namely, pouring temperature, Injection pressure and cooling were found to be insignificant. Table 4.3 shows the rank of various factors in the term of their relative significance. Coating has the highest rank, signifying highest contribution to surface roughness and the cooling has the lowest rank and was observed to be insignificant in affecting surface roughness. Main effect plot for the mean surface roughness is shown in the Figure 4.3 which shows the variation of surface roughness with the input parameters. As can be seen surface finish improves with oil type coating.

Table 4.2: Analysis of Variance for means of surface roughness (R_a)

Factors	Degree of Freedom(DOF)	Seq Sum of Square(ss)	Adj MS(variance)	F(fisher ratio)	P(percentage contribution)
Pouring Temperature	2	0.72349	0.36174	2.39866	24.5312
Injection Pressure	2	0.61496	0.30748	2.03883	20.8513
Coating	2	1.30921	0.6546	4.34055	44.391
Cooling	2	0.30162	0.15081	1.000	10.2269
Total	8	2.94927			
E pooled	6	0.30162	0.15081		

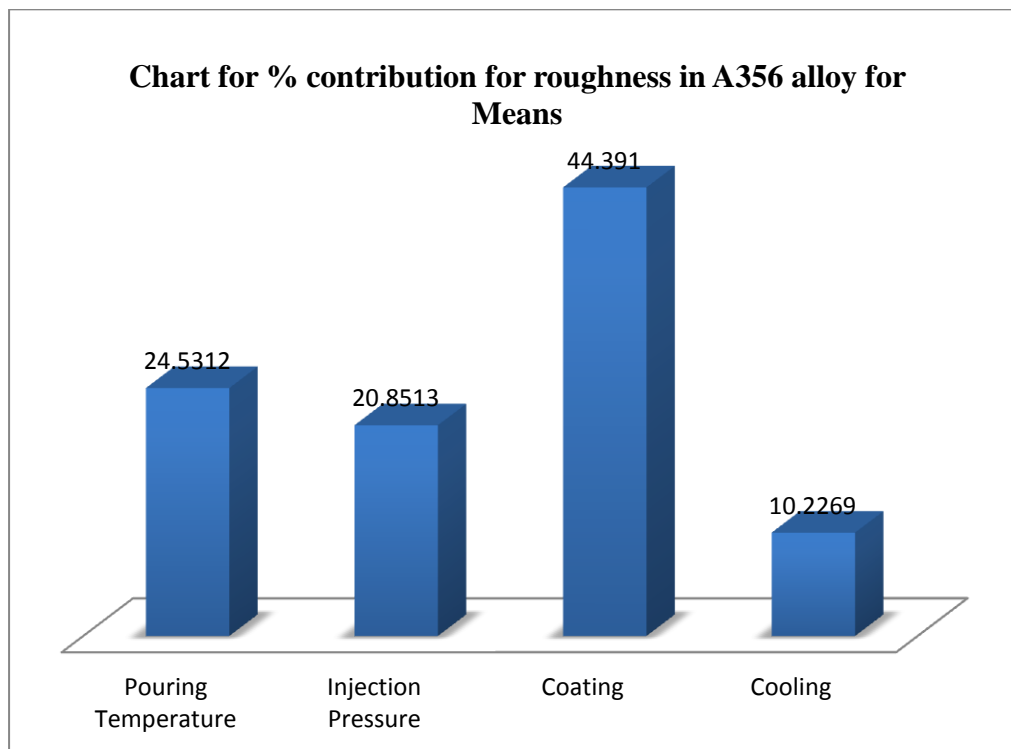


Figure 4.2: Bar chart for percentage contribution in roughness for Means.

Table 4.3: Response Table for Mean Surface Roughness for A356 Alloy (R_a)

Level	Pouring Temperature	Injection Pressure	Coating Type	Cooling Type
1	2.348	2.275	1.575	1.922
2	1.678	1.635	2.480	2.202
3	1.855	1.972	1.827	1.758
Delta	0.670	0.640	0.905	0.443
Rank	2	3	1	4

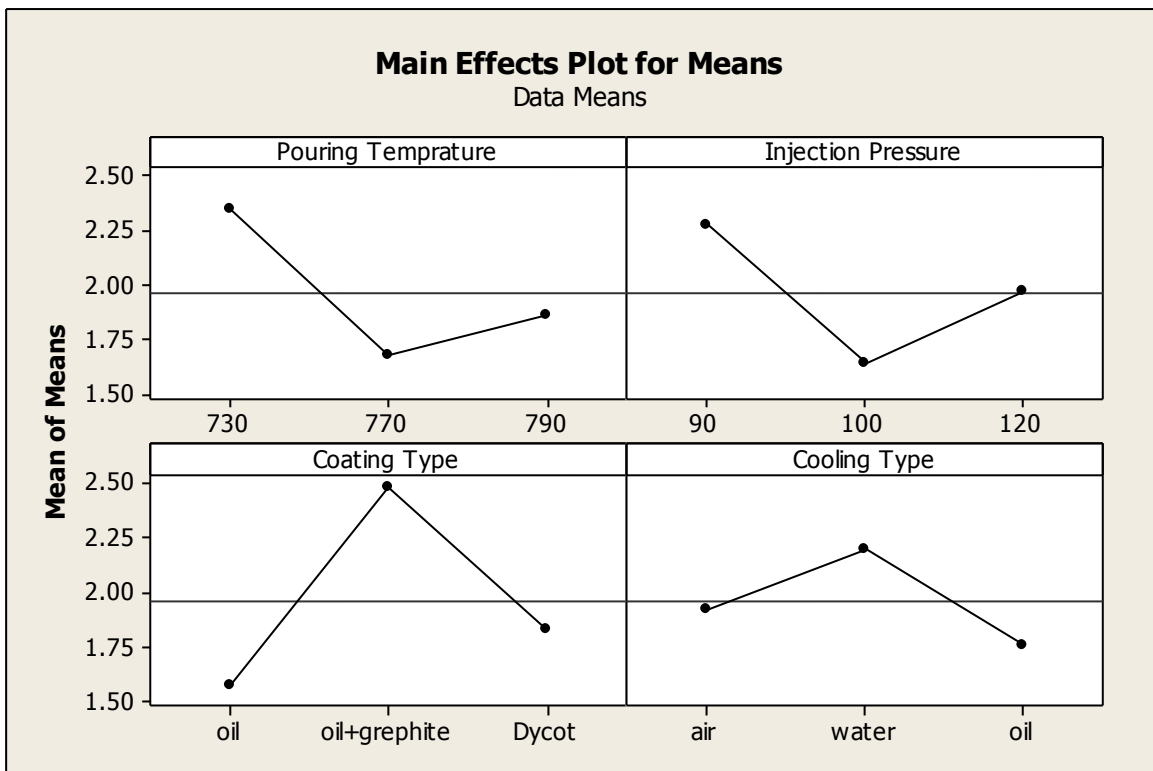


Figure 4.3: Main effect plot for surface roughness for Means

4.4 RESULTS FOR S/N RATIO – SURFACE ROUGHNESS

The S/N ratio consolidated several repetitions into one value and is an indication of the amount of variation present in the process. The S/N ratios have been calculated to identify the major contributing factors and interactions that cause variation in surface roughness. Surface roughness is a “lower the better” type response and is given by a logarithmic function based on the mean square deviation (MSD),

$$S / N_{LB} = -10 \log(MSD) = -10 \log\left(\frac{1}{r} \sum_{i=1}^r y_i^2\right)$$

$$\text{Where } MSD_{LB} = \frac{1}{r} \sum_{j=1}^r (y_j^2)$$

The S/N ratio values are given in the last column of Table 4.1, Table 4.4 shows the ANOVA results for S/N ratio of surface roughness at 95% confidence interval. Other than cooling, all other factors, namely coating, temperature and injection pressures were found to be significant in affecting surface roughness (R_a). According to F-test, coating was observed to be the most significant factor affecting the surface roughness, followed by injection pressure and pouring temperature according to F-test. Main effect plot of S/N ratio for surface roughness are shown in the Figure 4.6.

Table 4.4: Analysis of Variance for S/N ratios of surface roughness in A356 Alloy

Source	Seq SS	DOF	Adj MS	F	P
Pouring Temperature	15.3741	2	7.6871	2.87702	26.4357
Injection Pressure	13.4753	2	6.7376	2.52165	23.1707
Coating	23.9634	2	11.9817	4.48434	41.205
Cooling	5.3438	2	2.6719	1.0000	9.18864
e-pooled	5.3438	2	2.6719		
Total	58.1566	8			

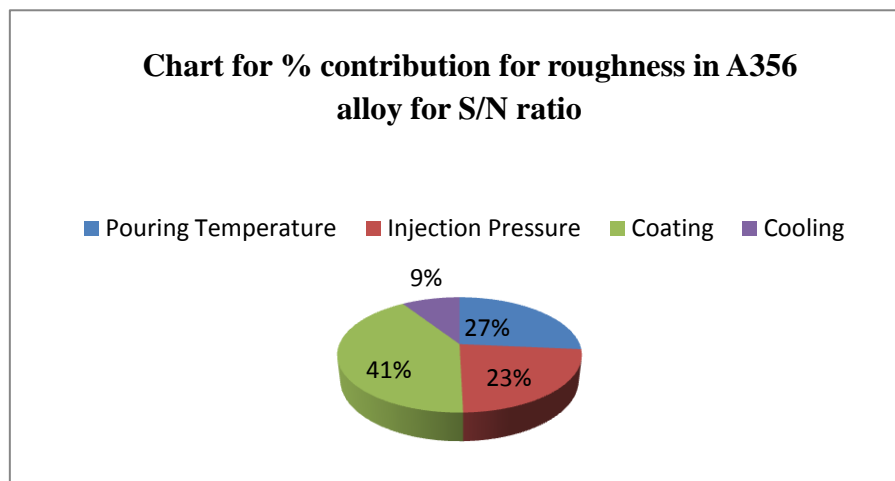


Figure 4.4: Pie chart for percentage contribution in surface roughness for s/n ratio.

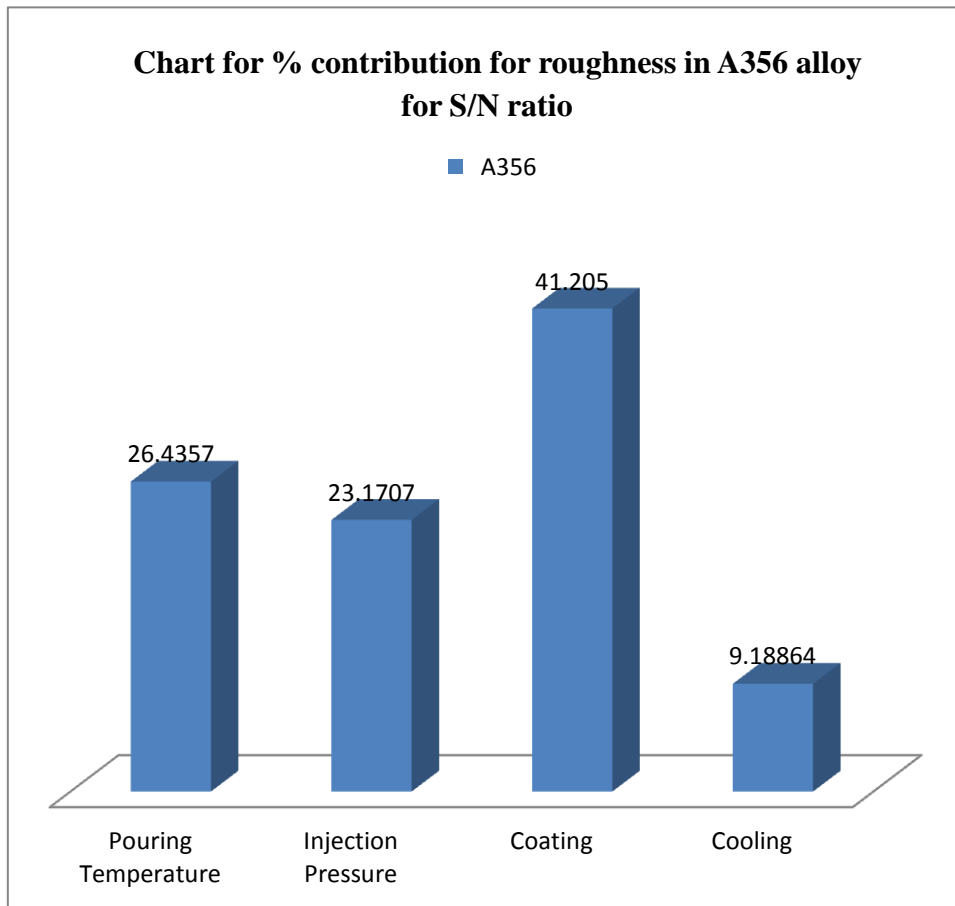


Figure 4.5: Bar chart for percentage contribution in surface roughness for s/n ratio.

Table 4.5: Response Table for S/N Ratio of Surface Roughness

Level	Pouring Temperature	Injection Pressure	Coating Type	Cooling Type
1	-7.325	-6.960	-3.662	-5.045
2	-4.478	-3.963	-7.619	-6.561
3	-4.633	-5.513	-5.154	-4.830
Delta	2.847	2.997	3.957	1.732
Rank	3	2	1	4

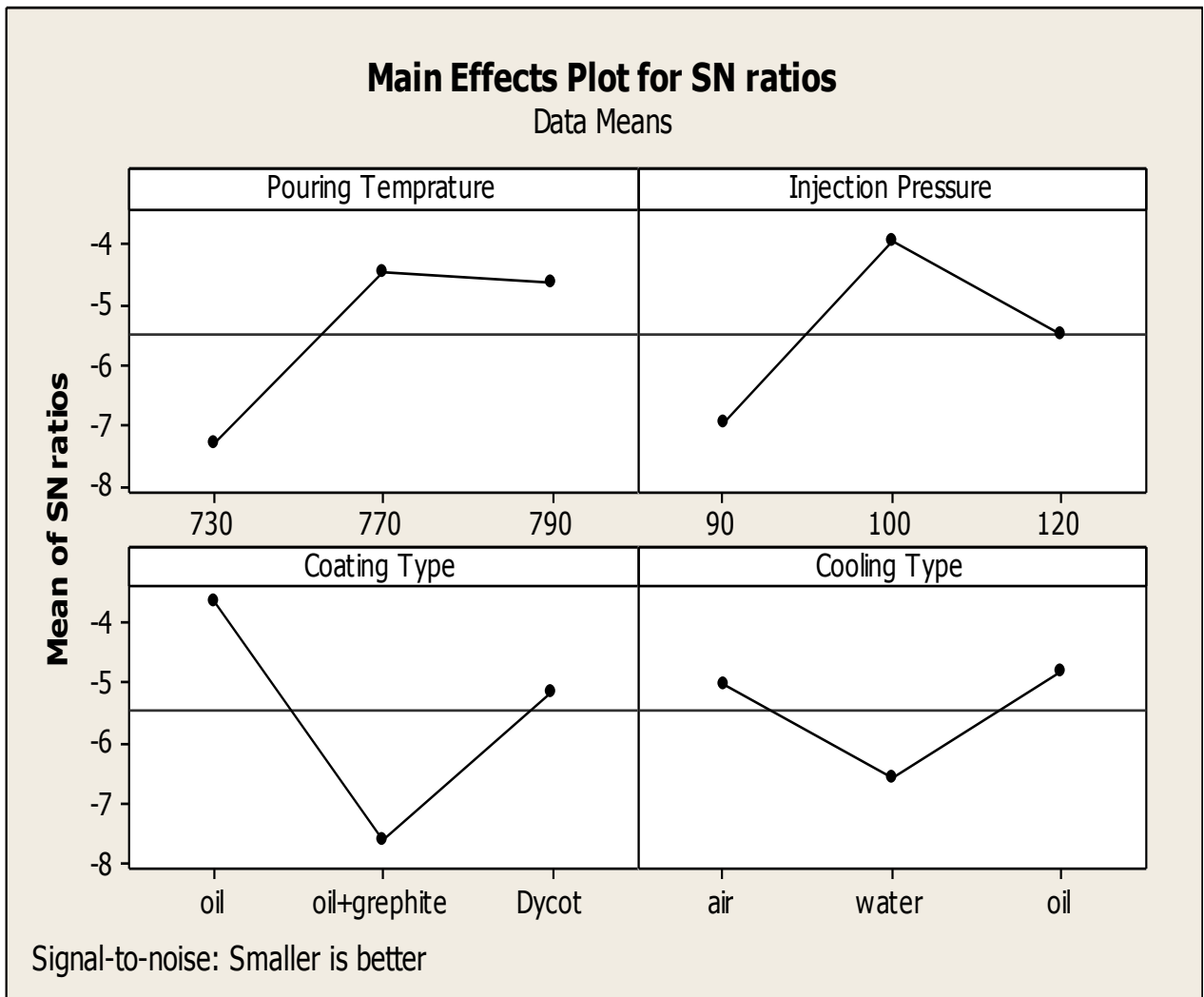


Figure 4.6: Main effects Plot for S/N ratio of surface roughness

4.5 OPTIMAL DESIGN FOR ROUGHNESS

The same level of all the significant factors provide a higher mean value and reduced variability so nothing has to be compromised. The level of factors which improves average and uniformity may conflict, so a compromise may have to be reached. Also a compromise has to occur when multiple responses are considered and the same factor level may cause one response to improve and other to deteriorate [66]. In this experimental analysis, the main effect plot in Figure 4.3 and estimate the mean surface roughness. From the, Table 4.6 it is concluded that lowest roughness was observed when Oil type coating is used and pressure was kept at 100 kg/cm². In S/N ratio lowest roughness was observed when coating type Oil+Grephite was used and pressure was kept at 90 kg/cm², pouring temperature at 730°C.

Table 4.6 Significant Factors and Their Levels

Factor	Affecting mean		Affecting variation	
	Contribution	Best level	Contribution	Best level
Pouring Temperature, A	insignificant	-	significant	Level -1 (730°C)
Injection Pressure, B	insignificant	-	significant	Level-2, (90kg/cm ²)
Coating, C	significant	Oil Level-1	significant	Oil+Grephte Level-2
Cooling, D	insignificant	-	insignificant	-

Estimating the mean

In experimental analysis, surface roughness is a lower average response is better (LB) characteristic. Depending on the characteristic, different treatment combinations has chosen to obtain satisfactory results. After conducting the experiments the optimum treatment condition within the experiments determined on the basis of prescribed combination of factor levels is determined to one of those in the experiment [66].

Mean value for Roughness

$$\begin{aligned} \mu_{A_1 B_2 C_2} &= \bar{A}_1 + \bar{B}_2 + \bar{C}_2 - 2\bar{T} \\ &= 1.855 + 2.275 + 2.48 - 2 \times 1.9605 = 3.921 \text{ micron} \end{aligned}$$

Confidence Interval around the Estimated Mean

The confidence interval is a maximum and minimum value between which the true average should fall at some stated percentage of confidence. The estimate of the mean μ is only a point estimate based on the averages of results obtained from the experiment. Statistically this provides a 50% chance of the true averages being greater than μ and a 50% chance of the true average being less than μ [66].

Confidence Interval around the estimated roughness mean

$$CI_1 = \sqrt{\frac{F_{\alpha, v_1, v_2} V_e}{n_{eff}}}$$

Where $F_{\alpha, v_1, v_2} = F \text{ ratio}$

$\alpha = \text{risk (0.05)}$

$\text{confidence} = 1 - \alpha$

$v_1 = \text{dof for mean which is always} = 1$

$v_2 = \text{dof for error} = v_e$

$n_{eff} = \text{Number of tests under that condition using the participating factors}$

$$n_{eff} = \frac{N}{1 + \text{dof}_{A,B,C}} = \frac{9}{1 + 2 + 2 + 2} = 1.28$$

$$CI_1 = \sqrt{\frac{F_{\alpha, v_1, v_2} V_e}{n_{eff}}} = \sqrt{\frac{5.99 \times 0.05027}{1.28}} = 0.485$$

So, the confidence interval around the Surface Roughness is given by 3.921 ± 0.485 micron.

4.6 RESULTS FOR DENSITY

The density of the cast material was obtained by using micrometer to conclude the volume and the weight was observed by using the electronic weighing scale available in Workshop at GRIMT, Radaur (Haryana). Density is denoted by $\rho = \frac{\text{Weight}}{\text{volume}}$. The result for density for each of the 9 experiments is given in Table in 4.7.

Table 4.7: Results for Density

Trial No.	Pouring temp.	Injection pressure	Coating type	Cooling type	Mean density	S/N ratio
1	770 ⁰	100	Oil Coating	Air Cooling	2.6733	8.540953968
2	770 ⁰	90	Oil+ Graphite	Water Coolig	2.6617	8.503182092
3	770 ⁰	120	Dycot	Oil Cooling	2.6838	8.575002971
4	790 ⁰	100	Oil+ Graphite	Oil Cooling	2.6772	8.553616327
5	790 ⁰	90	Dycot	Air Cooling	2.6624	8.505466092
6	790 ⁰	120	Oil Coating	Water Coolig	2.6761	8.550046761
7	730 ⁰	100	Dycot	Water Coolig	2.6711	8.533802947
8	730 ⁰	90	Oil Coating	Oil Cooling	2.6645	8.512314492
9	730 ⁰	120	Oil+ Graphite	Air Cooling	2.6853	8.579856237

4.7 ANALYSIS OF VARIANCE- DENSITY

The results were analyzed using ANOVA for identifying the significant factor affecting the performance measures. ANOVA for the mean density at 95% confidence interval is given in Table 4.8. ANOVA table shows that injection pressure (F value (134.5) and Cooling type (F value 12.5) are the factors that significantly affects the density. All other factors, namely, pouring temperature and coating type were found to be insignificant. Table 4.9 shows the rank of various factors in the term of their relative significance. Pressure has the highest rank, signifying highest contribution to density and the pouring temperature has the lowest rank and was observed to be insignificant. Main effect plot for the mean density is shown in the Figure 4.9 which shows the density increase with the increase in injection pressure.

Table 4.8: Analysis of Variance for Means density

Factors	DF	Seq SS	Adj MS	F	P
Pouring Temperature	2	0.000005	0.000002	1	0.81833061
Injection Pressure	2	0.000539	0.000269	134.5	88.2160393
Coating	2	0.000018	0.000009	4.5	2.94599018
Cooling	2	0.000049	0.000025	12.5	8.01963993
e-pooled	4	0.000005	0.000002		
Total	8	0.000611			

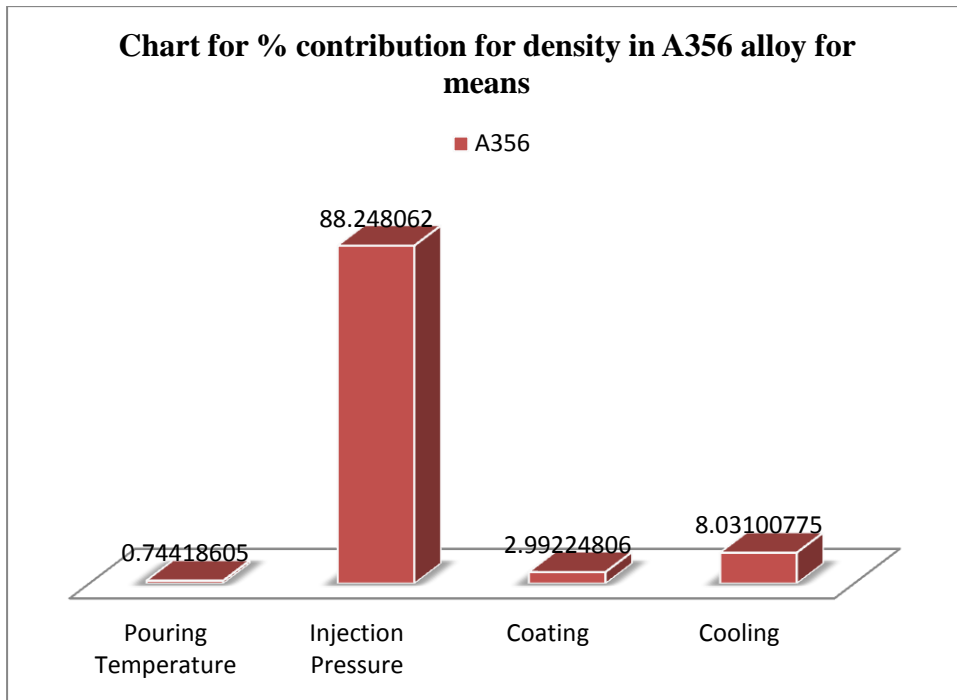


Figure 4.7: Bar chart for percentage contribution in density for Means.

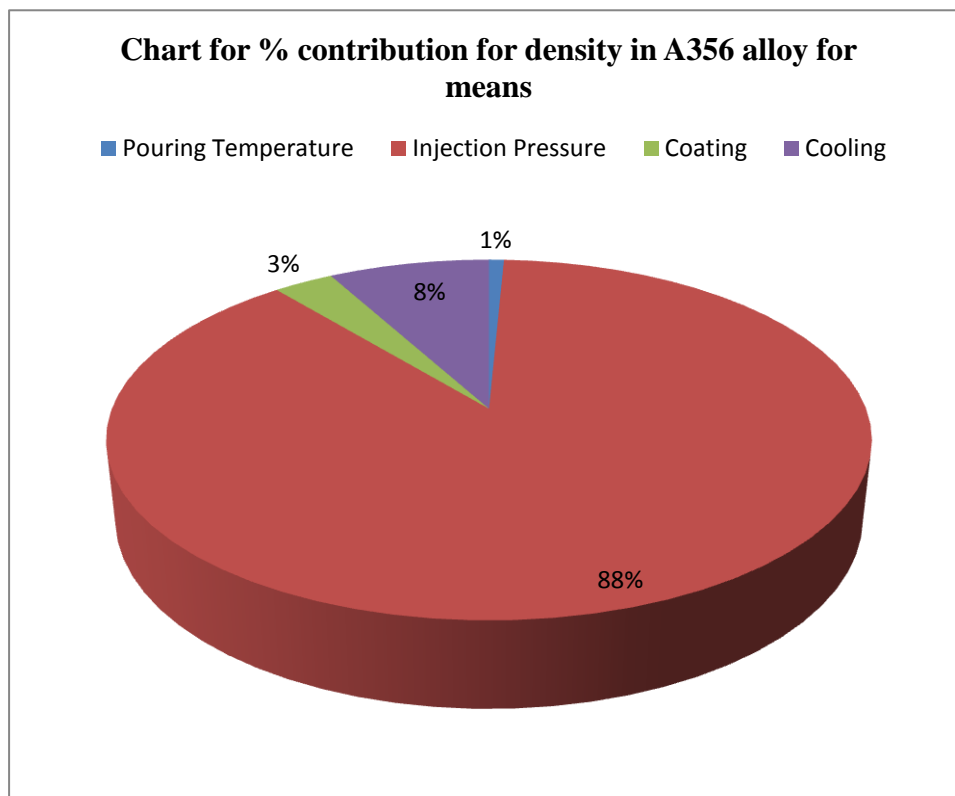


Figure 4.8: Pie chart for percentage contribution in density for Means.

Table 4.9: Response Table for Means for Density

Level	Pouring Temperature	Injection Pressure	Coating Type	Cooling Type
1	2.674	2.663	2.671	2.674
2	2.673	2.674	2.675	2.67
3	2.672	2.682	2.672	2.675
Delta	0.002	0.019	0.003	0.006
Rank	4	1	3	2

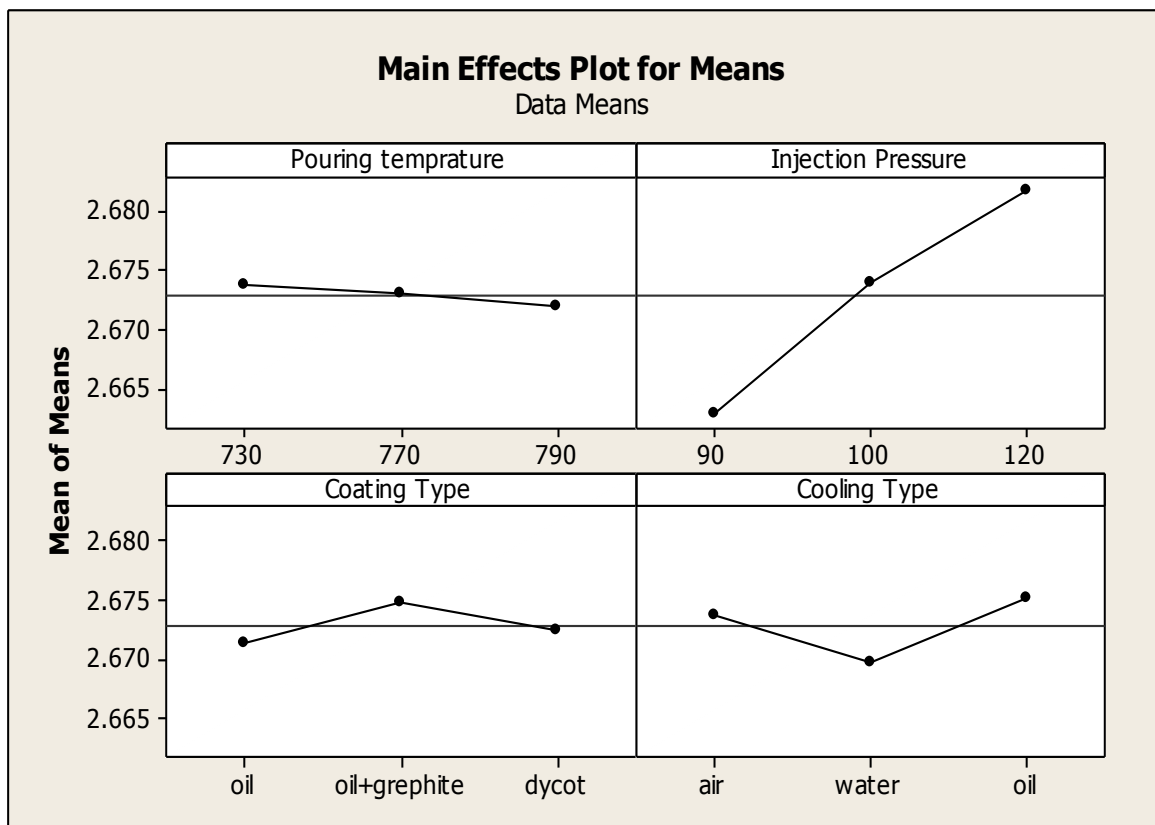


Figure 4.9 Main effect plots for mean density

4.8 RESULTS FOR S/N RATIO – DENSITY

The S/N ratios have been calculated to identify the major contributing factors and interactions that cause variation in density. Density a “Higher the better” type response is given by a logarithmic function based on the mean square deviation (MSD),

$$(S/N)_{HB} = -10 \log (MSD_{HB})$$

$$\text{Where } MSD_{HB} = \frac{1}{r} \sum_{j=1}^r \left(\frac{1}{y_j^2} \right)$$

MSD_{HB} = Mean Square Deviation for higher-the-better response.

Table 4.10 shows the ANOVA results for S/N ratio of density at 95% confidence interval. Except coating and Pouring temperature, the other two factors injection pressure and cooling Factor were found to be significant. According to F-test injection pressure was observed to be the most significant factor affecting the density, followed by Cooling Factor.

Table 4.10: Analysis of Variance for S/N ratio for Density

Factors	DF	Seq SS	Adj MS	F	P
Pouring Temperature	2	0.000048	0.000024	1	0.74418605
Injection Pressure	2	0.005692	0.002846	118.583333	88.248062
Coating Type	2	0.000193	0.000096	4	2.99224806
Cooling Type	2	0.000518	0.000259	10.7916667	8.03100775
e-pooled	2	0.000048	0.000024		
Total	8	0.00645			

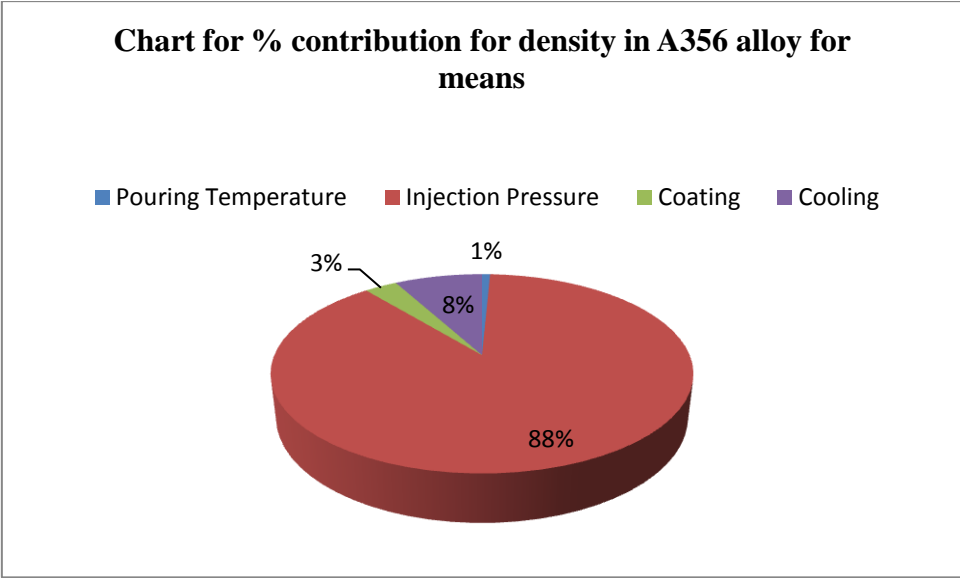


Figure 4.10: Pie chart for percentage contribution in density for s/n ratio.

Table 4.11: Response Table for S/N ratio for Density

Level	Pouring Temperature	Injection Pressure	Coating Type	Cooling Type
1	8.542	8.507	8.534	8.542
2	8.54	8.543	8.546	8.529
3	8.536	8.568	8.538	8.547
Delta	0.006	0.061	0.011	0.018
Rank	4	1	3	2

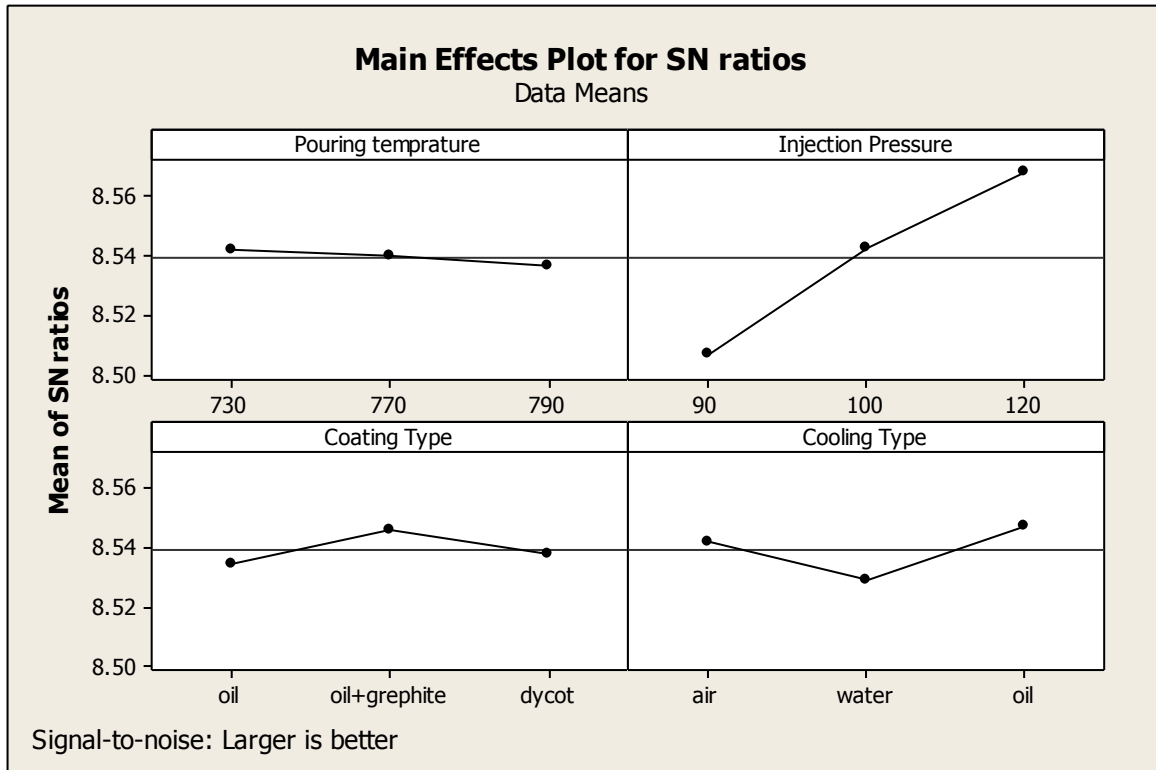


Figure 4.11: Main effect plots for S/N Ratio of density

4.9 OPTIMAL DESIGN FOR DENSITY

The same level of all the significant factors provide a higher mean value and reduced variability so nothing has to be compromised. In this experimental analysis, the main effect plot in Figure 4.9 and estimate the mean for density. From the, Table 4.11 it is concluded that highest density was observed when injection pressure was kept at 120 kg/cm² and Cooling Type Oil is used. In S/N ratio plot 4.12 shows same result.

Table 4.12 Significant Factor and their Levels

Factor	Affecting mean		Affecting variation	
	Contribution	Best level	Contribution	Best level
Pouring Temperature, A	Insignificant	-	Insignificant	-
Injection Pressure, B	significant	Level-3, (120kg/cm ²)	significant	Level-3, (120kg/cm ²)
Coating, C	insignificant	-	insignificant	-
Cooling, D	significant	Level-3 Oil	significant	Level-3 Oil

Estimating the mean

In experimental analysis, density is a higher average response is better (HB) characteristic. After conducting the experiments the optimum treatment condition within the experiments determined on the basis of prescribed combination of factor levels is determined to one of those in the experiment

Mean value for Density

$$\begin{aligned}\mu_{B_3D_3} &= \bar{B}_3 + \bar{D}_3 + - \bar{T} \\ &= 2.6817 + 2.6751 - 2.6728 = 2.684 \text{ gms/mm}^3\end{aligned}$$

Confidence Interval around the Estimated Mean

Confidence Interval around the estimated density mean

$$CI_1 = \sqrt{\frac{F_{\alpha, v_1, v_2} V_e}{n_{eff}}}$$

Where $F_{\alpha, v_1, v_2} = F$ ratio

$\alpha = \text{risk (0.05)}$ $\text{confidence} = 1 - \alpha$

$v_1 = \text{dof for mean which is always} = 1$

$v_2 = \text{dof for error} = v_e$

$n_{eff} = \text{Number of tests under that condition using the participating factors}$

$$n_{eff} = \frac{N}{1 + \text{dof}_{B,D}} = \frac{9}{1 + 2 + 2} = 1.8$$

$$CI_1 = \sqrt{\frac{F_{\alpha, v_1, v_2} V_e}{n_{eff}}} = \sqrt{\frac{0.2 \times 0.00646}{1.8}} = 0.0231$$

So, the confidence interval around the Density is given by $2.684 \pm 0.0231 \text{ gms/mm}^3$.

4.10 RESULTS OF HARDNESS

Hardness was measured on a Rockwell Hardness Tester, (model AVERY 6402) England, available at Mechanics of Solid lab, Thapar University, Patiala. The hardness measurement is dependent on the diameter of indentation on the samples. The indents formed in the pyramid shaped steel ball indenter were measured on B scale with a minor load of 10 kg for 20 Seconds. The result of hardness for each of the 9 experiments is given in Table in 4.13.

Table 4.13: Results of Hardness

Trial No.	Pouring temp.	Injection pressure	Coating type	Cooling type	Mean hardness	S/N ratio
1	750 ⁰	100	Oil Coating	Air Cooling	75.3333	37.5397
2	750 ⁰	90	Oil+ Graphite	Water Coolig	85.6667	38.6562
3	750 ⁰	120	Dycot	Oil Cooling	87.3333	38.8236
4	770 ⁰	100	Oil+ Graphite	Oil Cooling	80	38.0618
5	770 ⁰	90	Dycot	Air Cooling	82.3333	38.3115
6	770 ⁰	120	Oil Coating	Water Coolig	81	38.1697
7	790 ⁰	100	Dycot	Water Coolig	76	37.6163
8	790 ⁰	90	Oil Coating	Oil Cooling	75.6667	37.5781
9	790 ⁰	120	Oil+ Graphite	Air Cooling	79.3333	37.9891

4.11 ANALYSIS OF VARIANCE FOR HARDNESS

The results were analyzed using ANOVA for identifying the significant factor affecting the performance measures. The analysis of variance (ANOVA) for the mean hardness at 95% confidence interval is given in Table 4.14. ANOVA table shows that the pouring temperature (F value 7.000053), and Injection Pressure (F value 6.3746) and Coating (F value 5.221524) are the factor that significantly affects the hardness, whereas Cooling Factor was found to be insignificant. Table 4.15 shows the rank of various factors in the term of their relative significance. Pouring temperature has the highest rank; signifying highest contribution to

hardness and the Cooling has the lowest rank and was observed to be insignificant in affecting hardness. Main effect plot for the mean hardness is shown in the Figure 4.14.

Table 4.14: Analysis of Variance for Mean Hardness

Factors	DF	Seq SS	Adj MS	F	P
Pouring Temperature	2	53.062	26.5309	7.000053	35.7216
Injection Pressure	2	48.321	24.1605	6.374634	32.53
Coating	2	39.58	19.7901	5.221524	26.6455
Cooling	2	7.58	3.7901	1	5.1029
e-pooled	2	7.58	3.7901		
Total	8	148.543			

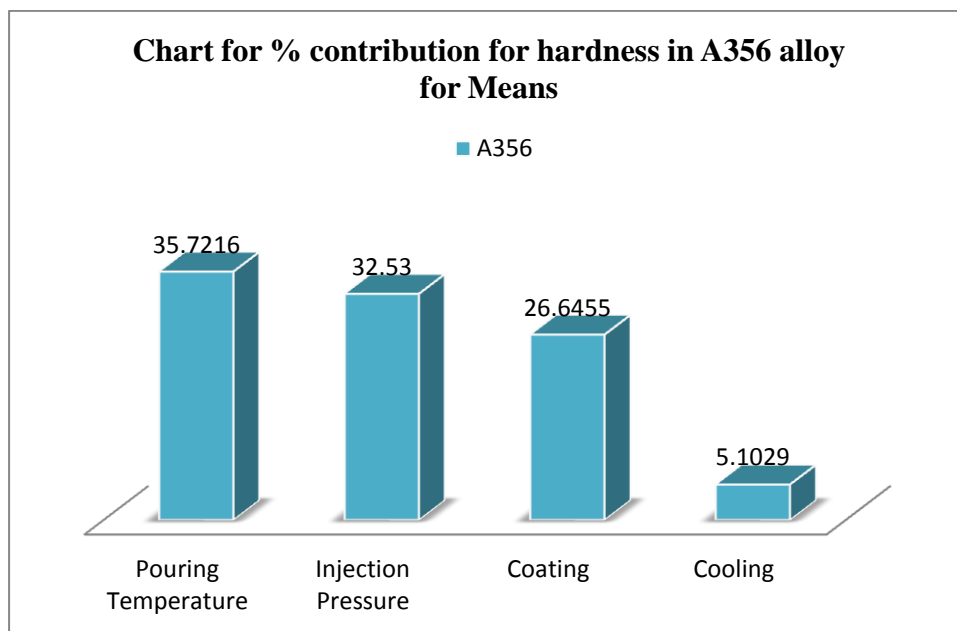


Figure 4.12: Bar chart for percentage contribution in hardness for Means.

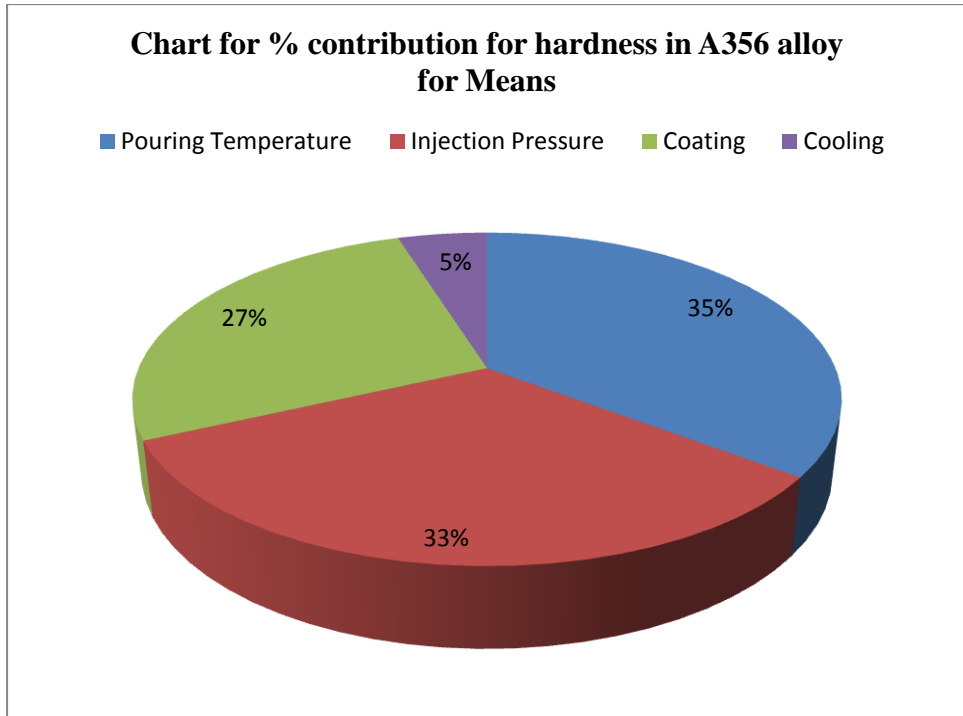


Figure 4.13: Pie chart for percentage contribution in hardness for Means.

Table 4.15: Response Table for Means for hardness

Level	Pouring Temperature	Injection Pressure	Coating Type	Cooling Type
1	77	81.22	77.33	79
2	82.78	77.11	81.67	80.89
3	81.11	82.56	81.89	81
Delta	5.78	5.44	4.56	2
Rank	1	2	3	4

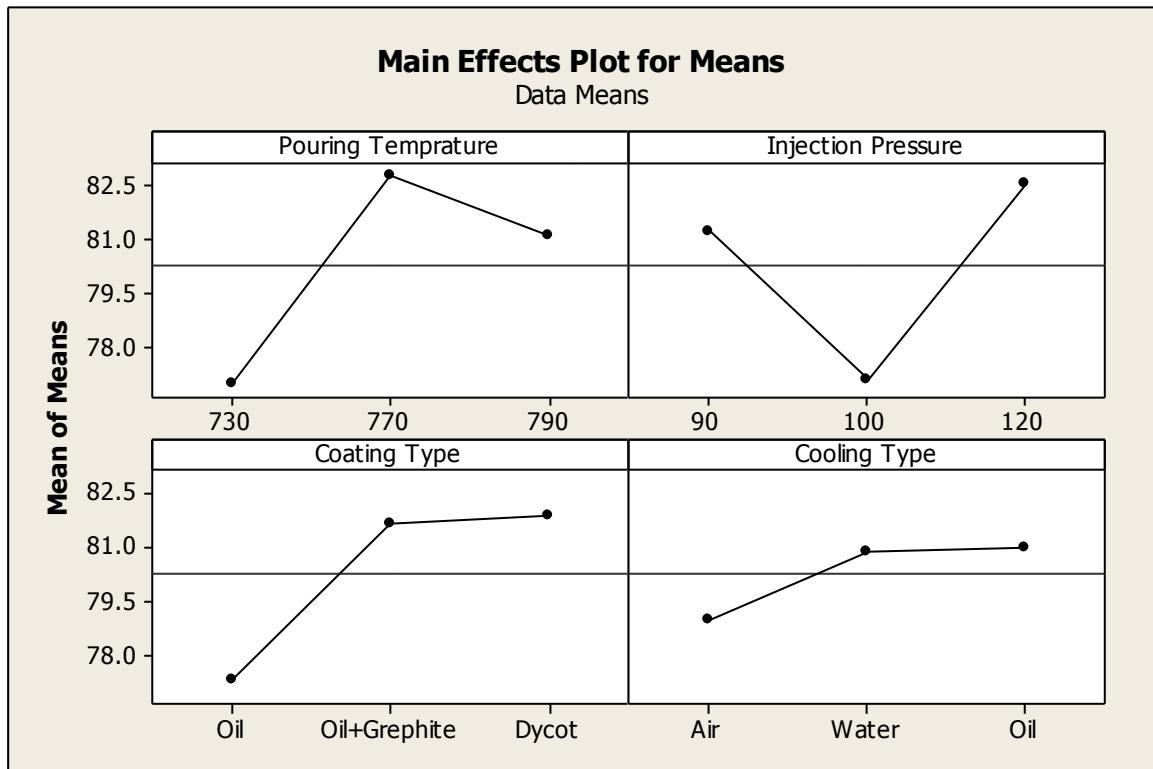


Figure 4.14: Main effects plot for mean hardness

4.12 RESULTS FOR S/N RATIO – HARDNESS

The S/N ratio consolidated several repetitions into one value and is an indication of the amount of variation present in the process. The S/N ratios have been calculated for hardness to identify the major contributing factors and interactions that cause variation in hardness. Hardness is a “Higher the better” type response is given by a logarithmic function based on the mean square deviation (MSD),

$$(S/N)_{HB} = -10 \log (MSD_{HB})$$

$$\text{Where } MSD_{HB} = \frac{1}{r} \sum_{j=1}^r \left(\frac{1}{y_j^2} \right)$$

MSD_{HB} = Mean square Deviation for higher-the-better response

Table 4.16 shows the ANOVA results for S/N ratio of hardness at 95% confidence interval. Except Cooling all other factors are significant. According to F-test Pouring temperature was observed to be the most significant factor affecting the hardness, followed by Injection pressure and coating according to F-test. Table 4.17 shows the rank of various factors in the term of their relative significance. Pouring temperature has the highest rank; signifying

highest contribution to hardness and the Cooling has the lowest rank and was observed to be insignificant in affecting hardness. Main effect plot of S/N ratio for hardness are shown in the Figure 4.16.

Table 4.16: Analysis of Variance for S/N Ratio of Hardness

Factors	DF	Seq SS	Adj MS	F	P
Pouring Temperature	2	0.60519	0.302596	7.253194	35.309
Injection Pressure	2	0.56312	0.281559	6.748939	32.8545
Coating	2	0.46224	0.231118	5.539874	26.9688
Cooling	2	0.08344	0.041719	1	4.8682
e-pooled	2	0.08344	0.041719		
Total	8	1.71398			

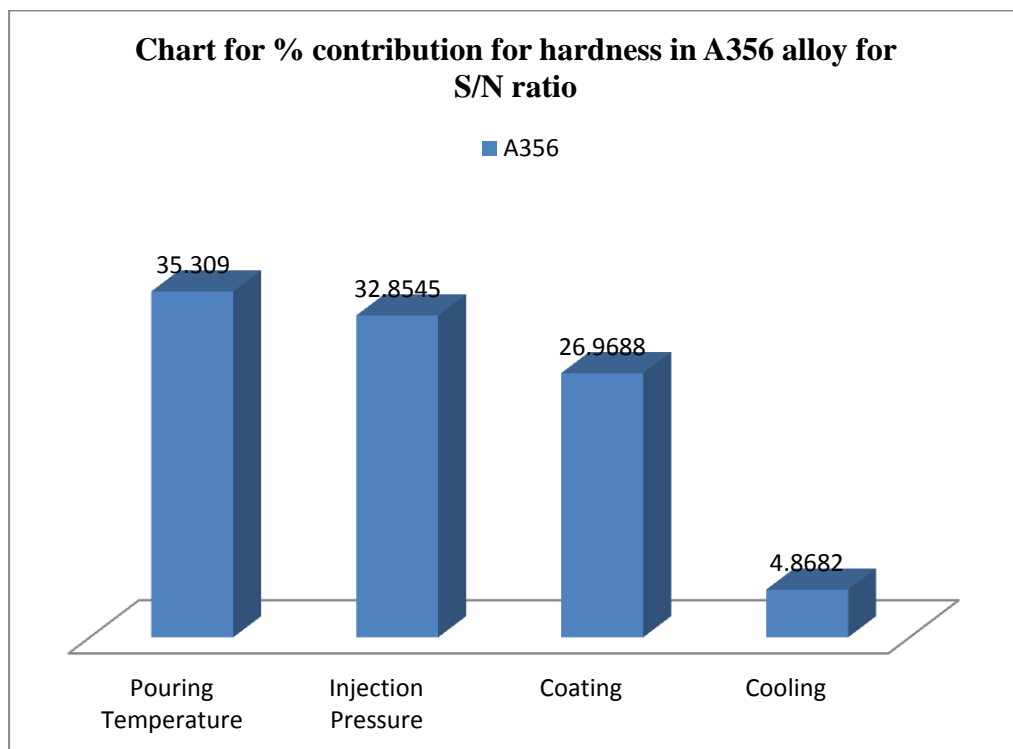


Figure 4.15: Bar chart for percentage contribution in Density for s/n ratio.

Table 4.17: Response Table for S/N Ratio of Hardness

Level	Pouring Temperature	Injection Pressure	Coating Type	Cooling Type
1	37.73	38.18	37.76	37.95
2	38.34	37.74	38.24	38.15
3	38.18	38.33	38.25	38.15
Delta	0.61	0.59	0.49	0.21
Rank	1	2	3	4

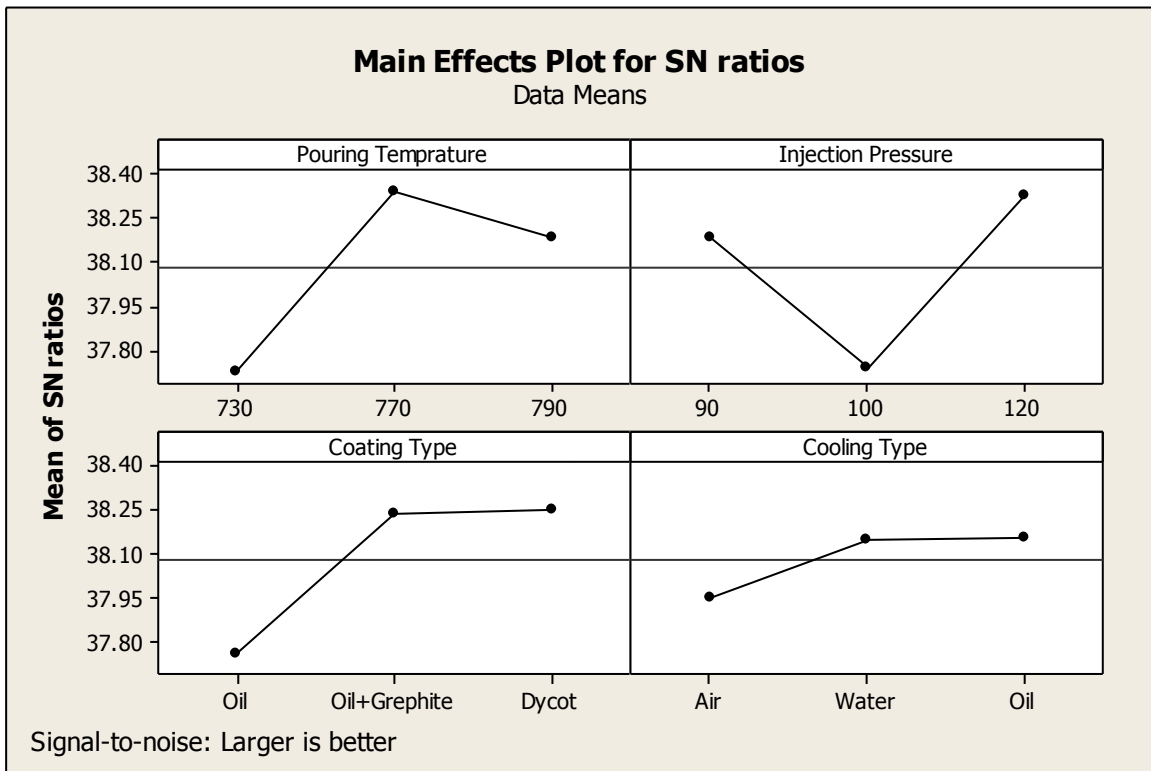


Figure 4.16: Main Effect Plot for S/N Ratio of Hardness

4.13 OPTIMAL DESIGN FOR HARDNESS

In this experimental analysis, the main effect plot in Figure 4.16 and estimate the mean Hardness. From the, Table 4.18 it is concluded that Higher hardness was observed when

Pouring Temperature was kept 770⁰c and injection pressure was kept at 120 kg/cm² and for coating Dycot was used during casting because these decrease variation.

Table 4.18 Significant Factors and Their Levels

Factor	Affecting mean		Affecting variation	
	Contribution	Best level	Contribution	Best level
Pouring Temperature, A	significant	Level -1 , (770°C)	significant	Level -1, (770°C)
Injection Pressure, B	significant	Level-3 (120 kg/cm ²)	significant	Level-3 (120 kg/cm ²)
Coating, C	significant	Level-3 (Dycot)	significant	Level-3 (Dycot)
Cooling, D	Insignificant	-	Insignificant	-

Estimating the mean

Mean value for Hardness

$$\mu_{A_1B_3C_3} = \bar{A}_1 + \bar{B}_3 + \bar{C}_3 - 2\bar{T}$$

$$= 82.777 + 82.555 + 81.888 - 2 * 80.296 = 86.628 \text{HRN}$$

Confidence Interval around the Estimated Mean

Confidence Interval around the estimated hardness mean

$$CI_1 = \sqrt{\frac{F_{\alpha, v_1, v_2} V_e}{n_{eff}}}$$

Where $F_{\alpha, v_1, v_2} = F \text{ ratio}$

$\alpha = \text{risk (0.05)}$ $\text{confidence} = 1 - \alpha$

$v_1 = \text{dof for mean which is always} = 1$

$v_2 = \text{dof for error} = v_e$

$n_{eff} = \text{Number of tests under that condition using the participating factors}$

$$n_{eff} = \frac{N}{1 + \text{dof}_{A,B,C}} = \frac{9}{1 + 2 + 2 + 2} = 1.28$$

$$CI_1 = \sqrt{\frac{F_{\alpha, v_1, v_2} V_e}{n_{eff}}} = \sqrt{\frac{18.5 \times 3.7901}{1.28}} = 7.4011$$

So, the confidence interval around the hardness is given by 86.628 ± 7.4011 HRN.

5.1 INTRODUCTION

The effect of various input parameters i.e. thermal characteristics (temperature of the molten metal), injection pressure of the molten metal, type of coating (Oil Coating, Oil + Graphite Coating, Dycot Coating), and the type of cooling (air cooling, water cooling and oil cooling). The three responses were selected for experimentation namely, surface roughness, density, hardness. The experiment was conducted using A356 and ADC12 aluminium alloy. In this chapter we only concentrate effects on ADC 12 aluminium alloy with same experimental condition explained below. The assignment of factor was carried out using statistical software MINITAB 16. All the factors were varied at three levels. The degree of freedom required for the experiment was calculated to be 8, thus orthogonal array that can be used should have degree of freedom (DOF) less than or equal to 8. L9, which can accommodate factors with 3-levels, was thus used for conduct of experiments to measure three responses namely the surface roughness, density and hardness. After conducting the 9 trials the mean value for all the above factors are tabulated. For the analysis of result Analysis of Variance (ANOVA) was performed.

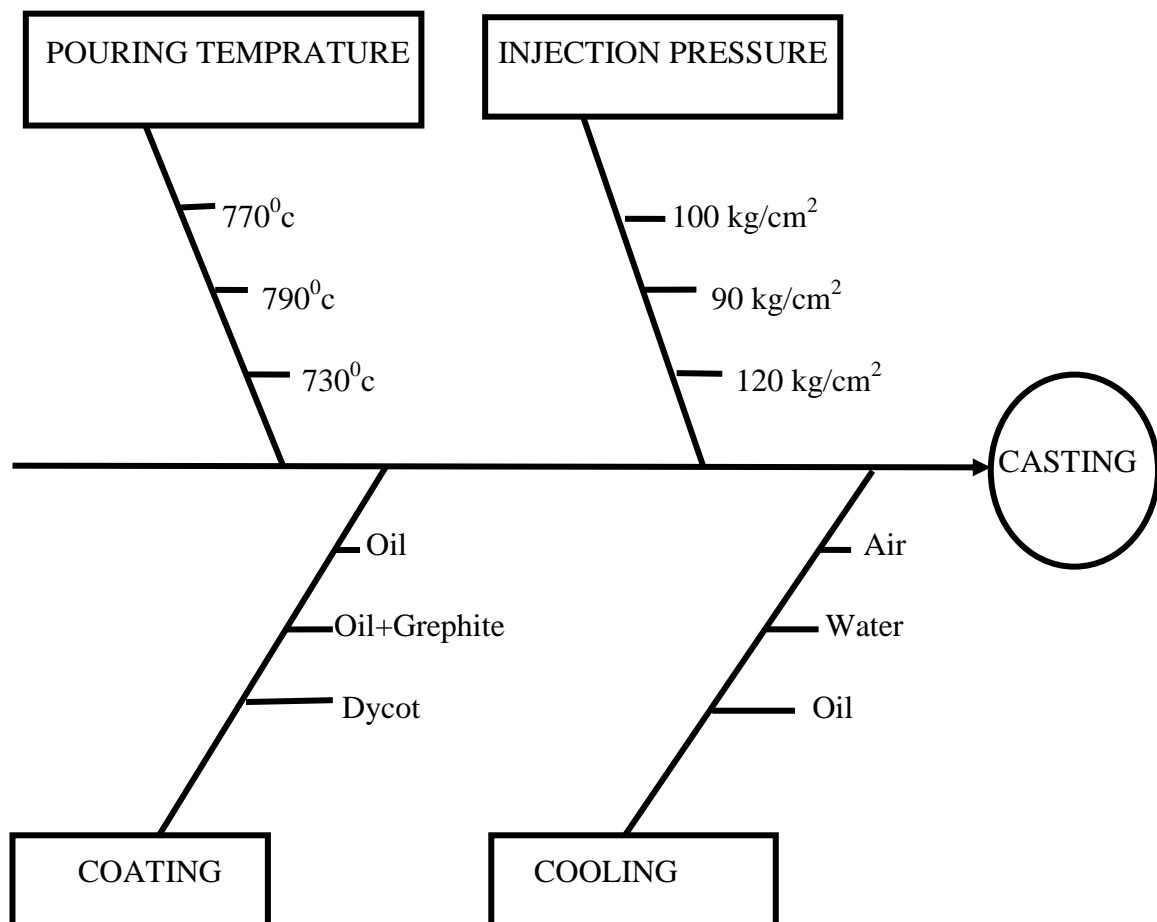


Figure 5.1: Fish bone diagram for process parameter and factors affecting them.

5.2 RESULTS OF SURFACE ROUGHNESS (R_a)

Surface roughness was measured using the Mitutoyo Surftest model SJ-400 available in the Metrology laboratory at Thapar University, Patiala. The result of surface roughness for each of the 9 experiments is given in Table in 5.1.

Table 5.1: Results for Surface Roughness (R_a) for ADC12 Alloy.

Trial No.	Pouring temp.	Injection pressure	Coating type	Cooling type	Mean surface roughness	S/N ratio
1	770	100	Oil	Air	2.78	-8.8809
2	770	90	Oil+Grephte	Water	1.68	-4.5062
3	770	120	Dycot	Oil	1.78	-5.0084
4	790	100	Oil+Grephte	Oil	1.39	-2.8603
5	790	90	Dycot	Air	2.12	-6.5267
6	790	120	Oil	Water	3.66	-11.27
7	730	100	Dycot	Water	1.86	-5.3903
8	730	90	Oil	Oil	1.75	-4.8608
9	730	120	Oil+Grephte	Air	1.81	-5.1536

5.3 ANALYSIS OF VARIANCE- SURFACE ROUGHNESS

The results were analyzed using ANOVA for identifying the significant factors affecting the surface roughness. ANOVA results for the mean surface roughness at 95% confidence interval are given in Table 5.2. The variation data for each factor was tested for F value to find significance of each factor. The principle of F-test is that the larger the F values for a particular parameter, the greater the effect of performance characteristics due to the change in that process parameter. ANOVA analysis showed that Coating (F value 3.83395) was the only factor that significantly affects the surface roughness. All other factors, namely, pouring temperature, Injection pressure and cooling were found to be insignificant. Table 5.3 shows the rank of various factors in the term of their relative significance. Coating has the highest rank, signifying highest contribution to surface roughness and the cooling has the lowest rank and was observed to be insignificant in affecting surface roughness. Main effect plot for the mean surface roughness is shown in the Figure 5.4 which shows the variation of surface roughness with the input parameters. As can be seen surface finish improves with oil+Grephte type coating.

Table 5.2: Analysis of Variance for means of surface roughness (R_a)

Factors	DOF	Seq SS	Adj MS	F	P
Pouring Temperature	2	0.51109	0.25554	1	12.9621
Injection Pressure	2	0.51209	0.25604	1.00196	12.9875
Coating	2	1.95949	0.97974	3.83395	49.6959
Cooling	2	0.96029	0.48014	1.87891	24.3545
Total	8	3.94296			
E pooled	2	0.51109	0.25554		

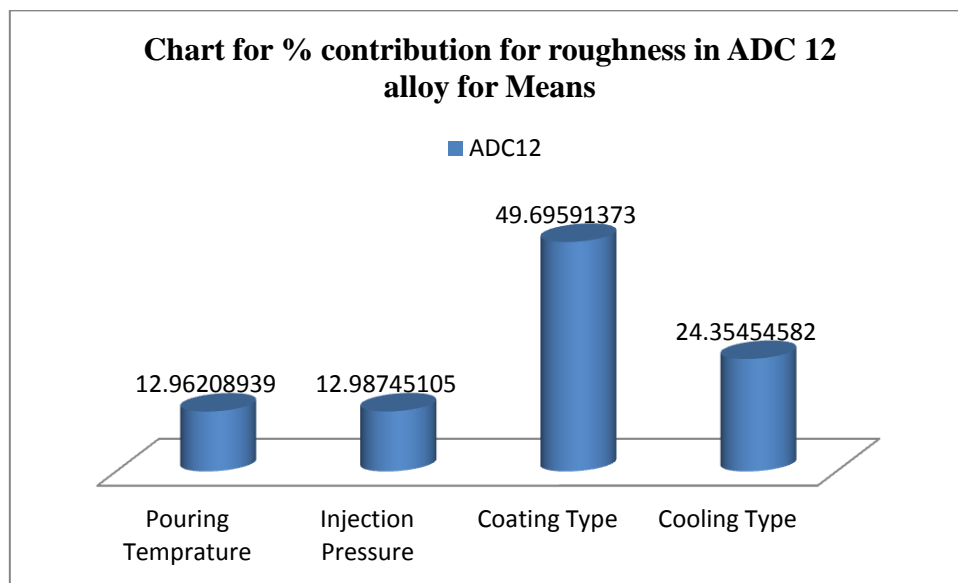


Figure 5.2: Bar chart for percentage contribution in roughness for Means.

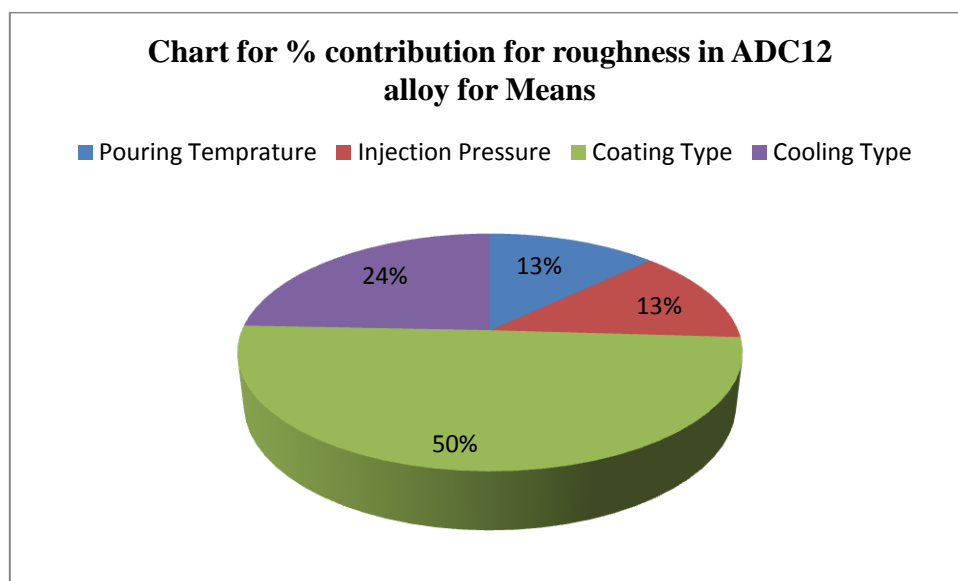


Figure 5.3: Pie chart for percentage contribution in roughness for Means.

Table 5.3: Response Table for Means in Surface Roughness For ADC12 Alloy (R_a)

Level	Pouring Temperature	Injection Pressure	Coating Type	Cooling Type
1	1.807	1.85	2.73	2.237
2	2.08	2.01	1.627	2.4
3	2.39	2.417	1.92	1.64
Delta	0.583	0.567	1.103	0.76
Rank	3	4	1	2

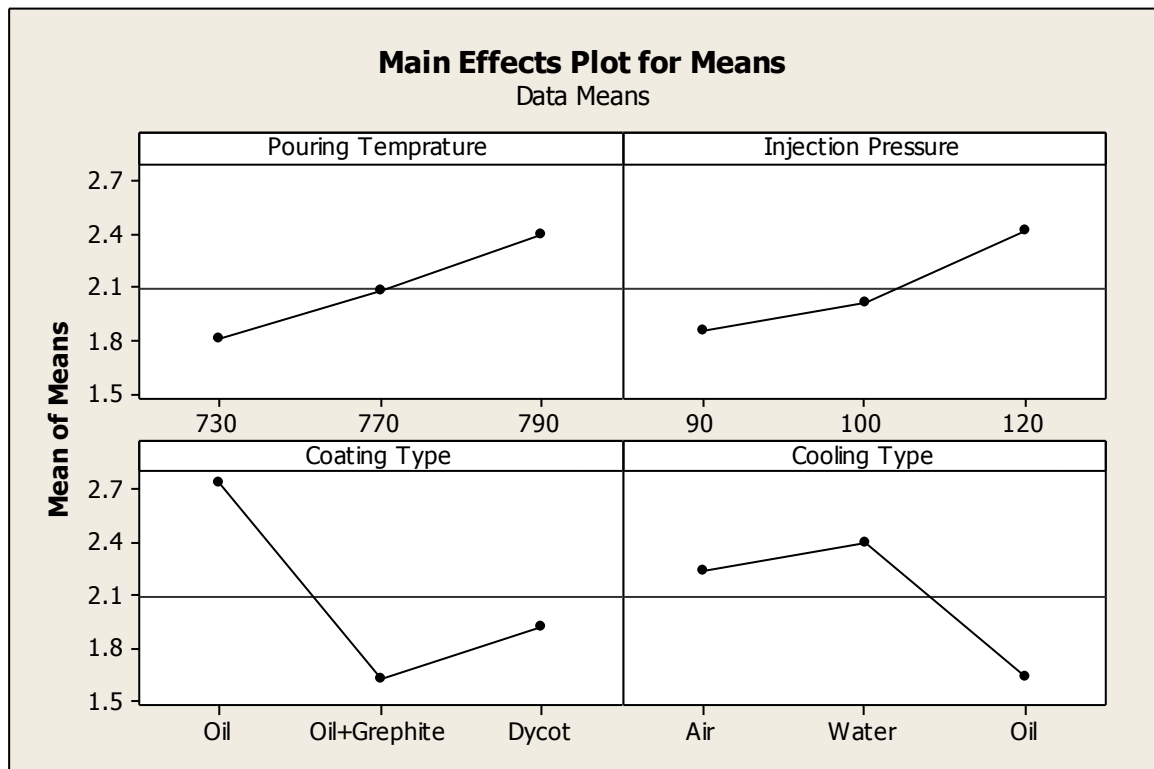


Figure 5.4: Main effect plot for surface roughness

5.4 RESULTS FOR S/N RATIO – SURFACE ROUGHNESS

The S/N ratio consolidated several repetitions into one value and is an indication of the amount of variation present in the process. The S/N ratios have been calculated to identify the major contributing factors and interactions that cause variation in surface roughness. Surface roughness is a “lower the better” type response and is given by a logarithmic function based on the mean square deviation (MSD),

$$S / N_{LB} = -10 \log(MSD) = -10 \log\left(\frac{1}{r} \sum_{i=1}^r y_i^2\right)$$

$$\text{Where } MSD_{LB} = \frac{1}{r} \sum_{j=1}^r (y_j^2)$$

The S/N ratio values are given in the last column of Table 5.1. Table 5.4 shows the ANOVA results for S/N ratio of surface roughness at 95% confidence interval. Other than cooling, all other factors, namely coating, pouring temperature and injection pressures were found to be significant in affecting surface roughness (R_a). According to F-test, coating was observed to be the most significant factor affecting the surface roughness, followed by Cooling and Injection Pressure according to F-test. Main effect plot of S/N ratio for surface roughness are shown in the Figure 5.7.

Table 5.4: Analysis of Variance for S/N ratios of surface roughness in ADC12 Alloy

Source	Seq SS	DOF	Adj MS	F	P
Pouring Temperature	2	4.6269	2.3135	1	8.93547
Injection Pressure	2	5.6324	2.8162	1.21729	10.8773
Coating	2	26.7577	13.3789	5.78297	51.6744
Cooling	2	14.7642	7.3821	3.19088	28.5126
e-pooled	2	4.6269	2.3135		
Total	8	51.7813			

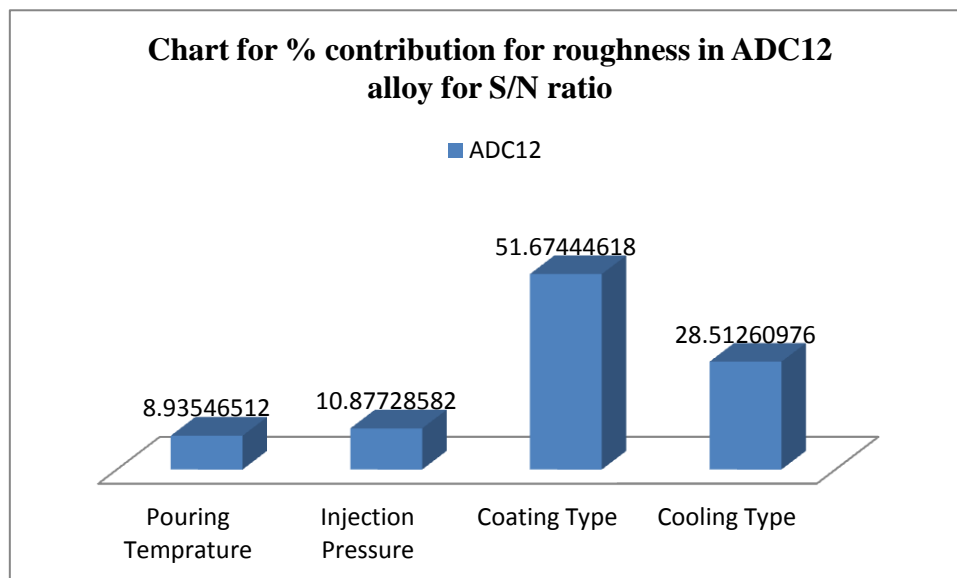


Figure 5.5: Bar chart for percentage contribution in roughness for S/N ratio.

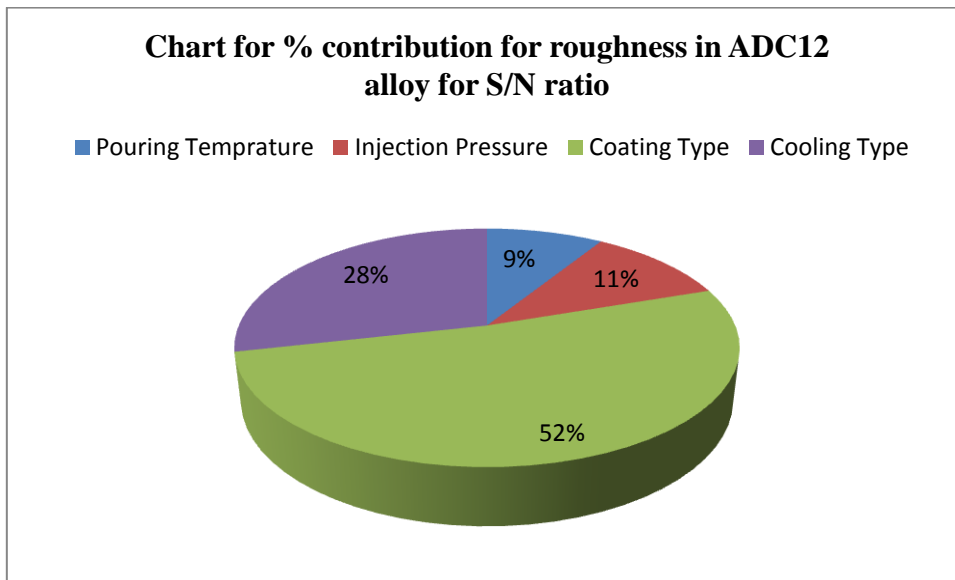


Figure 5.6: Pie chart for percentage contribution in roughness for S/N ratio.

Table 5.5: Response Table for S/N Ratio of Surface Roughness

Level	Pouring Temperature	Injection Pressure	Coating Type	Cooling Type
1	-5.135	-5.298	-8.337	-6.854
2	-6.132	-5.71	-4.173	-7.055
3	-6.886	-7.144	-5.642	-4.243
Delta	1.751	1.846	4.164	2.812
Rank	4	3	1	2

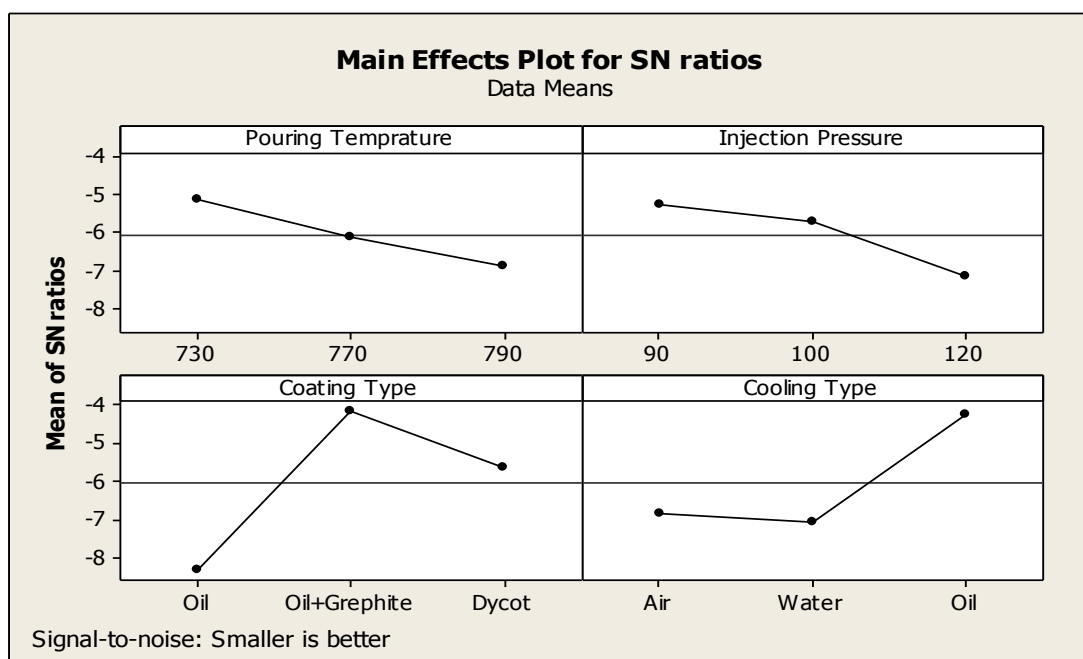


Figure 5.7: Main effects Plot for S/N ratio of surface roughness

5.5 OPTIMAL DESIGN FOR ROUGHNESS

The same level of all the significant factors provide a higher mean value and reduced variability so nothing has to be compromised. The level of factors which improves average and uniformity may conflict, so a compromise may have to be reached. Also a compromise has to occur when multiple responses are considered and the same factor level may cause one response to improve and other to deteriorate [65]. In this experimental analysis, the main effect plot in Figure 5.4 and estimate the mean surface roughness. From the, Table 5.6 it is concluded that lowest roughness was observed when coating type Oil+Grephte is used and pressure was kept at 90 kg/cm². In S/N ratio lowest roughness was observed when coating type Oil was used and pressure was kept at 120 kg/cm², and cooling type water cooling was used as they reduce the variation and improve the surface finish.

Table 5.6 Significant Factors and Their Levels

Factor	Affecting mean		Affecting variation	
	Contribution	Best level	Contribution	Best level
Pouring Temperature, A	insignificant	-	insignificant	Level -3, (790°C)
Injection Pressure, B	significant	Level-2	significant	Level-3, (120kg/cm ²)
Coating, C	significant	Oil+Grephte	significant	Level-1 (Oil)
Cooling, D	insignificant	-	significant	Level-2, (Water)

Estimating the mean

In experimental analysis, surface roughness is a lower average response is better (LB) characteristic. Depending on the characteristic, different treatment combinations has chosen to obtain satisfactory results. After conducting the experiments the optimum treatment condition within the experiments determined on the basis of prescribed combination of factor levels is determined to one of those in the experiment [66].

Mean value for Roughness

$$\begin{aligned} \mu_{B_2 C_2 D_2} &= \overline{B_2} + \overline{C_2} + \overline{D_2} - 2\overline{T} \\ &= 1.85 + 1.62 + 1.64 - 2 \times 2.092 = 0.926 \text{ micron} \end{aligned}$$

Confidence Interval around the Estimated Mean

The confidence interval is a maximum and minimum value between which the true average should fall at some stated percentage of confidence. The estimate of the mean μ is only a point estimate based on the averages of results obtained from the experiment. Statistically this provides a 50% chance of the true averages being greater than μ and a 50% chance of the true average being less than μ [2].

Confidence Interval around the estimated roughness mean

$$CI_1 = \sqrt{\frac{F_{\alpha, v_1, v_2} V_e}{n_{eff}}}$$

Where $F_{\alpha, v_1, v_2} = F$ ratio

$\alpha = \text{risk (0.05)}$ $\text{confidence} = 1 - \alpha$

$v_1 = \text{dof for mean which is always} = 1$

$v_2 = \text{dof for error} = v_e$

$$V_e = \frac{\text{Total pooled variation}}{\text{Total pooled DOF}}$$

$$n_{eff} = \frac{\text{No of Experiments}}{1 + \text{Total DOF associated with } \mu}$$

$$n_{eff} = \frac{N}{1 + \text{dof}_{B,C,D}} = \frac{9}{1 + 2 + 2 + 2} = 1.28$$

$$CI_1 = \sqrt{\frac{F_{\alpha, v_1, v_2} V_e}{n_{eff}}} = \sqrt{\frac{18.5 \times 0.2555}{1.28}} = 1.921$$

So, the confidence interval around the Surface Roughness is given by 0.926 ± 1.921 micron.

5.6 RESULTS FOR DENSITY

The density of the cast material was obtained by using micrometer to conclude the volume and the weight was observed by using the electronic weighing scale available in Workshop at GRIMT, Radaur (Haryana). Density is denoted by $\rho = \frac{\text{Weight}}{\text{volume}}$. The result for density for each of the 9 experiments is given in Table in 5.7.

Table 5.7: Results for Density

Trial No.	Pouring temp.	Injection pressure	Coating type	Cooling type	Mean density	S/N ratio
1	770	100	Oil	Air	2.760004	8.818194
2	770	90	Oil+Grepwhite	Water	2.7051	8.643666
3	770	120	Dycot	Oil	2.7649	8.833589
4	790	100	Oil+Grepwhite	Oil	2.725	8.70733
5	790	90	Dycot	Air	2.725	8.70733
6	790	120	Oil	Water	2.784	8.893385
7	730	100	Dycot	Water	2.75	8.786654
8	730	90	Oil	Oil	2.725	8.70733
9	730	120	Oil+Grepwhite	Air	2.784	8.893385

5.7 ANALYSIS OF VARIANCE- DENSITY

The results were analyzed using ANOVA for identifying the significant factor affecting the performance measures. ANOVA for the mean density at 95% confidence interval is given in Table 5.8. ANOVA table shows that injection pressure (F value (32.231) is the only factor that significantly affects the density. All other factors, namely, Pouring temperature, Coating and cooling type were found to be insignificant. Table 5.9 shows the rank of various factors in the term of their relative significance. Pressure has the highest rank, signifying highest contribution to density and the Pouring temperature has the lowest rank and was observed to be insignificant. Main effect plot for the mean density is shown in the Figure 5.10 which shows the density increase with the increase in injection pressure.

Table 5.8: Analysis of Variance for Means density

Factors	DF	Seq SS	Adj MS	F	P
Pouring Temperature	2	0.000165	0.000082	1	2.560521
Injection Pressure	2	0.005287	0.002643	32.23171	82.04531
Coating	2	0.000503	0.000252	3.073171	7.805711
Cooling	2	0.00049	0.000245	2.987805	7.603973
e-pooled	2	0.000165	0.000082		
Total	8	0.006444			

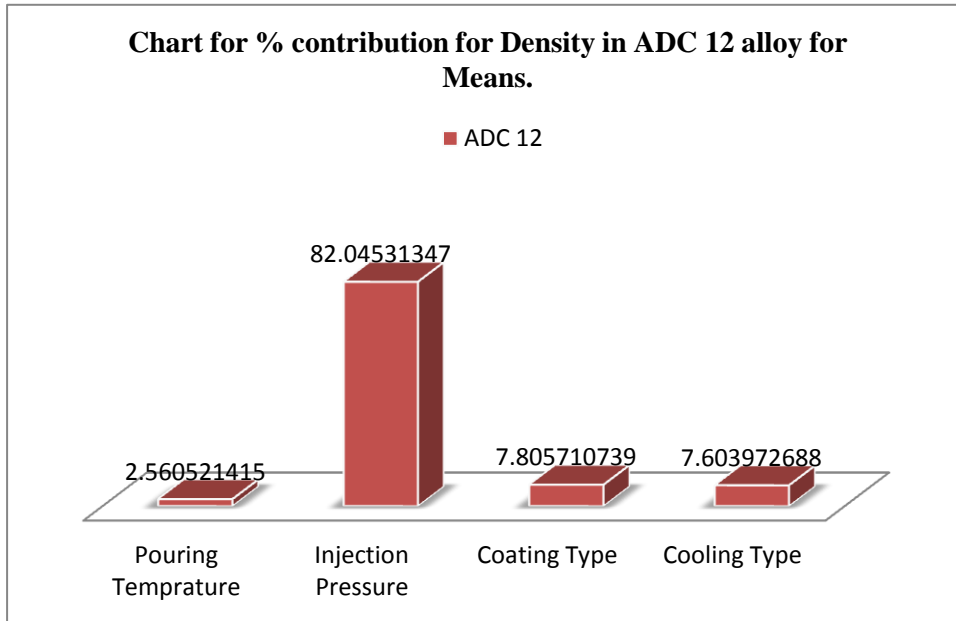


Figure 5.8: Bar chart for percentage contribution in Density for Means.

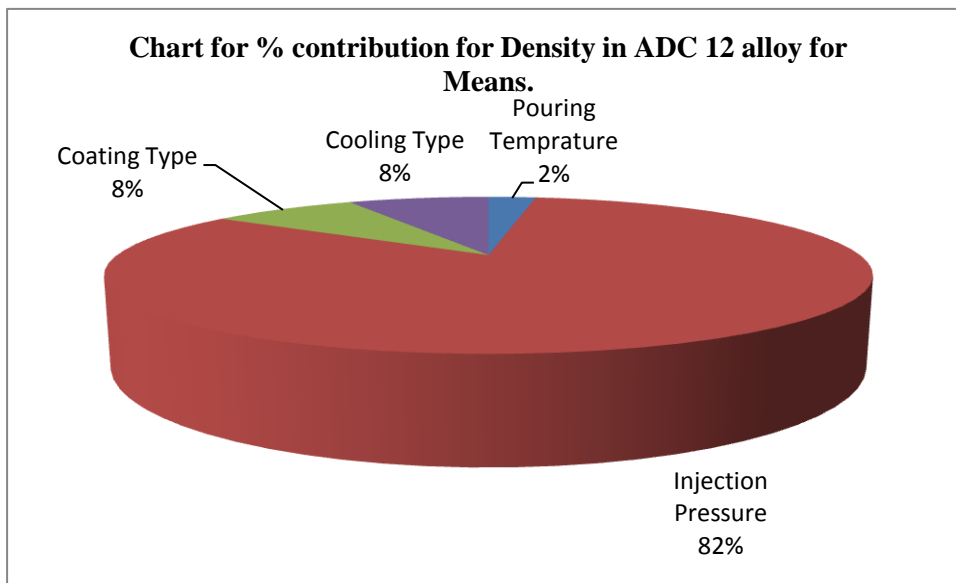


Figure 5.9: Pie chart for percentage contribution in Density for Means.

Table 5.9: Response Table for Means for Density

Level	Pouring Temperature	Injection Pressure	Coating Type	Cooling Type
1	2.753	2.718	2.756	2.756
2	2.743	2.745	2.738	2.746
3	2.745	2.778	2.747	2.738
Delta	0.01	0.059	0.018	0.018
Rank	4	1	2	3

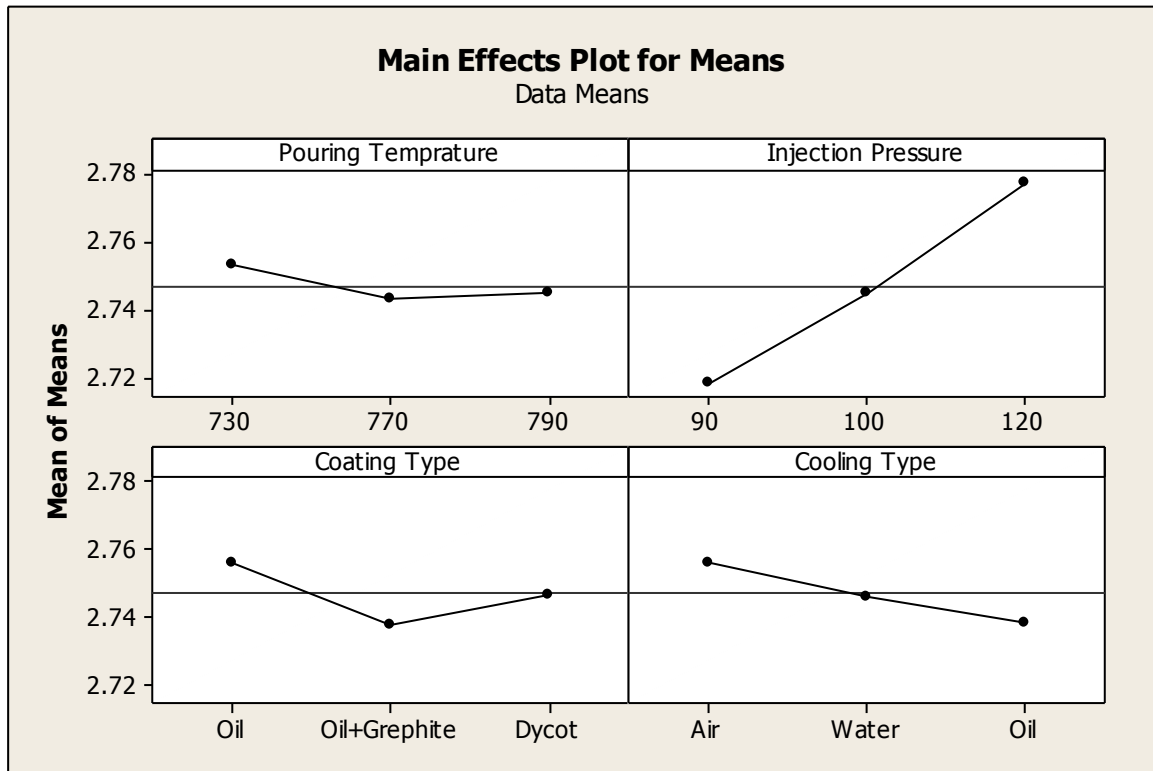


Figure 5.10 Main effect plots for mean density

5.8 RESULTS FOR S/N RATIO – DENSITY

The S/N ratios have been calculated to identify the major contributing factors and interactions that cause variation in density. Density a “Higher the better” type response is given by a logarithmic function based on the mean square deviation (MSD),

$$(S/N)_{HB} = -10 \log (MSD_{HB})$$

$$\text{Where } MSD_{HB} = \frac{1}{r} \sum_{j=1}^r \left(\frac{1}{y_j^2} \right)$$

MSD_{HB} = Mean Square Deviation for higher-the-better response.

Table 5.10 shows the ANOVA results for S/N ratio of density at 95% confidence interval. Except injection pressure all other factor namely Coating, Cooling and Pouring temperature are found to be insignificant. According to F-test injection pressure was observed to be the most significant factor affecting the density, followed at small level by Coating Factor.

Table 5.10: Analysis of Variance for S/N ratio for Density

Factors	DF	Seq SS	Adj MS	F	P
Pouring Temperature	2	0.001656	0.000828	1	2.57055
Injection Pressure	2	0.05281	0.026405	31.8901	81.9751
Coating Type	2	0.00508	0.00254	3.067633	7.885505
Cooling Type	2	0.004876	0.002438	2.944444	7.568843
e-pooled	2	0.001656	0.000828		
Total	8	0.064422			

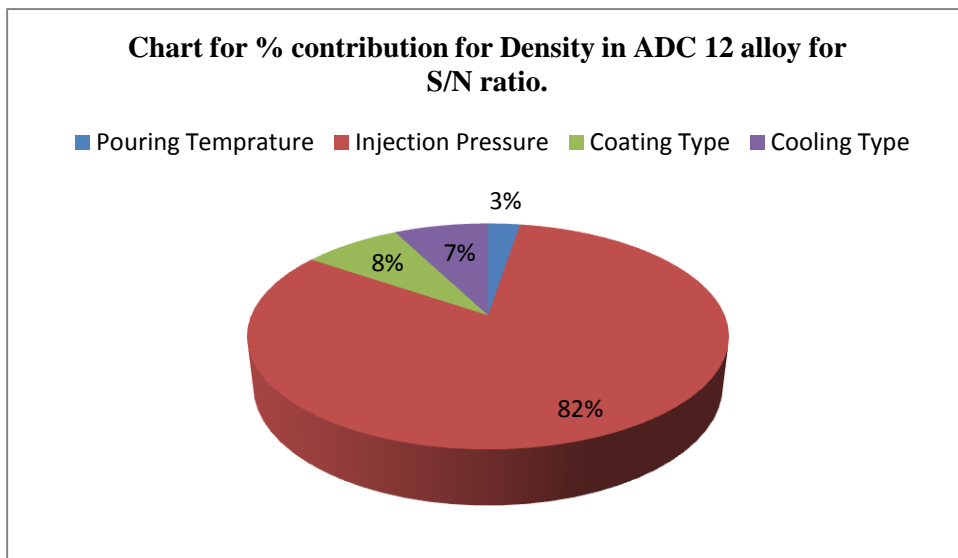


Figure 5.11: Pie chart for percentage contribution in Density for S/N ratio.

Table 5.11: Response Table for S/N Ratio for Density

Level	Pouring Temperature	Injection Pressure	Coating Type	Cooling Type
1	8.796	8.686	8.806	8.806
2	8.765	8.771	8.748	8.775
3	8.769	8.873	8.776	8.749
Delta	0.031	0.187	0.058	0.057
Rank	4	1	2	3

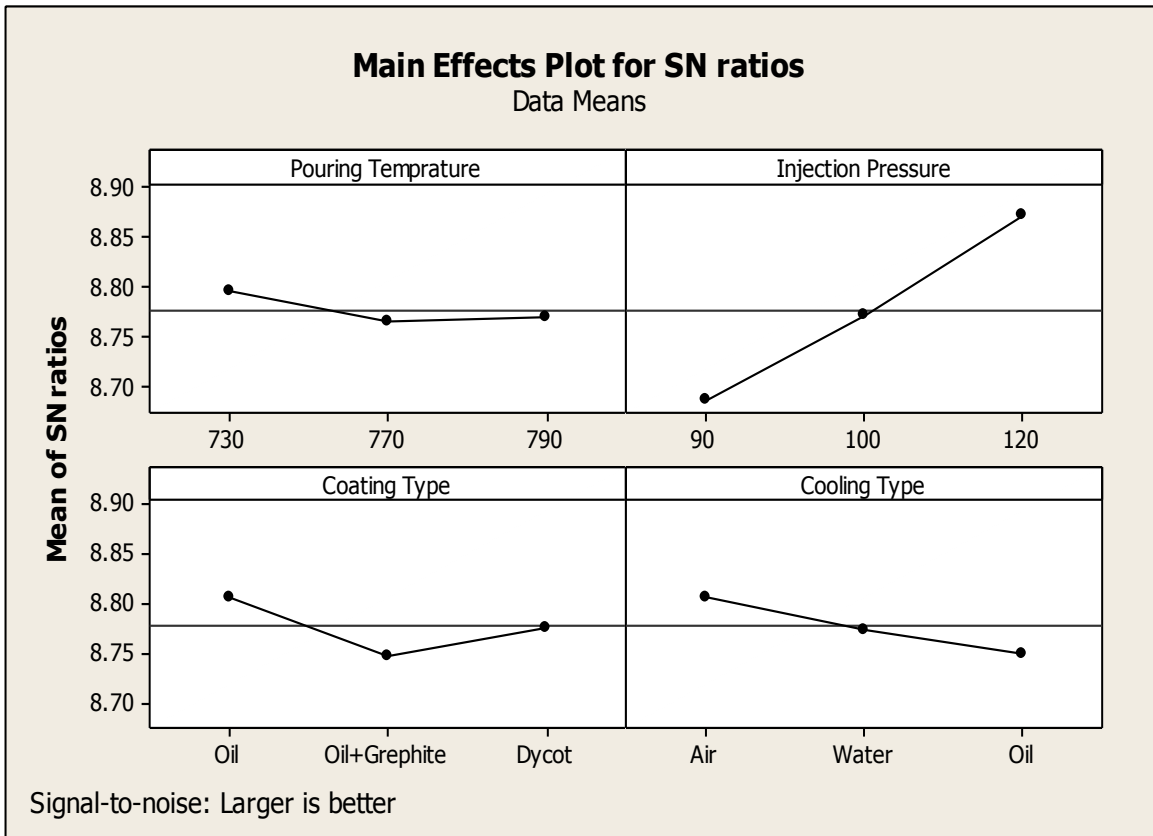


Figure 5.12: Main effect plots for S/N Ratio of density.

5.9 OPTIMAL DESIGN FOR DENSITY

The same level of all the significant factors provide a higher mean value and reduced variability so nothing has to be compromised. In this experimental analysis, the main effect plot in Figure 5.11 and estimate the mean for density. From the, Table 5.12 it is concluded that highest density was observed when injection pressure was kept at 120 kg/cm² and Coating Type Oil is used. In S/N ratio plot 5.12 shows same result.

Table 5.12 Significant Factor and their Levels

Factor	Affecting mean		Affecting variation	
	Contribution	Best level	Contribution	Best level
Pouring Temperature, A	Insignificant	-	Insignificant	-
Injection Pressure, B	significant	Level-3, (120kg/cm ²)	significant	Level-3, (120kg/cm ²)
Coating, C	significant	Level-1 Oil	significant	Level-1 Oil
Cooling, D	insignificant	-	insignificant	-

Estimating the mean

In experimental analysis, density is a higher average response is better (HB) characteristic. After conducting the experiments the optimum treatment condition within the experiments determined on the basis of prescribed combination of factor levels is determined to one of those in the experiment

Mean value for Density

$$\begin{aligned}\mu_{B_3C_1} &= \bar{B}_3 + \bar{C}_1 + - \bar{T} \\ &= 2.777 + 2.756 - 2.747 = 2.786 \text{ gms/mm}^3\end{aligned}$$

Confidence Interval around the Estimated Mean

Confidence Interval around the estimated density mean

$$CI_1 = \sqrt{\frac{F_{\alpha, v_1, v_2} V_e}{n_{eff}}}$$

Where $F_{\alpha, v_1, v_2} = F$ ratio

$\alpha = \text{risk (0.05)}$ $\text{confidence} = 1 - \alpha$

$v_1 = \text{dof for mean which is always} = 1$

$v_2 = \text{dof for error} = v_e$

$n_{eff} = \text{Number of tests under that condition using the participating factors}$

$$n_{eff} = \frac{N}{1 + \text{dof}_{A,B}} = \frac{9}{1 + 2 + 2} = 1.8$$

$$CI_1 = \sqrt{\frac{F_{\alpha, v_1, v_2} V_e}{n_{eff}}} = \sqrt{\frac{18.5 \times 0.000082}{1.8}} = 0.0290$$

So, the confidence interval around the Density is given by $2.786 \pm 0.0290 \text{ gms/mm}^3$.

5.10 RESULTS OF HARDNESS

Hardness was measured on a Rockwell Hardness Tester, (model AVERY 6402) England, available at Mechanics of Solid lab, Thapar University, Patiala. The hardness measurement is

dependent on the diameter of indentation on the samples. The indents formed in the pyramid shaped steel ball indenter were measured on B scale with a minor load of 10 kg for 20 Seconds. The result of hardness for each of the 9 experiments is given in Table in 5.13.

Table 5.13: Results of Hardness

Trial No.	Pouring temp.	Injection pressure	Coating type	Cooling type	Mean hardness	S/N ratio
1	770	100	Oil	Air	90.5	39.13297
2	770	90	Oil+Grephite	Water	84	38.48559
3	770	120	Dycot	Oil	104	40.34067
4	790	100	Oil+Grephite	Oil	104.5	40.38233
5	790	90	Dycot	Air	107	40.58768
6	790	120	Oil	Water	95	39.55447
7	730	100	Dycot	Water	112	40.98436
8	730	90	Oil	Oil	91.5	39.22842
9	730	120	Oil+Grephite	Air	89	38.9878

5.11 ANALYSIS OF VARIANCE- HARDNESS

The results were analyzed using ANOVA for identifying the significant factor affecting the performance measures. The analysis of variance (ANOVA) for the mean hardness at 95% confidence interval is given in Table 5.14. ANOVA table shows that coating (F value 14.767) and Injection Pressure (F value 3.4973) are the factor that significantly affects the hardness, whereas Pouring temperature and Cooling Factor was found to be insignificant. Table 5.15 shows the rank of various factors in the term of their relative significance. Coating has the highest rank; signifying highest contribution to hardness and the Cooling has the lowest rank and was observed to be insignificant in affecting hardness. Main effect plot for the mean hardness is shown in the Figure 5.15.

Table 5.14: Analysis of Variance for Mean Hardness

Factors	DF	Seq SS	Adj MS	F	P
Pouring Temperature	2	130.667	65.333	4.148127	17.71756
Injection Pressure	2	110.167	55.083	3.497333	14.9379
Coating	2	465.167	232.583	14.76717	63.07349
Cooling	2	31.5	15.75	1	4.271186
e-pooled	4	31.5	15.75		
Total	8	737.5			

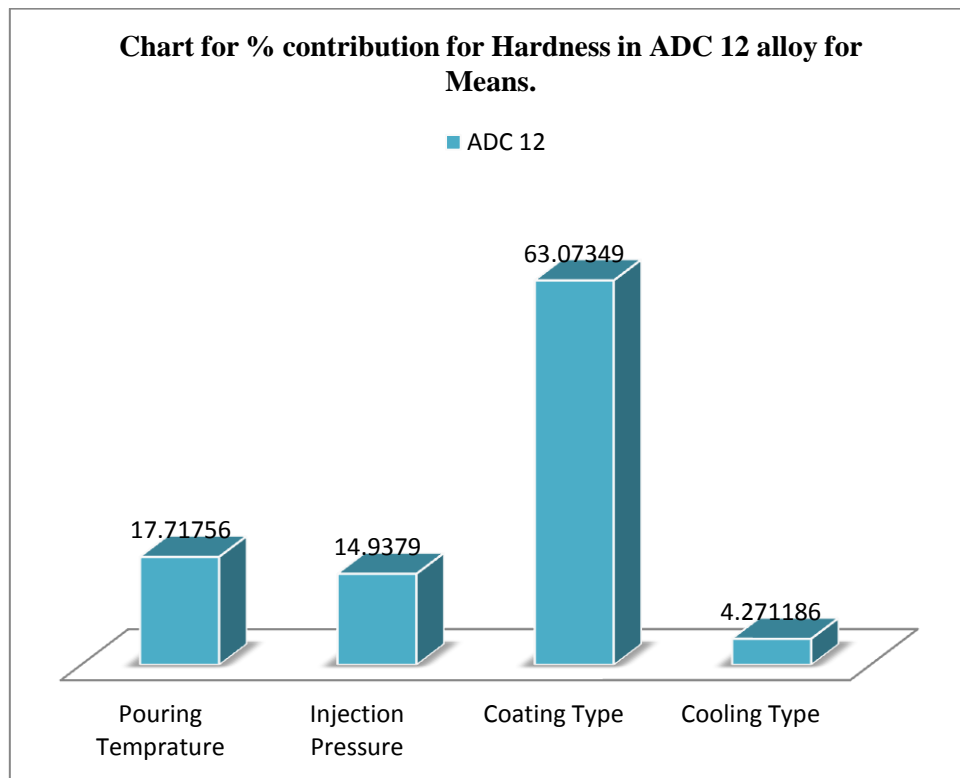


Figure 5.13: Bar chart for percentage contribution in Hardness for Means.

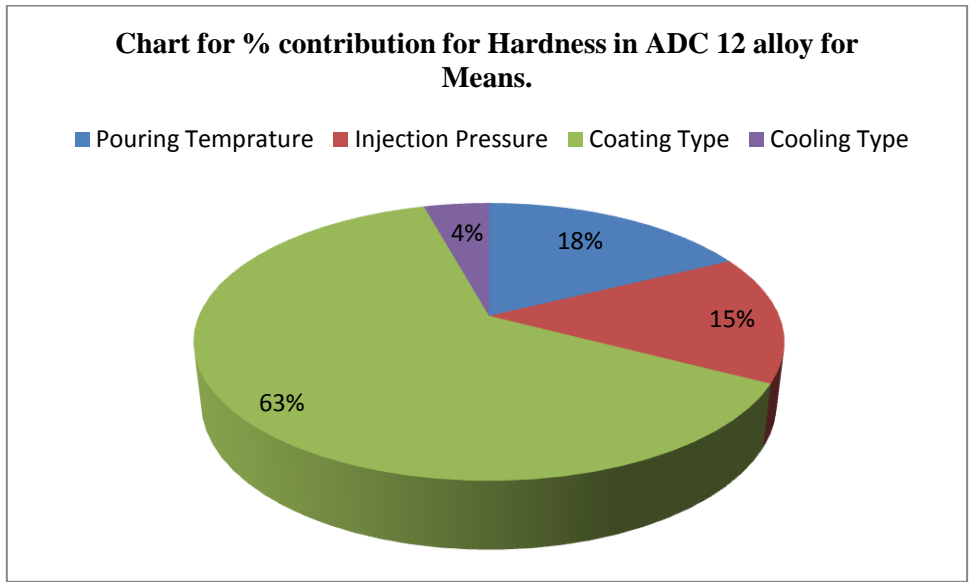


Figure 5.14: Pie chart for percentage contribution in Hardness for Means.

Table 5.15: Response Table for Means for hardness

Level	Pouring Temperature	Injection Pressure	Coating Type	Cooling Type
1	97.5	94.17	92.33	95.5
2	92.83	102.33	92.5	97
3	102.17	96	107.67	100
Delta	9.33	8.17	15.33	4.5
Rank	2	3	1	4

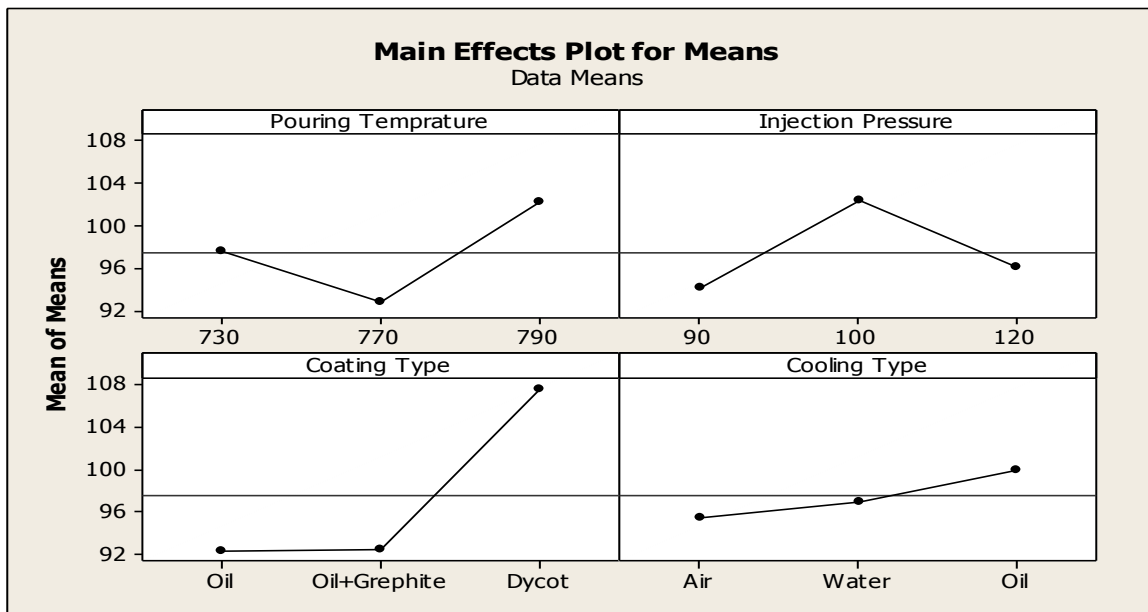


Figure 5.15: Main effects plot for mean hardness.

5.12 RESULTS FOR S/N RATIO – HARDNESS

The S/N ratio consolidated several repetitions into one value and is an indication of the amount of variation present in the process. The S/N ratios have been calculated for hardness to identify the major contributing factors and interactions that cause variation in hardness. Hardness is a “Higher the better” type response is given by a logarithmic function based on the mean square deviation (MSD),

$$(S/N)_{HB} = -10 \log (MSD_{HB})$$

$$\text{Where } MSD_{HB} = \frac{1}{r} \sum_{j=1}^r \left(\frac{1}{y_j^2} \right)$$

MSD_{HB} =Mean square Deviation for higher-the-better response

Table 5.16 shows the ANOVA results for S/N ratio of hardness at 95% confidence interval. Except pouring temperature and cooling, all other factors are significant. According to F-test coating was observed to be the most significant factor affecting the hardness, followed by injection Pressure according to F-test. Table 5.17 shows the rank of various factors in the term of their relative significance. Coating has the highest rank; signifying highest contribution to hardness and the Cooling has the lowest rank and was observed to be insignificant in affecting hardness. Main effect plot of S/N ratio for hardness are shown in the Figure 5.17.

Table 5.16: Analysis of Variance for S/N Ratio of Hardness

Factors	DF	Seq SS	Adj MS	F	P
Pouring Temperature	2	1.09713	0.54856	3.943071	18.77271
Injection Pressure	2	0.86475	0.43237	3.107892	14.79652
Coating	2	3.60417	1.80208	12.95342	61.67004
Cooling	2	0.27824	0.13912	1	4.760894
e-pooled	4	0.27824	0.13912		
Total	8	5.84428			

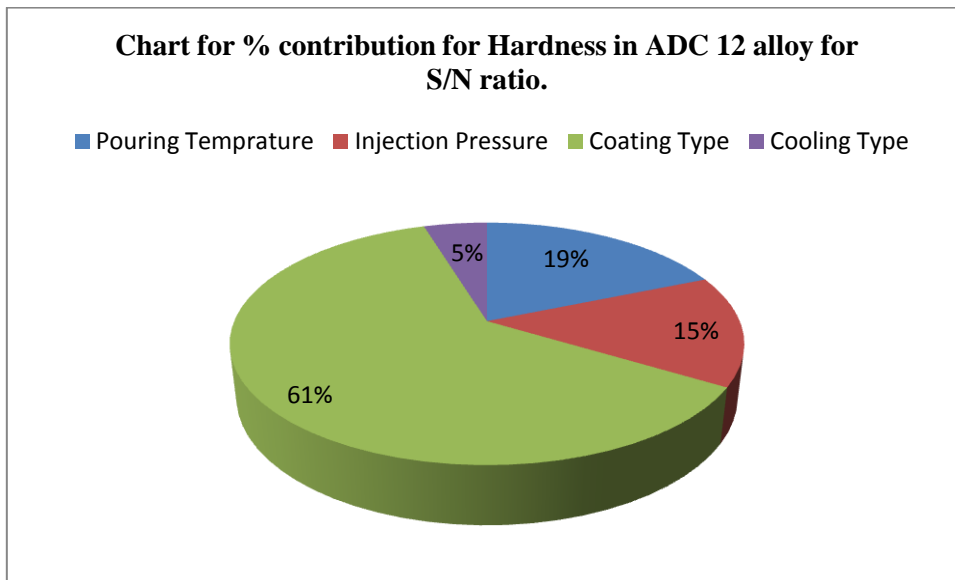


Figure 5.16: Pie chart for percentage contribution in Hardness for S/N ratio.

Table 5.17: Response Table for S/N Ratio of Hardness

Level	Pouring Temperature	Injection Pressure	Coating Type	Cooling Type
1	39.73	39.43	39.31	39.57
2	39.32	40.17	39.29	39.67
3	40.17	39.63	40.64	39.98
Delta	0.86	0.73	1.35	0.41
Rank	2	3	1	4

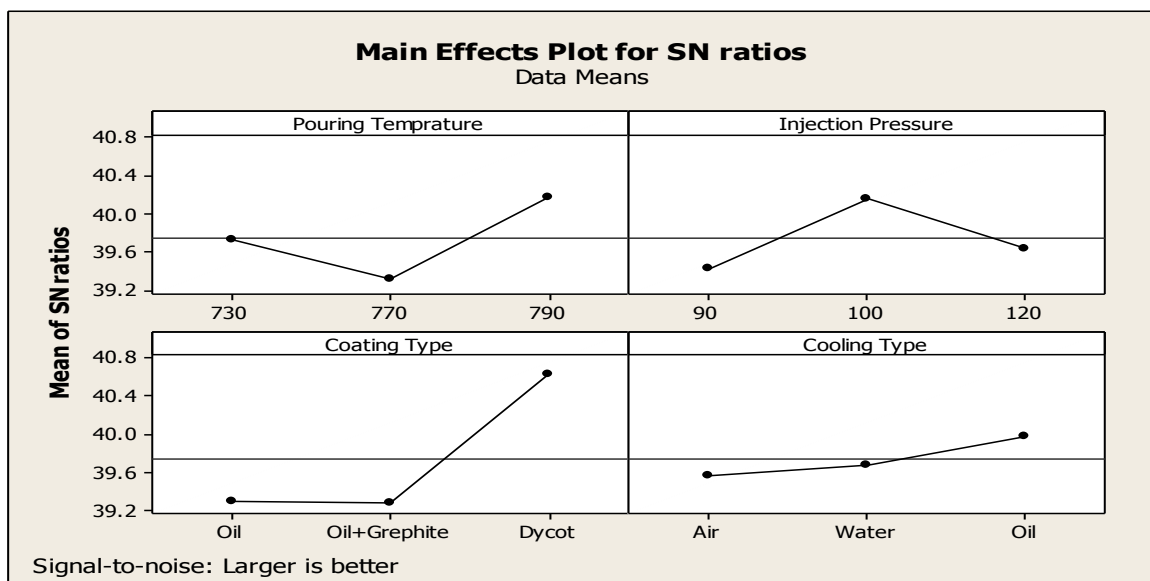


Figure 5.17: Main Effect Plot for S/N Ratio of Hardness

5.13 OPTIMAL DESIGN FOR HARDNESS

In this experimental analysis, the main effect plot in Figure 5.16 and estimate the mean Hardness. From the, Table 5.18 it is concluded that Higher hardness was observed when Coating Type Dycot was used and injection pressure was kept at 100 kg/cm² and for cooling oil cooling was used during casting because these decrease variation.

Table 5.18 Significant Factors and Their Levels

Factor	Affecting mean		Affecting variation	
	Contribution	Best level	Contribution	Best level
Pouring Temperature, A	Insignificant	-	Insignificant	-
Injection Pressure, B	significant	Level-1(100 kg/cm ²)	significant	Level-1 (100 kg/cm ²)
Coating, C	significant	Level-3, (Dycot)	significant	Level-3, (Dycot)
Cooling, D	Insignificant	-	Insignificant	-

Estimating the mean

Mean value for Hardness

$$\begin{aligned}\mu_{B_1C_3} &= \bar{B}_1 + \bar{C}_3 + - \bar{T} \\ &= 102.33 + 107.66 - 97.5 = 112.496 \text{HRN}\end{aligned}$$

Confidence Interval around the Estimated Mean

Confidence Interval around the estimated hardness mean

$$CI_1 = \sqrt{\frac{F_{\alpha, v_1, v_2} V_e}{n_{eff}}}$$

Where $F_{\alpha, v_1, v_2} = F$ ratio

$\alpha = \text{risk (0.05)}$ $\text{confidence} = 1 - \alpha$

$v_1 = \text{dof for mean which is always} = 1$

$v_2 = \text{dof for error} = v_e$

$n_{eff} = \text{Number of tests under that condition using the participating factors}$

$$n_{eff} = \frac{N}{1 + \text{dof}_{B,C}} = \frac{9}{1 + 2 + 2} = 1.8$$

$$CI_1 = \sqrt{\frac{F_{\alpha, v_1, v_2} V_e}{n_{eff}}} = \sqrt{\frac{7.71 \times 7.875}{1.8}} = 5.8078$$

So, the confidence interval around the hardness is given by 112.496 ± 5.807 HRN.

6.1 Introduction

Comparison of alloys is done on the basis of their responses to the input factors and the input factors for both the alloys A356 and ADC 12 are the following

Table 6.1 Analysis of results for A356 casting

Trial No.	Pouring temp. °C	Injection pressure kg/cm ²	Coating type	Cooling type	Mean surface roughness R _a	Mean Density	Mean Hardness
1	770	100	Oil Coating	Air Cooling	1.105	2.6733	75.3333
2	770	90	Oil+ Graphite	Water Coolig	2.93	2.6617	85.6667
3	770	120	Dycot	Oil Cooling	1.53	2.6838	87.3333
4	790	100	Oil+ Graphite	Oil Cooling	1.67	2.6772	80
5	790	90	Dycot	Air Cooling	1.82	2.6624	82.3333
6	790	120	Oil Coating	Water Coolig	1.545	2.6761	81
7	730	100	Dycot	Water Coolig	2.13	2.6711	76
8	730	90	Oil Coating	Oil Cooling	2.075	2.6645	75.6667
9	730	120	Oil+ Graphite	Air Cooling	2.84	2.6853	79.3333

Table 6.2 Analysis of results for ADC12 casting

Trial No.	Pouring temp. °C	Injection pressure kg/cm ²	Coating type	Cooling type	Mean surface roughness R _a	Mean Density	Mean Hardness
1	770	100	Oil Coating	Air Cooling	2.78	2.760004	90.5
2	770	90	Oil+ Graphite	Water Coolig	1.68	2.7051	84
3	770	120	Dycot	Oil Cooling	1.78	2.7649	104
4	790	100	Oil+ Graphite	Oil Cooling	1.39	2.725	104.5
5	790	90	Dycot	Air Cooling	2.12	2.725	107
6	790	120	Oil Coating	Water Coolig	3.66	2.784	95
7	730	100	Dycot	Water Coolig	1.86	2.75	112
8	730	90	Oil Coating	Oil Cooling	1.75	2.725	91.5
9	730	120	Oil+ Graphite	Air Cooling	1.81	2.784	89

Table 6.3: Percentage Contribution for roughness (R_a) for means.

Factors	P(A356)	P(ADC12)
Pouring Temperature	24.5312	12.9621
Injection Pressure	20.8513	12.9875
Coating	44.391	49.6959
Cooling	10.2269	24.3545

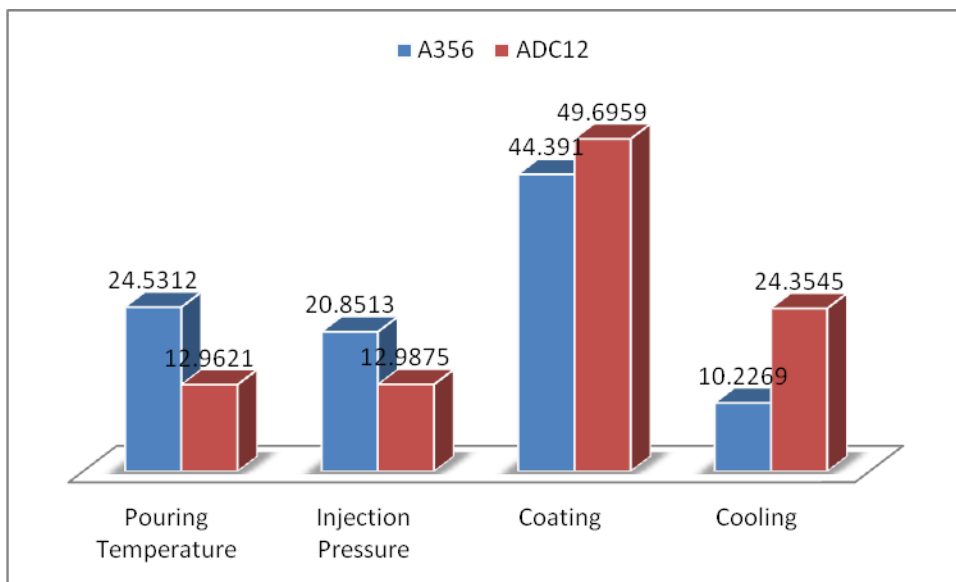


Figure 6.1: Bar chart for percentage contribution in roughness for Means.

6.2 Comparison for Roughness

From the above comparisons of for roughness it is very clear from fig 6.1 that pouring temperature has more influence for roughness in A356 alloy than ADC12 alloy and injection pressure has also the same influence on A356 but coating and cooling are more influencing in

ADC12 then A356 alloy so by controlling these input influencing parameter we can control the quality of the product

Table 6.4: Percentage Contribution for Density for means.

Factor	A356	ADC 12
Pouring Temperature	0.81833	2.560521
Injection Pressure	88.216	82.04531
Coating	2.94599	7.805711
Cooling	8.01964	7.603973

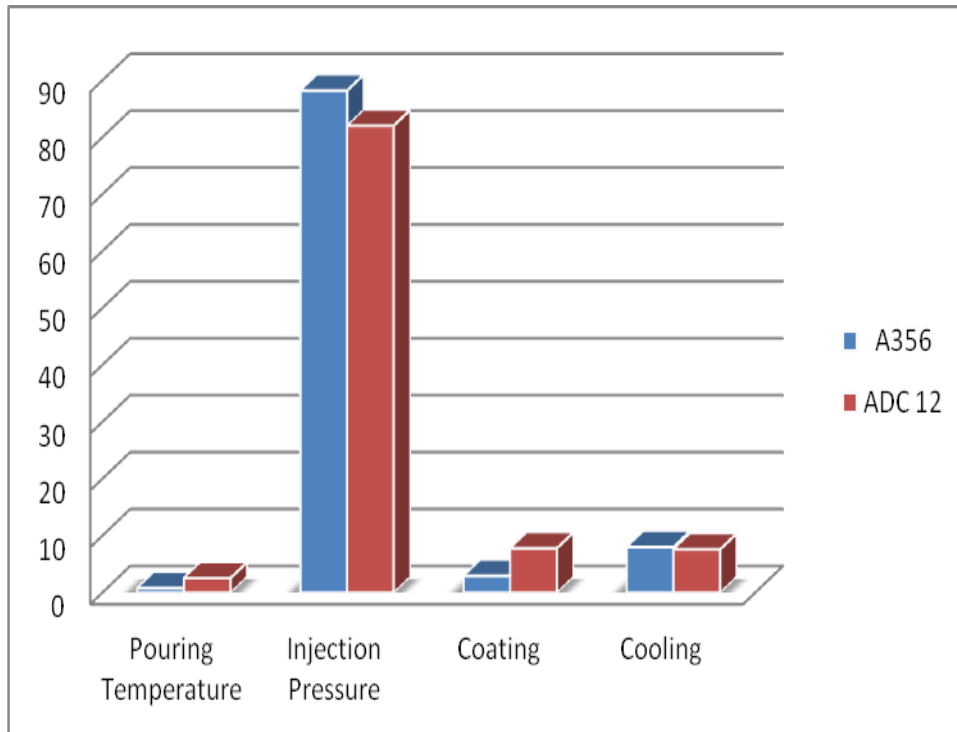


Figure 6.2: Bar chart for percentage contribution in Density for Means.

6.3 Comparison for Density

In this comparisons for density of A356 and ADC12 alloy all the input factor have nearly same influence but injection pressure shows the greatest influence on both the alloys and more in case of A356 alloy.

Table 6.5: Percentage Contribution for Hardness for means in A356 and ADC 12 alloy.

Factor	A356	ADC12
Pouring Temperature	35.7216	17.71756
Injection Pressure	32.53	14.9379
Coating	26.6455	63.07349
Cooling	5.1029	4.271186

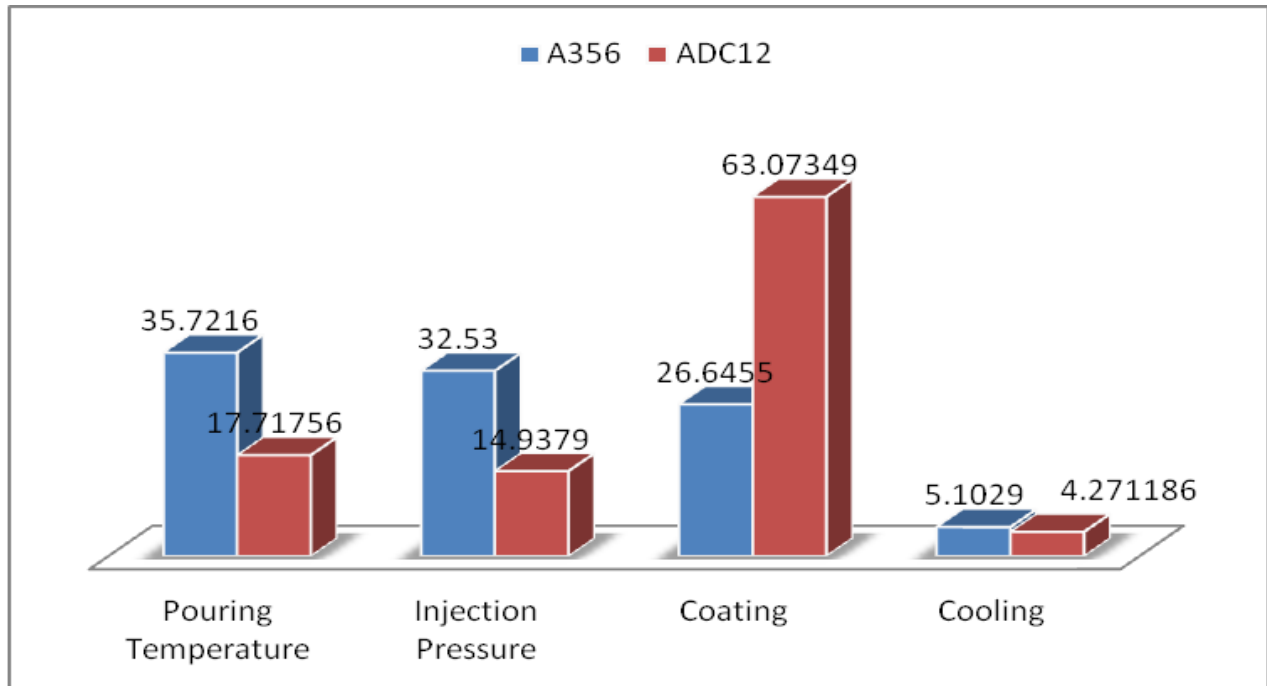


Figure 6.3: Bar chart for percentage contribution in Hardness for Means.

6.4 Comparison for Hardness

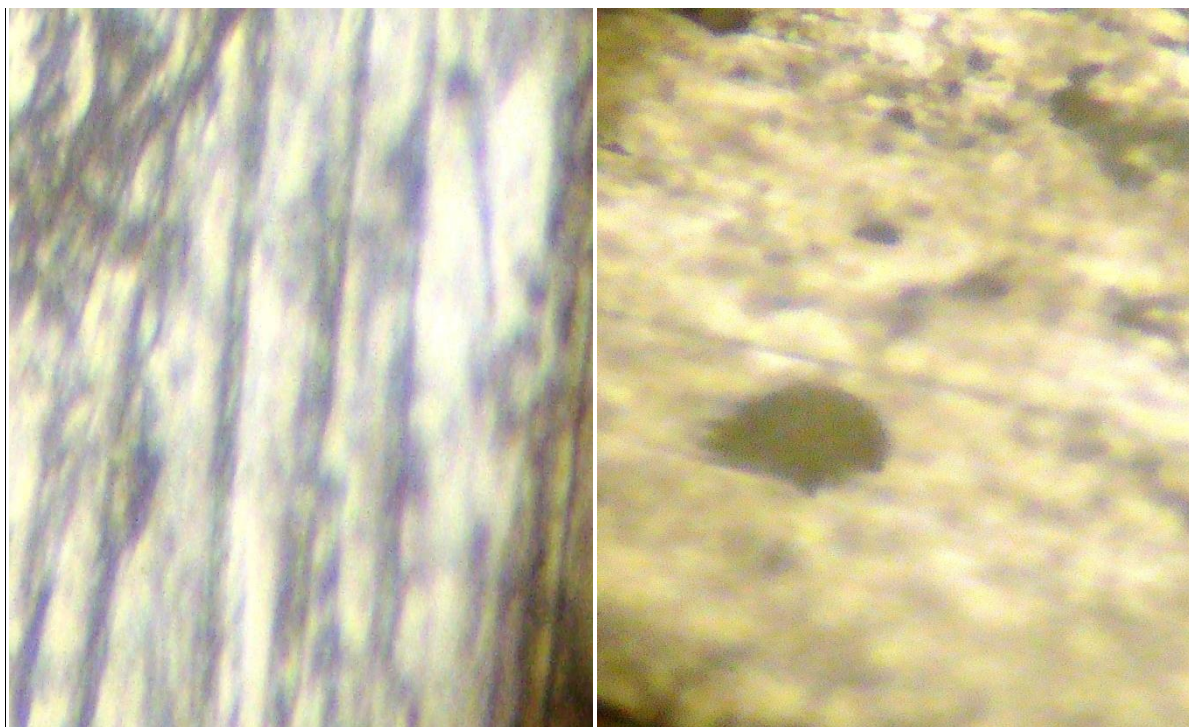
The above comparison for percentage contribution in Hardness show the variable effect of different input parameters on both the alloys. A356 is more influenced by pouring temperature, injection pressure and ADC12 is more influenced by coating used during the high pressure die casting process and moderately influenced by other input parameters.

So above comparisons gives us a conclusion that both the material of Aluminium alloy A356 and ADC12 under same input conditions show different behaviours and gives us an idea about cost saving and enhancing the quality of product by controlling the input conditions to both the product separately.

7.1 INTRODUCTION

Microstructure of the A356 and ADC12 alloy analyzed to know the difference between the alloys characteristics under the same condition of high pressure die casting at different stages and to check the suitability of process parameter with good microstructure of the alloys.

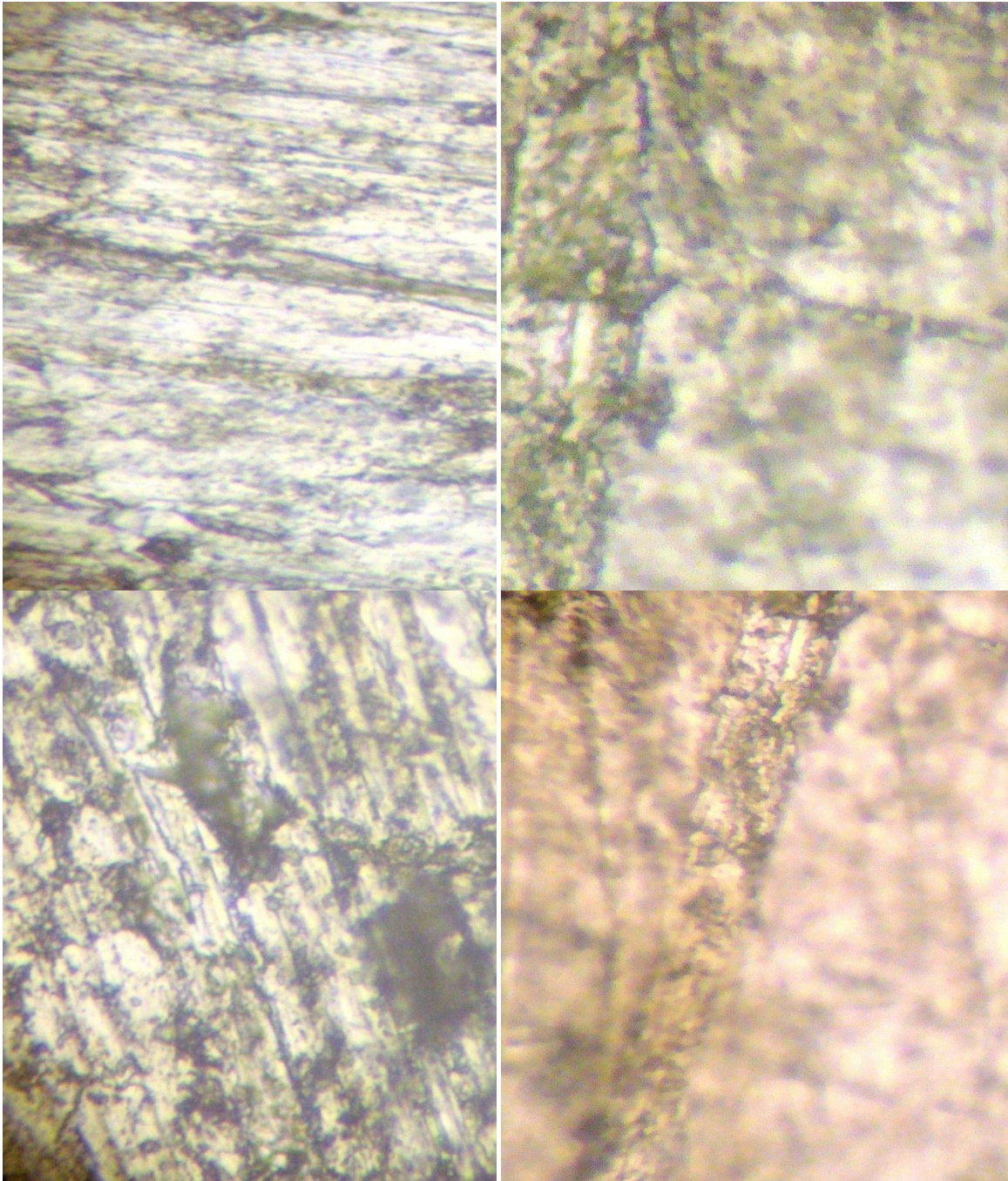
The aluminium-silicon alloys possess exceptional casting characteristics, which enable them to be used to produce intricate castings of thick and thin sections. Fluidity and freedom from hot tearing increase with silicon content and are excellent throughout the range. The ductility of alloys enables castings to be easily rectified or modified in shape, e.g., simple components may be cast straight, and later bent to the required contour. A356 is observed to be more ductile than ADC 12 and ADC12 is observed to be more harder than A356.



A356

ADC12

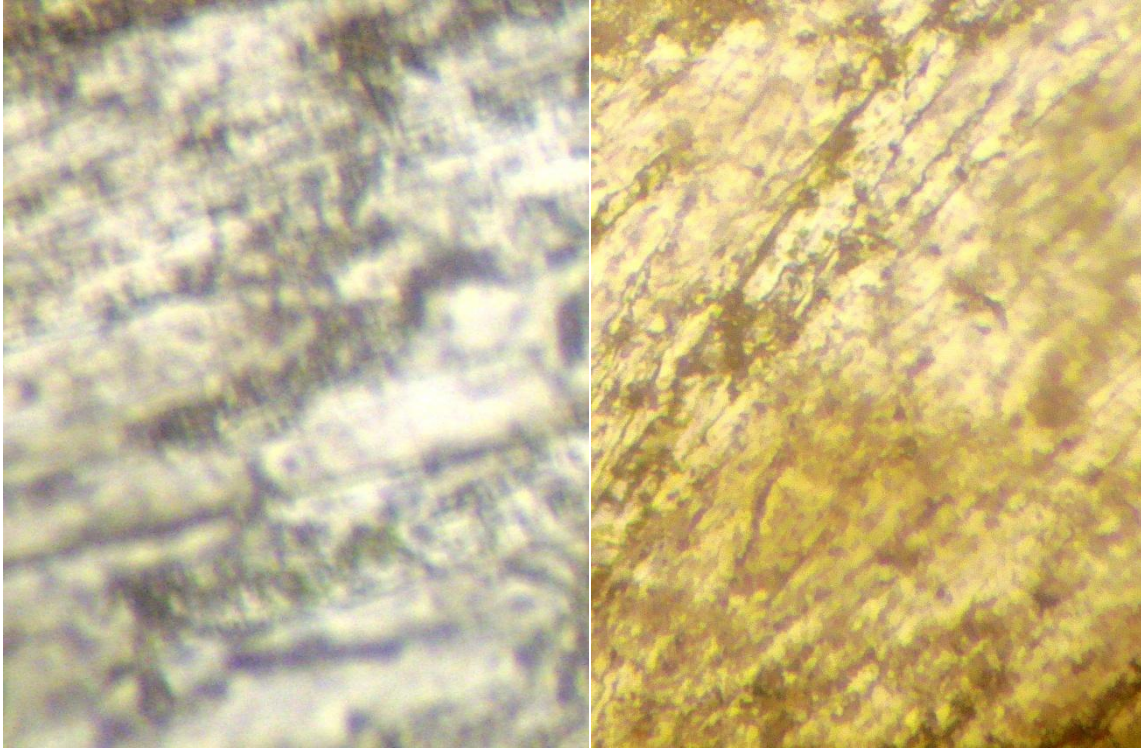
Figure 7.1 Microstructure of A356 and ADC 12 Pouring Temperature 770⁰c, and Injection pressure 100 Kg/cm², Oil Coating, Air Cooling.



A356

ADC12

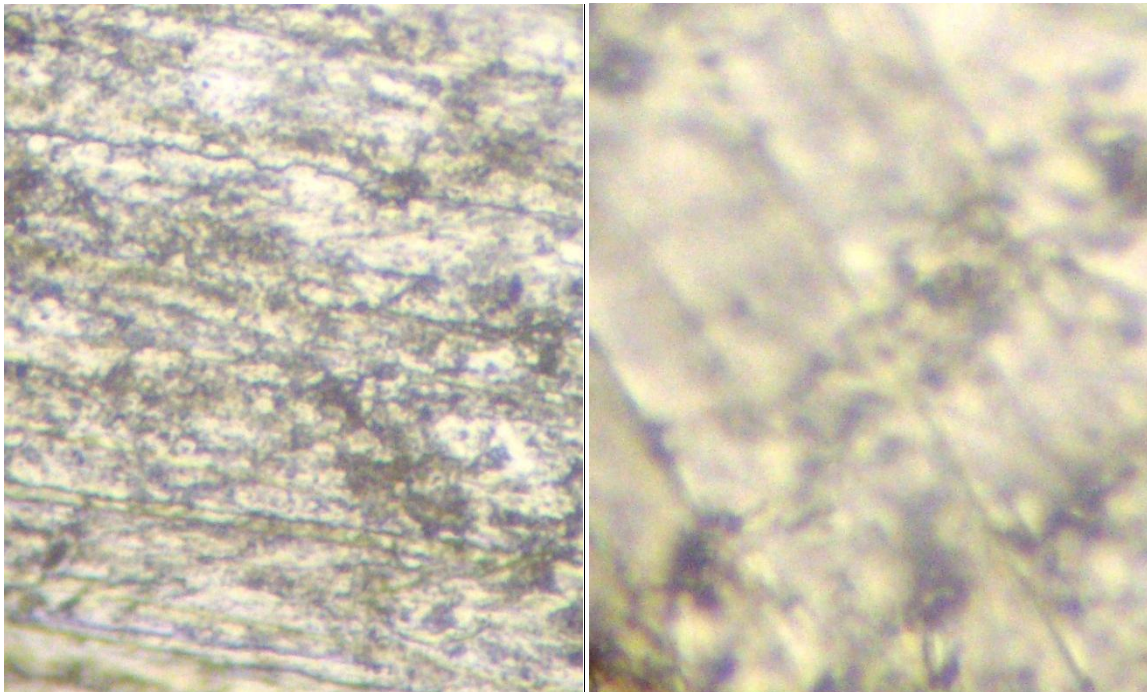
Figure 7.2 Microstructure of A356 and ADC 12, Pouring Temperature 770⁰c, Injection pressure 90 Kg/cm², Oil Graphite Coating, Water Cooling.



A356

ADC12

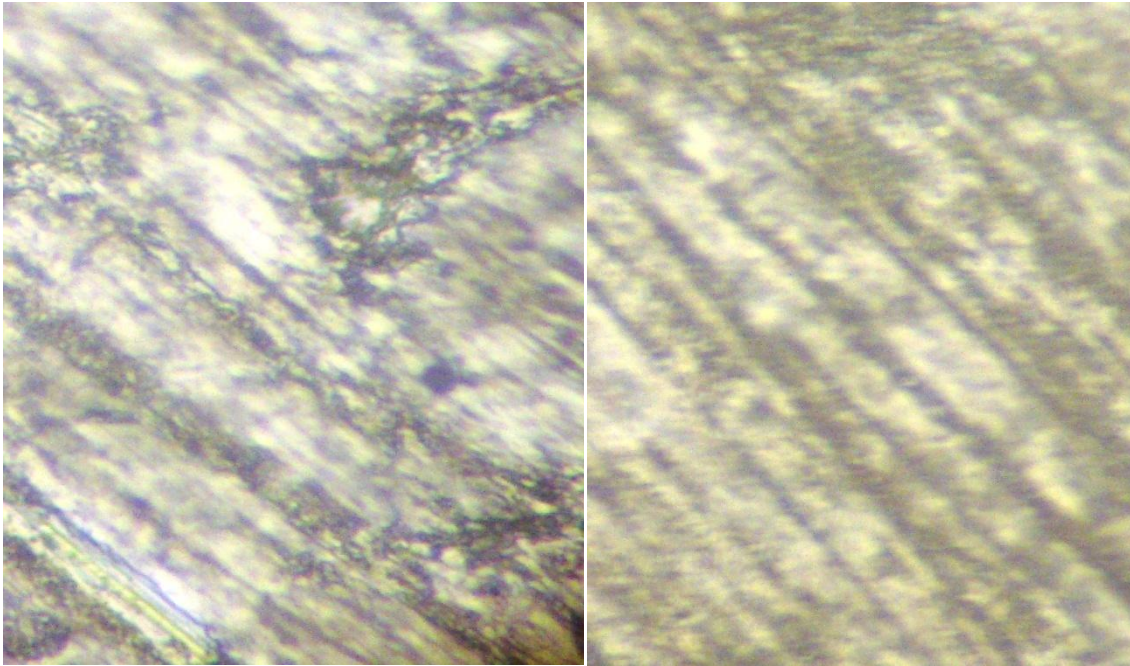
Figure 7.3 Microstructure of A356 and ADC12 Pouring Temperature 770⁰c and Injection pressure 120 Kg/cm², Dycot Coating, Oil Cooling.



A356

ADC12

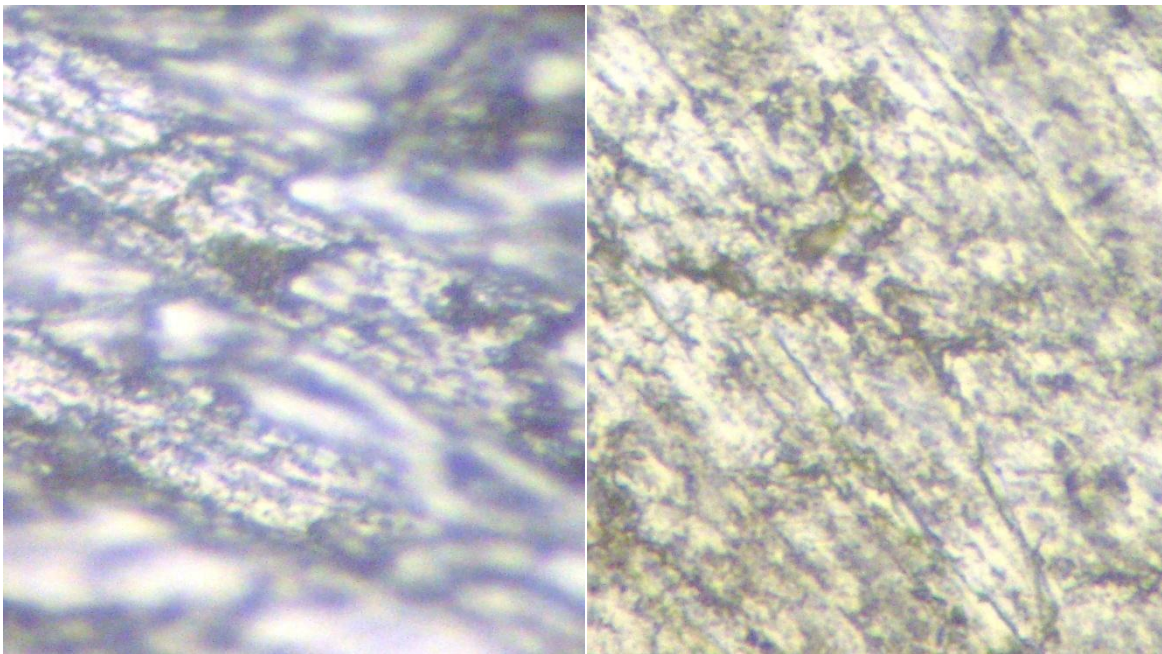
Figure 7.4 Microstructure of A356 and ADC12, Pouring Temperature 790⁰, and Injection pressure 100 Kg/cm², Oil Graphite Coating, Oil Cooling.



A356

ADC12

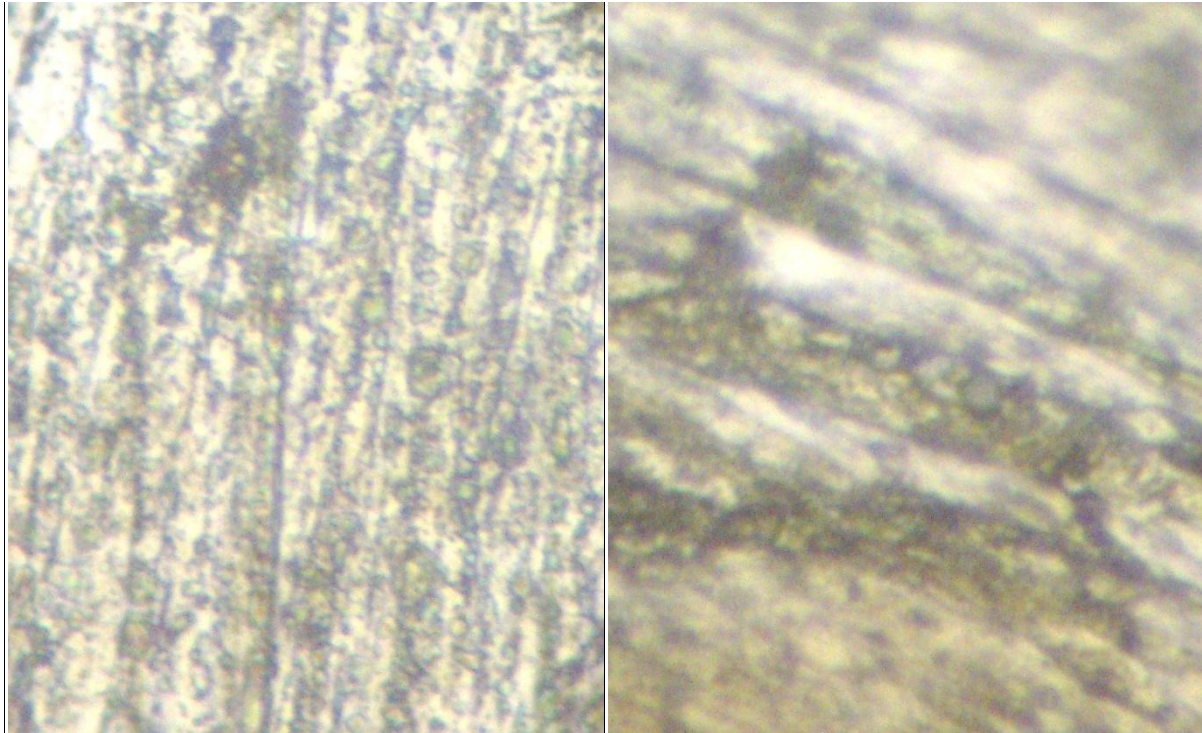
Figure 7.5 Microstructure of A356 and ADC12, Pouring Temperature 790⁰c , Injection pressure 90 Kg/cm², Dycot Coating, Air Cooling.



A356

ADC12

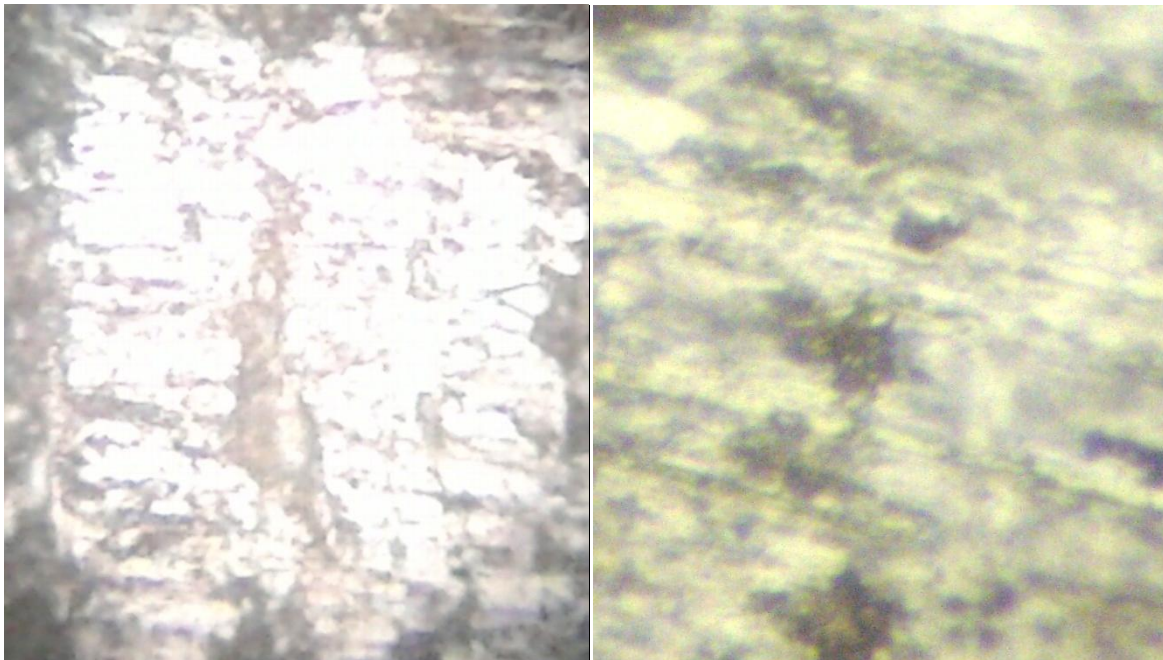
Figure 7.6 Microstructure of A356 and ADC12, Pouring Temperature 790⁰c, Injection pressure 120 Kg/cm², Oil Coating, and Water Cooling.



A356

ADC12

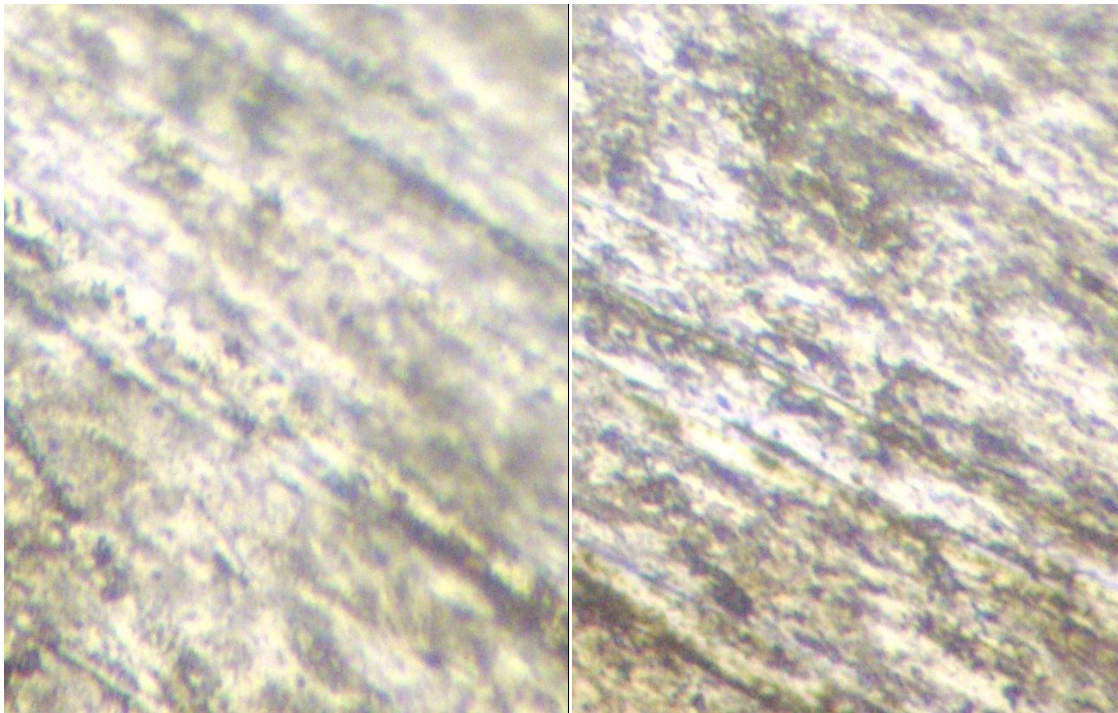
Figure 7.7 Microstructure of A356 and ADC12, Pouring Temperature 730⁰c ,Injection pressure 100 Kg/cm², Dycot Coating, Water Cooling.



A356

ADC12

Figure 7.8 Microstructure of A356 and ADC12, Pouring Temperature 730⁰c ,Injection pressure 90 Kg/cm², Oil Coating, Oil Cooling.



A356

ADC12

Figure 7.9 Microstructure of A356 and ADC12, Pouring Temperature 730⁰c, Injection pressure 120 Kg/cm², Oil Graphite Coating, Air Cooling

6.2 MICROSTRUCTURE ANALYSIS

Microstructure of die cast components made by aluminium A356 and ADC 12 alloy have been investigated by means of Leica Metallurgical Microscope at 50X zoom available at Thapar University, Patiala . The effects of parameters i.e. thermal characteristics (temperature of the molten metal), the injection pressure of the molten metal, type of coating (oil coating, oil + graphite coating, and dycot coating) on the microstructure of the cast product were observed on each of 9 experiments. The metallographic specimens were polished in usual manner with final polishing being carried out by hand, and they were etched in aqueous solution containing 2.5% HNO₃, 1.5 % HCL and 1% HF acid (etched with Keller's reagent) for about 20 seconds.

It is clear from fig 7.1 to 7.9 that the particle size of the alumina is very fine. From the fig it is easily detected that the distribution of the particles is almost uniform by comparing the above micrograph it was analyzed that microstructure of ADC12 is more fine then A356 but at some temperature pressure condition ADC 12 shows some micro cracks in his structure which can be controlled by controlling the input parameters.

RESULTS, CONCLUSIONS AND RECOMMENDATIONS

8.1 RESULTS

The effect of various input parameters i.e. thermal characteristics (temperature of the molten metal), injection pressure of the molten metal, type of coating (oil coating, oil + graphite coating, dycot coating), and the type of cooling (air cooling, water cooling and oil cooling) were evaluated using ANOVA and factorial design analysis. The purpose of the ANOVA was to identify the important parameters in prediction of surface roughness, density and hardness. Some results consolidated from ANOVA and plots are given below:

8.1.1 Surface Roughness

ANOVA analysis showed that Coating (F value 4.34055) was the only factor in A356 alloy and Coating (F value 3.83395) in ADC 12 that significantly affects the surface roughness. All other factors, namely, pouring temperature, coating and cooling were found to be insignificant.

For S/N ratio of surface roughness other than cooling, all other factors, namely, pressure temperature, injection pressure and coating were found to be significant in affecting surface roughness (R_a) in A356 alloy and in ADC 12 alloy except pouring temperature all other factor are found to be significant.

It is concluded that lowest roughness was observed when injection pressure was kept at 100 kg/cm² in A356 alloy and ADC 12 alloy In S/N ratio lowest roughness was observed in A356 when injection pressure was kept at 90 kg/cm², pouring temperature at 730°C and for coating Oil+Graphite was used during casting and in ADC12 when injection pressure 120 kg/cm², and pouring temperature 790 and coating type oil is used because these decrease variation.

8.1.2 Density

ANOVA table shows that injection pressure (F value (134.5) and Cooling type (F value 12.5) are the factors that significantly affects the density. All other factors, namely, coating and Pouring temperature were found to be insignificant in A356 alloy and in ADC12 alloy

injection pressure (F value (32.231) is the only factor that significantly affects the density. All other factors, namely, Pouring temperature, Coating and cooling type were found to be insignificant..

For S/N ratio of density in A356 alloy injection pressure and cooling Factor were found to be significant and in ADC 12, injection pressure and coating are found to be significant.

It is concluded that highest density was observed when injection pressure was kept at 120 kg/cm² and coating type Oil+graphite is used in both the alloys. In S/N ratio plot shows same result.

8.1.3 HARDNESS

ANOVA table shows that pouring temperature (F value 7.000053), and Injection Pressure (F value 6.3746) and Coating (F value 5.221524) are the factor that significantly affects the hardness, whereas Cooling Factor was found to be insignificant in A356 alloy and in ADC12 alloy coating (F value 14.767) and Injection Pressure (F value 3.4973) are the factor that significantly affects the hardness, whereas Pouring temperature and Cooling Factor was found to be insignificant..

For S/N ratio of hardness in A356 alloy, except cooling, all other factors are significant. According to F-test Pouring temperature was observed to be the most significant factor affecting the hardness, followed by Injection pressure and coating according to F-test and in ADC12 alloy According to F-test coating was observed to be the most significant factor affecting the hardness, followed by injection Pressure according to F-test.

- [1]. Knowledge Article From <http://www.Diecasting.Org>
- [2]. Lalit Kumar, “Multi Response Optimization Of Process Parameter In Cold Chamber Pressure Die Casting”, 2010, ME THESIS, THAPAR UNIVERSITY, PATIALA.
- [3]. Asm Casting Hand Book, “William T. Becker, Roch J. Shipley” Isbn-0871707047, 9780871707048 Page(127-154).
- [4]. Knowledge Article From <http://www.Custompartnet.Com/Wu/Die-Casting>.
- [5]. 1-64th-Model-Minis. Wikispaces.Com
- [6]. Dycot Manuals Of Foseco Gmbh, Germany. “Mfd.&Mkt. By M/S Technologies Die Casting”.
- [7]. Ching-Chih Tai., “The optimization accuracy control of a die-casting product part”, Journal of Materials Processing Technology, April 1998, Vol. 103, pp.173-188.
- [8]. Stephanie Dalquist., Timothy Gutowski., “ Massachusetts Institute of Technology”, (LMP)”, December 2004, pp.1-7.
- [9]. Jiang Zheng ., Qudong Wang ., Pang Zhao., Congbo Wu., “optimization of high pressure die casting parameters using artificial neural network”, International Journal of Advance Manufacturing and Technology, November 2008, vol.44, pp.667-674.
- [10]. B. Baradarani., R. Raiszadeh., “Precipitation hardening of cast Zr-containing A356 aluminium alloy”, Journal of Materials Processing Technology, August 2010, Vol. 32, pp.935- 940.
- [11]. C.G. Kang., P.K. Seo., S.S. Kang., “The effect of injection velocity on liquid segregation and mechanical properties in arm part fabricated by semi-solid die casting process”, Journal of Materials Processing Technology ,Feb 2006 ,vol.176, pp.32–40.
- [12]. P.W. Cleary., M. Prakash ., T. Nguyen., “3D SPH flow predictions and validation for high pressure die casting of automotive components”, Journal of Applied Mathematical Modelling, April 2006, vol. 30, pp.1406–1427.
- [13]. Guilherme Ourique Verran ., Rui Patrick Konrad Mendes., Marco Aur´elio Rossi., “ influence of injection parameter on defect formation in die casting Al12Si1,3Cu alloy”, Journal of Materials Processing Technology 2006, vol.179, pp.190-195.

- [14]. Guo Zhipeng., Xiong Shoumei., Liu BaiCheng., LI Mei., Allison John., “Understanding of the influence of process parameters on the heat transfer behavior at the metal/die interface in high pressure die casting process”, international journal of material processing and technology, Science in China Series E: Technological Sciences , Jan. 2009 , vol. 52 ,no. 1, pp. 172-175.
- [15]. Chen Zheng zhou., “Preparation of semi-solid A356 Al-alloy slurry by introducing grain process”, Journal of Trans. Nonferrous Met. Soc. China , March 2012, Vol.22, PP. 1307–1312.
- [16]. Zhi-Peng a Guo, Shou-Mei a Xiong, Bai-cheng a Liu, Bai-cheng a Liu, Li b Mei, Allison b Jhon., (2008) “Determination of the heat transfer coefficient at metal-die interface of high pressure die casting process of AM50 alloy” International journal of heat and mass transfer 51, pp. 6032-6038.
- [17]. Ahuett Horacio., Garza R., Miller Allen., “The effect of heat released during fill on the deflection of die casting”, Journal Of Materials Processing Technology , August 2006, vol.142., pp. 648-658.
- [18]. J.D. Zhu., S.L. Cockcroft., and D.M. Maijer., “ Modeling of microporosity formation in A356 aluminium alloy casting”, Journal of Metallurgical and materials Transaction(China), March 2006 , vol.37A, pp.1075-1083.
- [19]. S. M. H. Mirbagheri., “Modelling of metal–mold interface resistance in the A356 Aluminium alloy casting process”, Journal of Wiley InterScience and technology, June 2006, vol.23., pp.295-312.
- [20]. Vinod kumar., “ automatic selection of optimum parting line and parting direction in Die Casting A review”, National Conference on Advancements and Futuristic Trends in Mechanical and Materials Engineering Oct. 2011., pp.1-5.
- [21]. R.W. Lewis., R.S. Ransingh., “ A correlation to describe the interfacial heat transfer during Solidification Simulation and Its Use in the Optimal Feeding Design of Castings”, Journal of Metallurgical and materials transactions, , APRIL 1998, VOL. 29B , PP.437-447.
- [22]. G. Dour., M. Dargusch., C. Davidson ., A. Nef., “Development of a non-intrusive heat transfer coefficient gauge and its application to high pressure die casting effect

- of the process parameters”, *Journal of Materials Processing Technology*, March 2005, vol. 169, PP. 223–233.
- [23]. Guo Zhipeng., Xiong Shoumei., Cho SangHyun., “Interfacial heat transfer coefficient between metal and die during high pressure die casting process of aluminum alloy”, *Journal of Front. Mech. Eng. China*, Oct.2007, Vol.2, PP. 283–287.
- [24]. A. Hamasaiid., G. Dour., M.S. Dargusch., T. Loulou., C. Davidson., G. Savage., “Heat-Transfer Coefficient and In-Cavity Pressure at the Casting-Die Interface during High-Pressure Die Casting of the Magnesium Alloy AZ91D” , *Journal of Metallurgical and materials transactions*, Vol.39A, April 2008, PP.853-863.
- [25]. K. Gnanamurthy., “Realisation of lightweight machine tool components by modern foundry technology”, *Indian foundry Journal*, Vol 57 No. 2 ,February 2011, PP.23-30.
- [26]. V. Jaiganesh., G. Sajay Surya., S. Bharath Shanker., J. Suresh Kumar., S. Sownder., “Applying Gauge Repeatability and Reproducibility Analysis for a Cast Dimension in a Foundry A Case Study”, *Indian Foundry Journal*, Vol. 57 No. 3 , March 2011, PP 37-43.
- [27]. Guo Zhipeng., Xiong Shoumei., Cho SangHyun., Choi JeongKil., “Interfacial heat transfer coefficient between metal and die during high pressure die casting process of aluminum alloy”, *Journal of Front. Mech. Eng. China*, 2007, vol.2, PP. 283–287.
- [28]. Yongyou Cao., Zhipeng Guo., “Determination of the metal/die interfacial heat transfer coefficient of high pressure die cast B390 alloy, IOP conf series Material science and Engineering ,Jan. 2012, Vol.33, PP.1-10.
- [29]. Pearsson Anders., Hogmark Sture., Bergstrm Jens., “Temperature profile and condition for thermal fatigue cracking in brass die casting dies”, *Journal of materials processing and technology*, March 2004, vol.152, pp.228-236.
- [30]. Matthew Patrzalek., Ebrahim Shayan., Dario Toncich., “Control of cooling in casting dies based on thermal feedback”, *IOP conf series Material science and Engineering* ,Feb. 2010, PP.1-6.
- [31]. H. Yamagata., C. Kasprzak., M. Aniolek., H. Kurita., J. H. Sokolowski., “The effect of average cooling rates on the microstructure of Al-20% Si High Pressure Die Casting Alloy used for monolithic cylinder blocks” *Journal of Materials Processing Technology*, Oct.2007, vol.203, PP.333-341.

- [32]. Matthew Patrzalek.,Ebrahim Shayan.,Dario Toncich., “Control of cooling in casting dies based on thermal feedback”,IOP conf series Material science and Engineering ,Feb. 2010,PP.64-70.
- [33]. Horacio Ahuett Garza., R. Allen Miller., “The effects of heat released during fill on the deflections of die casting dies”,Journal of Materials Processing Technology,vol.142,May2003PP.648–658.
- [34]. Henry Hu., Fang Chen., Xiang Chen., Yeou-li Chu.,Patrick Cheng., “Effect of cooling water flow rates on local temperatures and heat transfer of casting dies”, Journal of Materials Processing Technology,vol.148,Jan 2004,PP.57–67.
- [35]. Giulio Timelli.,Otto Lohne.,Lars Arnberg.,Hans Ivar Laukli., “Effect of solution heat treatments on the microstructure and mechanical properties of a Die-Cast AlSi7MgMn Alloy”,Journal of Metallurgical and materials Transactions, Vol. 39A, JULY 2008,PP.1747-1758.
- [36]. Emma Sjolander., Salem Seifeddine., “The heat treatment of Al–Si–Cu–Mg casting alloys”, Journal of Materials Processing Technology,vol.210,March 2010,PP.1249–1259.
- [37]. H. Moller., G. Govender.,W.E. Stumpf., “Application of shortened heat treatment cycles on A356 automotive brake calipers with respective globular and dendritic microstructures”, Journal of Trans. Nonferrous Met. Soc. China, vol.20, June 2010 PP.1780–1785.
- [38]. Hiroshi horikawa., sanji kitaoka., “Aluminium alloy casting material for heat treatment excelling in heat conduction and process for producing the same”,United State Patent Application Publication, July 2012,PP.1-6.
- [39]. C.G. Kang.,P.K. Seo ., S.S. Kang., “The effect of injection velocity on liquid segregation and mechanical properties in arm part fabricated by semi-solid die casting process”, Journal of Materials Processing Technology,vol. 176,Feb 2006,PP.32–40.
- [40]. Rosendo Zamora., Felix Faura., Joaquin Lopez., Julio Hernandez., “Experimental verification of numerical predictions for the optimum plunger speed in the slow phase of a high-pressure die casting machine”, International Journal of Advance Manufacturing Technology,May 2006,vol.33,PP.266-276.
- [41]. R. Kimura.,M. Yoshida.,G. Sasakia.,J. Pan.,H. Fukunag., “Characterization of heat insulating and lubricating ability of powder lubricants for clean and high quality

- die casting, *Journal of Materials Processing Technology*, VOL.130,2002,PP. 289–293.
- [42]. James L.Graff., Lothar H. Kallien., “The effect of die lubricant spray on the thermal balance of dies”, *Journal of Chem-Trend*, PP. 1-26.
- [43]. C. Mitterer.,F. Holler.,F. U Stel.,D. Heim., “Application Of Hard Coatings In Aluminium Die Casting Soldering, Erosion And Thermal Fatigue Behaviour” *Journal of Surface And Coatings Technology*, vol. 125, 2000, PP. 233–239.
- [44]. Yucong Wang., “A study of PVD coatings and die materials for extended die-casting die life”, *Journal of Surface and Coatings Technology*, Vol. 94-95,1997,PP. 60-63.
- [45]. D. Heim.,F. Holler,C. Mitterer., “Hard coatings produced by PACVD applied to aluminium die casting”, *Journal of Surface and Coatings Technology*, Vol.116–119,1999,PP. 530–536.
- [46]. A. Lousa.,J. Romero., E. Martinez., J. Esteve., F. Montala., L. Carreras., “Multilayered chromium/chromium nitride coatings for use in pressure”, *Journal of Surface and Coatings Technology*,Vol. 146 –147, 2001,PP. 268–273.
- [47]. M.S. Dargusch., A.L. Bowles., K. Pettersen., P. Bakke., G.L. Dunlop., “The Effect of Silicon Content on the Microstructure and Creep Behavior in Die-Cast Magnesium AS Alloys”, *Journal of Metallurgical and materials Transactions*, Vol. 35A, June 2005, PP.1905-1909.
- [48]. H. Yamagata., W. Kasprzak., M. Aniolek., H. Kurita., J.H. Sokolowski., “The effect of average cooling rates on the microstructure of the Al–20% Si high pressure die casting alloy used for monolithic cylinder blocks”, *Journal of materials processing technology*, vol . 2 0 3,Oct.2007,PP. 333–341.
- [49]. Anthony E. Hughes., Nick Birbilis., Johannes M.C. Mol., Santiago J. Garcia, Xiaorong Zhou.,George E. Thompson., “High Strength Al-Alloys: Microstructure, Corrosion and Principles of Protection”,*Journal of Recent Trends in Processing and Degradation of Aluminium Alloys*,2007,PP.223-262.

- [50]. S. Otarawanna., C.M. Gourlay., H.I. Laukli., A.K. Dahle., “Microstructure formation in high pressure die casting”, *Journal of Transactions of The Indian Institute of Metals*, Vol. 62, Issues 4-5, August-October 2009, pp. 499-503.
- [51]. H. Moller., G. Govender., W. E. Stumpf., “Application of shortened heat treatment cycles on A356 automotive brake calipers with respective globular and dendritic microstructures”, *Journal of Trans. Nonferrous Met. Soc. China*, vol.20, June 2010 PP.1780–1785.
- [52]. Nonjabuliso E. Mazibuko., Ulyate A. Curle., “Effect of Solution Heat Treatment Time on a Rheocast Al-Zn-Mg-Cu Alloy” *Journal of Materials Science and Manufacturing*, Council for Scientific and Industrial Research (CSIR), Pretoria, South Africa,
- [53]. J.A. Taylor., G.B. Schaffer., D.H. St John., “The Role of Iron in the Formation of Porosity in Al-Si-Cu Based Casting Alloys: Part 1 Initial Experimental Observations”, *Journal of Metallurgical and materials Transactions*, VOL. 30A, JUNE 1999, PP.1643-1650.
- [54]. A.S. Sabau., S. Viswanathan., “Microporosity Prediction in Aluminum Alloy Castings”, *Journal of Metallurgical and materials Transactions*, VOL. 33B, APRIL 2002, PP.243-255.
- [55]. J.D. Zhu., S.L. Cockcroft., D.M. Maijer., “Modeling of Microporosity Formation in A356 Aluminum Alloy Casting”, *Journal of Metallurgical and materials Transactions*, VOL. 37A, March 2006, PP.1075-1085.
- [56]. V.D. Tsoukalas., “Optimization of porosity formation in AlSi9Cu3 pressure die castings using genetic algorithm analysis”, *Journal of Materials and Design*, Vol 29 April 2008, PP. 2027–2033.
- [57]. Yoshihiko Hangai., Shota Maruhashi., Soichiro Kitahara., Osamu Kuwazuru., Nobuhiro yoshikawa., “Nondestructive Quantitative Evaluation of Porosity Volume Distribution in Aluminum Alloy Die Castings by Fractal Analysis”, *Journal of Metallurgical and materials Transactions*, Vol. 40A, Dec. 2009, PP.2789-2793.
- [58]. Thoguluva Raghavan Vijayaram., “Metal Casting Dies”, *Indian Foundry Journal*, Vol 57, No. 10, Oct. 2011, PP.25-28.
- [59]. Kevin Morasch., Douglas M Woehlke., Kevin R. Anderson., Raymond J. Donahue., “Restoration process for porosity defect in metal casting products”, *United State Patent Application Publication*, July 2012, PP.1-8.

- [60]. Zhi-Peng a Guo., Shou-Mei a Xiong., Bai-cheng a Liu., Bai-cheng a Liu., Li b Mei., Allison b Jhon.,(2008)“Determination of the heat transfer coefficient at metal-die interface of high pressure die casting process of AM50 alloy” International journal of heat and mass transfer 51, pp. 6032-6038.
- [61]. Zhi-Peng a Guo, Shou-Mei a Xiong, Bai-cheng a Liu, Bai-cheng a Liu, Li b Mei, Allison b Jhon. (2008), “Effect of process parameter, casting thickness and alloys on the interfacial heat transfer coefficient in the high pressure die casting process” Metallurgical and material transactions, The minerals, metals and materials society and ASM international 2008. Vol.39A.pp. 2896.
- [62]. W. D. Griffiths., K. Kawai., “The Effect Of Increased Pressure On Interfacial Heat Transfer In The Aluminium Gravity Die Casting Process”, international journal of material processing and technology,Jan. 2010,Vol.45,PP. 2330–2339.
- [63]. R. K. Nayak., S. Venugopal., M. S. Velpari.,“Determination Of Interface Heat Transfer Coefficient (Ihtc) For Investment Casting Simulation- Asensitivity Study” Indian Foundry Journal Vol 57, No. 9 ,September 2011,PP 34-38.
- [64]. Knowledge Article From <http://www.espint.com>.
- [65]. Die casting alloys. *Internet Files\OLK\Die Casting Alloys.Doc*.
- [66]. Ross Phillip J., “Taguchi Techniques for Quality Engineering”, McGraw-Hill, ISBN 0-07-053866-2.